Australian
Geomechanics
Society

Australian Geomechanics

Journal and News of the Australian Geomechanics Society

Volume 48 No 4 December 2013

Offshore Geotechnics

ISSN 0818-9110

INTRODUCTION – OFFSHORE/NEARSHORE EDITION OF AUSTRALIAN GEOMECHANICS

In early 2010, the then President of the International Society of Soil Mechanics and Geotechnical Engineering (ISSMGE), Professor Jean-Louis Briaud, committed to re-establish a Technical Committee dedicated to Offshore Geotechnics (TC-209). This followed a long period during which offshore geotechnics was not truly represented within ISSMGE.

Dr Philippe Jeanjean (BP America) accepted an invitation to Chair the Technical Committee, with Professor Mark Randolph (The Centre for Offshore Foundation Systems and Advanced Geomechanics) as Vice Chair. Other committee members joined shortly after, and the group has been highly active ever since.

Many initiatives have been undertaken by TC-209, primarily following the objectives outlined in the terms of reference prepared by Professor Briaud for the 2010 to 2013 period. One such objective was to:

- *Disseminate knowledge and practice within the TC's subject area to the membership of the ISSMGE*

As part of the Technical Committee's plan to meet this objective, it was proposed to prepare a special edition of Australian Geomechanics dedicated to offshore and nearshore geotechnics. A number of authors subsequently committed to provide papers, covering a range of interesting themes.

I would like to thank the other members of the local committee, namely Nathalie Boukpeti (The Centre for Offshore Foundation Systems), Fiona Chow (WorleyParsons), Sarah Elkhatib (Arup), Nina Levy (Advanced Geomechanics), Elio Novello (URS) and Marc Senders (Woodside Energy). I would also like to thank the reviewers of the papers, who provided valuable feedback to the authors. Finally, I would like to thank the AGS National Committee and AG Journal editorial staff for their support of this initiative.

I hope you enjoy reading the contributions.

Phil Watson

Director, Advanced Geomechanics

Member of TC-209

Committee Chair - Offshore/Nearshore Edition of Australian Geomechanics

WEST PILBARA IRON ORE PROJECT, PORT OFF-LOADING FACILITY, ANKETELL POINT, WESTERN AUSTRALIA

Tony Gourlay[1], Ben Follett[2], Gavin Wearne[3], Bob Lamont-Smith[4] and Peter MacKenzie[5]
[1,2,3,4] AECOM Australia Pty Ltd., [5] API Management Pty Ltd

ABSTRACT

API Management Pty Ltd (API), a 50/50 Joint Venture between Aquila Resources and AMCI propose to construct a multi-user port off-loading facility at Anketell Point in the Pilbara region of Western Australia, which will form part of the West Pilbara Iron Ore Project (WPIOP). The port off-loading facility will have an initial iron ore handling capacity of 30 million tonnes per annum.

This paper describes the nearshore geotechnical investigations that have been completed at Anketell Point. It outlines the purpose of the investigations and provides a geotechnical account of the planning, occupational health and safety and operational aspects of the investigations that led to the successful completion and factual geotechnical reporting of the investigations within program and budget. An overview of the logging, field testing, on site sub-sampling, laboratory testing and the ground conditions is provided.

1 INTRODUCTION

The West Pilbara Iron Ore Project (WPIOP) is a substantial iron ore export operation proposed for the Pilbara region of Western Australia and will comprise the development of new mining and ore processing facilities, rail transport to a new port, port stockyard and storage facilities and port marine and wharf facilities. API is currently developing Stage 1 of the project, which is based on mining and exporting pisolite iron ore deposits located 30 km to 85 km south west of Pannawonica. Pannawonica is located about 140 km south west of Karratha.

The multi-user port off-loading facility forms part of the WPIOP and has an estimated construction cost of A$1.5B. Stage 1 of the port off-loading facility will comprise a single sided 342 m long ship-loader wharf, 324 m long approach jetty and 2,720 m long causeway structure. The wharf will be connected to an approximate 200 m wide, 18 km long dredged shipping channel.

AECOM was commissioned by API in 2008 as the engineering consultant for the multi-user port off-loading facility. AECOM led pre-feasibility and definitive feasibility studies which included nearshore geotechnical investigations, environmental studies, dredgability assessments, ship handling simulations, metocean condition assessments, maritime and coastal engineering assessments, concept designs, project risk assessments, capital expenditure and operational cost estimates as well as preliminary project schedule development.

This paper discusses the nearshore geotechnical investigations undertaken for concept design of the multi-user port off-loading facility.

2 BACKGROUND

The project site is located at Anketell Point at the eastern extent of Nickol Bay, approximately 1,500 km north of Perth, 30 km northwest of Karratha and approximately 7 km northwest of Wickham in the West Pilbara Region of Western Australia (See Figure 1).

Three potential port off-loading wharf sites were considered by API. These included Anketell Point, Cape Preston and Onslow. At these sites, a number of ship-loader wharf locations and shipping channel options were also considered. Following completion of the pre-feasibility study, Anketell Point was selected as the preferred site with two potential wharf option locations. The first option, referred to as the "Dixon Island Option" comprised a causeway extending approximately 800 m off Dixon Island to a 216 m long jetty and 342 m long ship-loader wharf. A bridge structure would connect Dixon Island to Anketell Point. The second option, referred to as the "Anketell Point Option" comprises a 2,720 m long causeway extending off Anketell Point to a 324 m long approach jetty and 342 m long ship-loader wharf. Both options connect to an approximately 18 km long and 200 m wide shipping channel. The Anketell Point option is currently being considered for development (See Figure 1).

The selection of preferred port location was based on a capital cost comparison of the design concepts at each location. Anketell Point provided the most favourable site conditions facilitating the most cost effective facility for the proposed 30Mtpa operation. Primarily soft ground conditions and reasonably close proximity to deep water permitted the dredging of an access channel to cater for bulk carriers with a laden daft of approximately 18.5 m CD. Anketell Point

also received natural protection from the incident operational wave climate from offshore Islands allowing an open ocean export wharf without the requirement of a breakwater. Other factors such as direct access to suitable land for port landside facilities and proximity to potential rail corridors also significantly contributed to the selection of Anketell Point as the preferred port location.

Figure 1: Site location and Wharf Options

The port off-loading facility for the Anketell Point option will be constructed approximately 3 km offshore in water depths typically ranging from -3 m CD to -11 m CD with tidal level fluctuations of up to about 6.2 m. The ship-loader wharf has been designed to accommodate up to 250,000 dead weight tonne iron ore carriers. It will consist of a steel pile substructure and steel superstructure comprising steel rail girders, transverse beams and bracing. The wharf superstructure supports the ship-loader, loading conveyors, an access roadway, maintenance walkways and access stairs to catwalks at dolphin level. Steel berthing and mooring dolphins have been designed and spaced accordingly to accommodate the proposed vessel sizes. The access jetty will comprise a trestle steel superstructure and will be supported on a steel pile substructure. The approach causeway structure will comprise a core of engineered fill protected by layers of armour rock.

Dredging will be required at the turning basin and ship berthing pocket locations as well as within the shipping channel. Dredge levels will typically range from about -11.5 m CD to -14.8 m CD at the turning basin and ship berthing pocket locations respectively. Dredge levels will typically range from -15.5 m CD to -16.3 m CD within the shipping channel. Overall, approximately 22 million cubic metres of dredging is anticipated for the Stage 1 development, which will likely be undertaken using trailer hopper suction and cutter suction dredging equipment.

3 REGIONAL GEOLOGY

The geologic framework and interpretation of environments is based largely on ideas presented by Hickman (2002) and Blake (1993) for the WPGGT and by Thorne and Trendall (2001) for the Fortescue Group.

The site lies within the northwest part of the Pilbara Craton and covers parts of the West Pilbara Granite–Greenstone Terrane (WPGGT) and northern exposures of the Hamersley Basin. Deposition of greenstones of the WPGGT commenced in the Archaean, shortly before 3270 Ma, where rocks assigned to the Roebourne Group were laid down. In the vicinity of the site the Roebourne Group is represented by the felsic metavolcanic and metasedimentary rocks of the Nickol River Formation and the peridotitic komatite, metabasalt and chert of the Regal Formation. The Roebourne Group is unconformably overlain by banded iron-formation (BIF), chert, and fine-grained clastic sedimentary rocks of the 3020 Ma Cleaverville Formation. Locally, the rocks of the WPGGT are overlain by the Mount Roe Basalt (2763

Ma) which is dominated by sub aerial basaltic lavas, subaqueous basaltic (pillow) lavas and waterlain volcaniclastic rocks. Superficial deposits currently covering the bedrock at the study site are formed by Cenozoic to Recent marine and terrestrial sediments, typically composed of carbonates and clasts of bedrock.

4 NEARSHORE GEOTECHNICAL INVESTIGATIONS

4.1 PLANNING

4.1.1 Geotechnical Aspects

Detailed geotechnical planning of the nearshore geotechnical investigations was undertaken with reference to the following documents:

- "Site Investigation Requirements for Dredging Works", published by the Permanent International Association of Navigation Congresses (PIANC), dated February 2000
- "Geotechnical and Geophysical Investigations for Offshore and Nearshore Developments", published by the International Society for Soil Mechanics and Geotechnical Engineering, dated September 2005

Combined with AECOM's previous involvement on similar projects in the Pilbara region, the nearshore investigations were undertaken in the following distinct phases:

- Desktop study (pre-feasibility study)
- Preliminary field investigations (pre-feasibility and definitive feasibility study)
- Detailed field investigations (post DFS)

Undertaking the fieldworks in a phased approach was extremely beneficial as it allowed the lessons learnt from one phase to be incorporated into the next and resulted in smoother run fieldwork programs. It also allowed the concept design of the port facilities to be optimised leading to significant potential cost savings.

4.1.2 Operational Aspects

Planning of the operational aspects of the nearshore geotechnical investigations was undertaken with API, the main contractor and subcontractors as part of interactive one or two day hazard identification workshops. These workshops included the open discussion of not only safety aspects of the project, but also integrated key operational issues such as developing and maintaining team morale, logistics of the fieldworks, cyclone evacuation procedures and preparedness, personnel rosters, vessel suitability, managing environmental incidents, night operations and managing community expectations. This collaborative planning process was very effective in "setting the tone" of the fieldworks which ensured all parties knew what their roles and responsibilities entailed, but more importantly they took ownership of them. This ultimately led to a series of successful overwater fieldwork campaigns which were completed within program and budget.

4.2 OPERATIONAL ASPECTS OF THE FIELDWORKS

4.2.1 Logistics and Personnel Rosters

Given the comparatively smaller scope of work, the preliminary overwater investigations for the pre-feasibility and definitive feasibility studies were undertaken relatively cost effectively as a day-time operation, where personnel worked 12 hour shifts. All field personnel were accommodated onshore at either Wickham or Point Samson. To manage fatigue, crews worked 2 weeks on and 2 weeks off and also took a rostered day off every 14 days. The drawback of this operation was that approximately 30% of each 12 hour shift was lost to transferring site personnel from Point Samson to the work site, which is located about 12 km from Point Samson.

Given the much larger scope of work for the detailed overwater drilling investigations, to reduce the overall length of the fieldworks program and expenditure, a 24 hour, 7 day per week operation was implemented whereby a 12 hour day and night shift was worked. All personnel were accommodated offshore on a dedicated accommodation vessel. The benefit of this approach was that the accommodation vessel could be moored close to the work site, vastly reducing the time required to transfer personnel to and from the drilling rig, increasing overall productivity during each shift. Therefore transfer times were significantly reduced to approximately 5% of each 12 hour shift, thus increasing overall drilling productivity. To manage fatigue, crews either worked 2 weeks on and 1 week off or 4 weeks on and 2 weeks off. Personnel rotated from day shift to night shift midway through their swing on site. A key benefit that was realised

in undertaking 24 hour drilling operations was that it allowed a better response to adverse weather conditions and opportunistic weather windows.

4.2.2 Support Vessels

Typically 31 personnel were on site at any one time. Personnel were accommodated on a three level, 36 Berth Catamaran where all meals and a daily clothes washing service was provided. This arrangement did pose issues around confinement of personnel, however these were overcome by allowing beach walks, the provision of exercise equipment, television, access to the internet, movies and a library on board the accommodation vessel.

An 1800 Horse Power (HP) Catamaran was used as a "work or tug boat" to tow the jack-up barge to each borehole location and to act as a standby vessel in the event of an emergency on the jack-up barge. If required this vessel could also be used a back-up transfer vessel.

A small 300 HP Catamaran with a shallow draft and a capacity for 22 personnel was used as a transfer vessel to transfer the drilling crew from the accommodation vessel to the jack-up barge at the beginning and end of each shift as well as from Point Samson to the accommodation during crew changeovers. The transfer vessel was also used to transfer materials and equipment for the drilling operations and provide supplies to the accommodation vessel. The shallow draft of the transfer vessel was fit for the purpose of getting in and out of Point Samson which was access restricted during low tide.

4.2.3 Weather, Sea State and Tidal Conditions

The daily weather, sea state and tidal conditions (i.e. temperature, sea wave, sea swell, wind speed, wind direction, tide levels) dictated whether the fieldworks could be undertaken or not. It was therefore essential to have up-to-date forecast information to allow forward planning of the works. Therefore, specialist "site specific" Bureau of Meteorology (BOM) forecasts were used to plan and respond appropriately to changing weather and sea state conditions together with predicted tidal data for the area. This information was particularly useful in planning tropical cyclone evacuations to ensure it would be safe to tow the jack-up barge back to Point Samson in readiness for the cyclone and staging access to those boreholes affected by large tidal variations.

4.2.4 Team Morale

A large part of the success of the nearshore geotechnical investigation campaigns can be attributed to the strong relationship and subsequent team morale that developed on site between all parties. Furthermore, open and honest day-to-day communications were maintained both on site and in the office and between the site and the office. Clear lines of communication were established prior to undertaking the fieldworks to ensure that important information was not miscommunicated. On site, all personnel were encouraged to speak their mind and contribute ideas or concerns at any time on the project. Team building activities leading to increased morale also extended to the "Clean-up Australia Day" campaign at Point Samson where the local community were very appreciative of the field team's efforts to rid the town and local beaches of visible rubbish.

4.2.5 Continuity of Senior Personnel

It is important to note that during all fieldwork campaigns there was continuity of key senior personnel from all parties involved. This was a major benefit as key senior personnel were aware of the history of the project and could bring this knowledge and any lessons learnt from earlier phases of the project into subsequent phases of the project. This led to more efficient working and improved safety and environmental outcomes.

4.3 HEALTH, SAFETY AND ENVIRONMENTAL MANAGEMENT

Health, Safety and Environmental (HSE) Management formed an integral part of the success of the nearshore investigations in terms of ensuring that the works were completed without any Lost Time Injuries or Reportable Environmental Incidents. Due to the scale of the overwater drilling investigations, the number of personnel present on site, the type of plant and equipment employed and the overall risks associated with managing health, safety and the environment on a 24 hour, 7 days per week overwater operation, full-time HSE advisors were employed on site for the duration of the fieldworks. In this way, a positive safety culture was developed from day one and reinforced throughout the project.

Some of the key HSE risks that were identified as part of a Hazard Identification Workshop included:

- Managing fatigue – typically caused by working long days, hot and humid climatic conditions on site, sea sickness, shift work and living in the confines of a boat.

- Cyclone Readiness – the fieldworks programs were conducted during cyclone season as the metocean conditions were typically more favourable for overwater work during this time of the year. Although winter periods avoid infrequent cyclone events, ocean swells combined with persistent easterly trade winds provided less favourable operational conditions.
- Planning and managing jack-up barge moves (towing, elevating and lowering) – this activity needed to be well timed so that the metocean conditions were favourable throughout the overall process. Additionally, managing the potential risk of "punch throughs" whilst jacking up was essential. This was achieved by jacking up in short 0.5 m lifts, alternately loading each pair of legs whilst jacking to encourage penetration through shallow soft layers of soil and then finally maintaining the jack-up just above the waterline for a period of at least 30 minutes prior to jacking to final height. The benefit of local knowledge, lessons learnt from earlier phases of work and site specific BOM reports were also invaluable in accomplishing this process safely.
- Personnel and equipment transfers from vessel to vessel – similar to the jack-up barge moves, transfers needed to be well timed so that metocean conditions were favourable throughout the overall process.
- Managing environmental incidents – although infrequent, hydraulic spills posed the greatest risk in terms of causing potential damage to the environment. This was managed by bunding all equipment, having spill kits readily available and suitably trained and experienced personnel on board the jack-up to respond to any incident.

These key risks were managed by implementing a comprehensive project specific HSE Management Plan, ensuring that all personnel engaged on the project were suitably qualified, experienced and had undergone site specific training and safety inductions. Key safety issues were raised regularly during daily pre-start meetings and at weekly tool box meetings combined with weekly safety drills. Safety audits were conducted regularly during the fieldworks to ensure safety systems and procedures were effective and being complied with.

4.4 PRE-FEASIBILITY STUDY

4.4.1 Desktop Study

A high level desktop study was conducted during the pre-feasibility study stage to identify potential sites for the port off-loading facility. This work included an assessment of possible wharf and shipping channel locations that could be included as part of a preliminary geotechnical investigation.

4.4.2 Seismic Refraction and Hydrographic Survey

At Anketell Point, overwater investigations comprised 34 seismic refraction lines, typically spaced at approximately 80 m centres (totalling about 162 km) together with a hydrographic survey along the same seismic lines. This work was conducted from 4 to 23 August 2008. The purpose of this work, following the earlier desktop study, was to:

- Assess the depths, thickness and distribution of the rock and soil layers relevant to dredging and pile foundations at the ship loader wharf locations
- Evaluate two alternative shipping channel alignments

Similar scopes of work were undertaken at the Cape Preston and Onslow sites.

Real time seismic refraction velocities were provided on site by the geophysicist for review and assessment of potential geotechnical hazards. This allowed for the request of additional surveys during the fieldworks to better assess the significance of such risks before demobilising from site.

4.5 DEFINITIVE FEASIBILITY STUDY

4.5.1 General

Following completion of the pre-feasibility study, Anketell Point was selected as the preferred site for the multi-user port off-loading facility. Two ship-loading wharf location options (i.e. Dixon Island and Anketell Point) were identified and a single shipping channel alignment option. To assess the feasibility of these options, a preliminary nearshore geotechnical investigation comprising the following was undertaken as part of the Definitive Feasibility Study (DFS):

- Seismic refraction and hydrographic survey
- Overwater geotechnical boreholes with *in situ* and laboratory testing
- Jet probing

The fieldwork locations were selected using the results of the pre-feasibility seismic refraction survey, however it was acknowledged the borehole locations might need to be modified as the investigations proceeded and as more information became available.

The purpose of the DFS nearshore investigations was to provide sufficient geotechnical data to facilitate a ±15% cost estimate for the port marine infrastructure.

4.5.2 Seismic Refraction and Hydrographic Survey

A total of 29 seismic refraction lines typically spaced at typically 80 m to 300 m centres (totalling approximately 73 km) were undertaken together with a bathymetric survey along the seismic lines at the location of the two ship-loading wharf options from 31 March to 16 April 2009. The objective of this work was to:

- Provide an assessment of the depth to the local basement rock
- Provide an assessment of the depths, thickness and distribution of the rock and soil layers relevant to dredging and pile foundation conditions for assessment of preliminary design and costing
- Assist in positioning the wharf head options based on the depth to the local basement rock and soil layers
- Assist in optimising the borehole locations for the jetty and wharf options
- Complement the borehole information and assist in the preparation of a geological model for the site.

The seismic refraction survey was conducted in three stages. Stage 1 and 2 were carried out over a relatively coarse grid covering the two wharf option locations with seismic refraction lines spaced at approximately 300 m to 500 m apart in both a north-south (Stage 1) and east-west (Stage 2) direction. As the seismic refraction data was collected each day, it was processed overnight by a site based geophysicist, so that preliminary results were available the following morning for review. Using this data, a preliminary geological model of the sub seabed conditions was developed and updated on a daily basis. Using this model it was possible to make decisions to shorten, lengthen, move or delete the Stage 1 and 2 seismic refraction lines and to decide whether the proposed position of the two wharf head options needed to be adjusted to ensure that the required dredge levels did not intersect rock and require costly drill and blast dredging techniques for removal.

Stage 3 comprised “infill seismic refraction lines” which were defined based on the preliminary geological model of the sub seabed conditions and the adjusted location of the wharf heads. The Stage 3 seismic refraction data was once again processed overnight by the site based geophysicist with the preliminary results available for review and incorporation into the preliminary geological model. Once again the position and length of the lines were adjusted as required. The nominated borehole positions were then confirmed once the position of the wharf head for the two options had been adjusted on the basis of the preliminary Stage 3 seismic refraction results.

This novel, staged and flexible approach to undertaking the geophysical survey led to significant program and cost savings to the project, with the risk of encountering rock requiring costly drill and blast dredging techniques greatly reduced. This outcome was only possible by having flexibility in being able to adjust the location of the wharf heads with close cooperation between the site team, geotechnical engineers and port planning specialists.

4.5.3 Overwater Boreholes

Nineteen boreholes ranging in depth from 3 m to 35 m below seabed level totalling approximately 297 m of drilling were undertaken from 25 March and 22 May 2009. Boreholes were drilled as close as possible to the seismic refraction lines for correlation purposes and were spaced at approximately 50 m to 110 m centres along the wharf and jetty locations. A limited number of boreholes were drilled in the turning basins and berth pockets due to time constraints. Some boreholes were drilled within the shipping channel alignment spaced at approximately 1.5km to 2.5 km centres. Operational water depths ranged between approximately 10 m at the access jetty location and 23 m in the shipping channel. Average drilling rates of 5.1 m/day were achieved including approximately 16% standby time. Standby time comprised about 10 days” downtime due to poor sea state.

The objective of this work was to provide an assessment of:

- The soil and rock conditions beneath the offshore facilities and in particular the conditions within the significant foundation support zone for the jetty and wharf structures and the areas to be dredged
- The geotechnical properties of the materials to be dredged in the shipping channel, turning basins and berthing pockets
- The underwater dredge slope stability at the shipping channel, turning basin and berthing pocket locations

- The consistency and strength of the sub seabed materials at the wharf and jetty locations to assist with foundation selection, material parameter selection and foundation design for the wharf and jetty structures
- Pile driveability at the wharf and jetty locations
- The consistency and strength of the sub seabed materials at the causeways to assist with foundation and stability assessment of the causeway structures
- Calibration of the geophysical data.

The overwater boreholes were undertaken using a drilling rig mounted on a four legged self-elevating (jack-up) barge. All boreholes were cored from seabed level using PQ3 wire-line diamond coring equipment. Core runs were limited to 1.5 m lengths and were typically 0.5 m to 1.0 m to maintain good core recovery in both consolidated soil and rock units. In the unconsolidated soil sediments the PQ-3 coring equipment was used as a wash boring tool and therefore core samples were not recovered.

Standard Penetration Tests (SPTs) were carried out in all boreholes typically at 0.5 m to 1.5 m centres in the unconsolidated soil and weathered rock to assess the *in situ* density/consistency. Pocket Penetrometer tests were undertaken on the sides of the recovered PQ-3 core to provide an approximate assessment of the unconfined compressive strength (or inferred undrained shear strength) of cohesive soils as well as cemented sands and carbonate rocks. Field Point Load Strength Index (Is_{50}) testing was carried out on the recovered rock core at approximately 1 m centres to indirectly assess the rock strength. Following completion of the drilling program, the geophysical survey results were correlated with the boreholes and quite good agreement was observed.

4.5.4 Jet Probing

A subsequent separate jet probing investigation was carried out following the offshore borehole drilling investigation. The jet probing investigation was carried out along the alignment of the Bouguer Passage Causeway, Dixon Island Bridge and Access Jetty Causeway areas where previous geotechnical investigations had not been carried out. In total, Jet Probing was conducted at 17 locations between 28 and 29 September 2009. The objective of the jet probing investigation was to:

- Assess the seabed levels across Bouguer Passage on the alignment of the bridge crossing from Anketell Point to Dixon Island
- Provide an assessment of the depth to possible competent founding material below seabed level on the alignment of the bridge crossing to assist with concept design and costing of the bridge foundations
- Assess the potential thickness of any soft/loose sediment that may impact the stability and cost of construction of the approach causeway structure.

Jet probing, whilst cost effective, provided limited information as it refused at shallow depth but provided sufficient information for the DFS stage of the investigations.

4.6 POST DFS

4.6.1 General

Detailed geotechnical investigations were subsequently carried out following completion of the DFS investigations to assess the preferred wharf option. The investigations comprised the following:

- Overwater geotechnical boreholes with *in situ* and laboratory testing
- Overwater Electric Friction Cone Penetration Testing
- Seismic reflection and hydrographic survey

The purpose of these investigations was to obtain sufficient geotechnical information for developing the project execution strategy and for preparing construction tender packages.

4.6.2 Overwater Boreholes – Phase 1

Following completion of the DFS investigations, the “Dixon Island Option” was selected as the preferred wharf option and a detailed investigation comprising a total of eighty seven (87) boreholes was drilled to depths ranging from 5 m to 46.50 m below seabed level, with a total of approximately 1,757 m of drilling undertaken between 8 October 2010 and 11 May 2011. Operational water depths ranged between approximately 1.0 m in Bouguer Passage and 20.0 m in the shipping channel. Average drilling rates of 9.6 m/day were achieved including approximately 30% standby time.

Standby time comprised a 14 day shutdown over Christmas, about 47 days' downtime due to poor sea state, about 7 days due to mechanical breakdowns and 15 days' standby due to three cyclones (Vince, Bianca and Carlos).

Typically one borehole was drilled at every dolphin location with boreholes spaced at approximately 30 m to 150 m along the length of the wharf, jetty and causeway structures. In the shipping channel boreholes were typically spaced at 50 m to 150 m centres and in the turning basin and ship berthing pocket, boreholes were spaced at approximately 100 m to 200 m centres. Where possible, all boreholes were drilled as close as possible to the seismic refraction lines for correlation purposes. Using the preliminary geotechnical model developed as part of the DFS, borehole positions were adjusted (where required) so that potential geotechnical hazards such as shallow cemented calcareous rock that could impact dredgability or soft/loose deposits that could impact the stability of the causeway structure could be investigated. As the investigation proceeded the preliminary geological model was regularly updated which lead to some boreholes being curtailed, added or locations adjusted as required. Towards the end the Phase 1 drilling program (16 April 2011) API requested that the investigations be extended to include drilling ten boreholes (269 m) at the "Anketell Point (wharf) Option" as a mitigation strategy pending the release of the final Anketell Point port master plan by the Department of State Development (DSD). The additional drilling was however terminated prematurely due to unfavourable metocean conditions.

The objective of this phase of drilling work was to:

- Provide a detailed assessment of the soil and rock conditions beneath the offshore facilities, in particular the conditions within the foundation support zone for the jetty and wharf structures and the areas to be dredged for the ship approach channel and turning basin
- Provide information for preparation of dredging design and construct tender documentation
- Provide information for preparation of pile design and construct tender documentation
- Provide information for preparation of other marine design and construct tender packages.

4.6.3 Overwater Boreholes – Phase 2

Following completion of the Phase 1 drilling campaign, the port master plan was released by the DSD indicating that the "Anketell Point (wharf) Option" was preferred due to heritage issues on Dixon Island. As a result, Phase 2 detailed investigations comprising a total of 44 boreholes were drilled to depths ranging from 5.4 m to 46.5 m below seabed level, with a total of approximately 1193 m of drilling undertaken between 16 January 2012 and 24 April 2012. Operational water depths ranged between approximately 2.5 m and 11 m. Average drilling rates of 11.7 m/day were achieved including approximately 21% standby time. Standby time comprised about 14 days' downtime due to poor sea state, one day due to mechanical breakdowns and seven days standby due to cyclone Iggy.

Borehole positions and spacing at the wharf, jetty, causeway structure, shipping channel, turning basin and ship berthing pocket were similar to the Phase 1 investigations. All boreholes were drilled as close as possible to the seismic refraction lines for correlation purposes and the preliminary geotechnical model developed as part of the DFS, was used to adjust borehole positions (where required) so that potential hazards could be investigated. As the investigation proceeded the preliminary geological model was regularly updated which lead to some boreholes being curtailed, added or adjusted as required.

The objective of this work was the same as the objective for the Phase 1 drilling work.

4.6.4 Overwater Electric Friction Cone Penetration Testing – Phase 2

Electric Friction Cone Penetration Testing (EFCPT) using a piezocone was undertaken between 26 April and 30 April 2012. A total of six EFCPTs were undertaken to depths of between 4.8 m and 11.2 m below seabed level, with a total depth of 48.6 m of probing along the length of the causeway structure. The EFCPTs were spaced at approximately 200 m to 300 m centres along the length of the causeway structure and where appropriate adjacent to existing boreholes.

The EFCPTs were undertaken using a portable modular rig mounted over the moon pool of the same jack-up barge used for the drilling works. Porewater dissipation tests were conducted in soft/loose sediments for permeability assessment. Parameters recorded with depth during the test included tip resistance, shaft resistance, friction ratio and pore pressure.

The objective of EFCPT work was to:

- Provide a detailed assessment of the soil and rock conditions beneath the causeway structure for foundation and stability assessment
- Provide information for assessment of the extent of potentially liquefiable materials in the vicinity of the causeway

4.6.5 Overwater Seismic Reflection and Hydrographic Survey – Phase 2

A marine geophysical and hydrographic survey was undertaken between 9 and 15 June 2012. The area surveyed included the ship turning basins, berthing pockets, berthing and mooring dolphins, wharf, tug harbour and approach causeway.

The completed scope of work comprised approximately 163.7 line kilometres of seismic reflection survey and approximately 280.4 line kilometres of multi-beam bathymetric survey. Due to shallow water depths in parts of the survey area, operations were tidally constrained and so not all nearshore areas for survey were accessible. The survey area extended from the shallow intertidal zone to approximately 5.8 km offshore and included a short section of the shipping channel, ship turning basins, berthing pockets, berthing and mooring dolphins, wharf(s), tug harbour and approach causeway, covering a total seafloor area of approximately 3.4 square kilometres.

The objective of the geophysical survey work was to:

- Provide additional geophysical data to supplement the DFS seismic refraction data obtained in 2009
- Provide a more detailed assessment of the depths and thickness and distribution of the rock and soil layers relevant to the dredging, pile foundations and approach causeway
- Provide an up-to-date and more complete hydrographic survey of the adopted wharf option, especially given that the wharf alignment had changed slightly following selection of this option
- Provide additional information to compliment the borehole and EFCPT information and inform the geological model.

4.7 LOGGING

Geotechnical logging was undertaken on site, on a full-time basis, by experienced geotechnical engineers and geologists from AECOM. For the non-carbonate soils and rocks, the geotechnical logging of the boreholes was undertaken in general accordance with Australian Standard AS1726–1993 with reference to the AECOM soil and rock explanatory sheets. For the calcareous sediments and sedimentary rocks, the Clark and Walker classification system (Clark & Walker, 1977) was adopted for logging these materials. Log descriptions were based on tactile and visual assessments of the samples recovered during drilling and these were compared with the field and laboratory test results. Where appropriate, the engineering logs were modified in light of the laboratory results. With this in mind, it was recognised that undertaking sufficient strength testing was essential so that correlations between field and laboratory Point Load Strength Index and UCS could be assessed to overcome (in part) the difference in strength classification systems of Clarke and Walker and AS1726-1993. Therefore both axial and diametral Point Load testing was undertaken in the field and in the laboratory. The ratio of axial to diametral testing was approximately 1.3:1.

To ensure that the quality of the logging was maintained during the fieldworks, regular feedback was provided to the field personnel on a daily basis as logs were reviewed in the office. Additionally the project manager and senior geologist visited the site on alternate weeks to assist field personnel and to conduct quality audits of the logging and the logging process. All field logs were digitised in the office using the proprietary borehole logging software gINT.

4.8 ON-SITE SUBSAMPLING

Following the DFS overwater drilling investigation, subsampling of the rock core on the jack-up barge was implemented for both Phase 1 and 2 of the detailed overwater drilling investigations. This was considered essential due to the fractured nature of the rock which was found to develop additional core breaks along pre-existing planes of weakness during transportation of the core from site to Perth. This resulted in core lengths often being too short or unsuitable for laboratory strength testing and therefore limited scheduled tests could be conducted during the DFS investigation.

During the Phase 1 and 2 investigations, rock core subsamples were identified by the AECOM field engineer/geologist and then they were cut to length by an experienced on-site geotechnician. All subsamples were then labelled (inside and out), wrapped in gladwrap, laid on flat plastic, placed in PVC splits and then wrapped in multiple layers of bubble wrap. Subsamples were transported to laboratories in Perth in smaller lockable steel boxes and where required, sent to other laboratories interstate. All steel boxes were labelled according to borehole and depth and an inventory prepared, a copy of which was included in each box for easy identification by the laboratory. This process ultimately resulted in intact samples arriving at the laboratory for strength testing. On-site subsampling reduced sample preparation time in the laboratory as core did not need to be removed from the core boxes and cut in the laboratory. This in turn resulted in quicker turn-around times for strength testing. Overall, whilst an additional cost was incurred for having a full-time geotechnician on the jack-up, the overall benefit more than outweighed the cost. It is important to note that the soil samples were also carefully wrapped, labelled and transported in lockable steel boxes to protect them in transit.

4.9 LABORATORY TESTING

Laboratory testing was undertaken on selected disturbed and undisturbed soil and rock samples recovered from the boreholes (as part of each phase of drilling). Due to the magnitude of the testing undertaken, a range of approved NATA accredited laboratories located in Perth and in New South Wales were engaged to undertake the testing to ensure that the length of the testing program was minimised. Laboratory testing was progressively scheduled whilst the fieldworks were being undertaken and this was achieved by ensuring collected samples were couriered to Perth typically on a weekly basis. Regular liaison and management of each laboratory was required to ensure that schedule could be maintained. This involved holding each laboratory accountable for progress on work in hand and understanding their capacity to take on further work as new laboratory schedules were prepared.

To provide information for classification and characterisation of the materials encountered in the boreholes in relation to dredging and piling conditions on site, the following soil and rock tests were undertaken as outlined in the table below.

Table 1: Laboratory Testing Undertaken

Test	Soil	Rock
Moisture Content	✓	✓
Atterberg Limits & Linear Shrinkage	✓	×
Particle Size Distribution & Hydrometer	✓	×
Dry (Bulk) Density	✓	✓
Wet (Bulk) Density	✓	✓
Particle Density	✓	✓
Particle Density & Water Absorption of Aggregate	×	✓
Porosity & Dry Density	×	✓
Organic Content	✓	×
Calcium Carbonate	✓	✓
X-ray Diffraction Analysis	✓	✓
Petrographic Analysis	✓	✓
Point Load Strength Index (Axial and Diametral)	×	✓
Uniaxial Compressive Strength (UCS)	×	✓
UCS with Young's Modulus	×	✓
CERCHAR Abrasivity	×	✓
Indirect Brazilian Tensile	×	✓
Ultrasonic Pulse Velocity	×	✓

During the overwater drilling investigation, preliminary laboratory schedules were prepared on site in hard copy format and in a spreadsheet which included a list of all samples including sub-samples of core. As each borehole was completed on site, the preliminary laboratory schedules were e-mailed to the office for review (against the field logs and core photographs) and finalisation prior to sending to a nominated laboratory. This saved a significant amount of time in the scheduling process. Furthermore, following completion of the DFS nearshore investigations a preliminary geological model was developed which included the identification of a series of stratigraphic units. During subsequent nearshore investigations, stratigraphic units were included on the draft field logs by the field personnel as well as on the preliminary laboratory schedules to assist with selection of soil and rock samples for laboratory scheduling. As the laboratory testing proceeded, the total number of tests conducted on particular stratigraphic units could be monitored (using a purpose designed spreadsheet) to ensure sufficient tests were conducted on a range of material types encountered in the boreholes.

Lessons learnt from the DFS overwater investigations and Phase 1 detailed overwater investigations, which comprised scheduling, managing and reviewing thousands of laboratory test results, led to the development of an in-house laboratory results tracking spreadsheet which was linked to the laboratory scheduling spreadsheet. Prior to commencement of the laboratory testing for Phase 2 of the post DFS investigations, agreement was sought with each laboratory to provide individual test results in pdf format, with each file named in accordance with a pre-agreed naming format to identify each individual test result. All laboratories were required to send the laboratory results to a dedicated project e-mail address accessible to the engineering team. Results received were then saved into a specific project directory where the file names were automatically checked against the laboratory schedules using the tracking spreadsheet. At the end of this efficient process, the total number of tests completed versus the number of uncompleted

tests was known and the laboratories could be followed up to check the status of outstanding test results. This innovative approach of tracking laboratory test results saved countless hours of work and significantly reduced human error in the checking process.

Following completion of this project, discussions were had with a number of laboratories regarding how the management of such large laboratory testing programs and the data that is generated can be better managed in the future. This has led to some laboratories looking at improving their systems, data management processes and how they can best provide the laboratory results in a format that is easily checked and imported into spreadsheets and data bases used by geotechnical consultants. One such format that the authors believe should be considered is the AGS format that is currently used by laboratories in the UK. Other ideas include using a web based approach to scheduling laboratory tests as well as posting results so that the overall process is trackable and therefore auditable with results in a standard or client specific format. It is the authors' understanding that NATA accredited laboratories are still unable to issue results in electronic format unless the results for individual tests are signed by an approved NATA signatory. Due to this NATA restriction, it therefore precludes issuing results in AGS format. If the Australian testing industry is to move forward, the industry needs to work with NATA to find a sensible solution that benefits the industry as a whole without compromising quality and ensuring results are trackable and auditable. With the current computing technology available in the market, this is not insurmountable.

5 INVESTIGATION FINDINGS

5.1 SUMMARY OF GROUND CONDITIONS

The ground conditions encountered on site can typically be summarised as follows:

- Unconsolidated calcareous sediments comprising mostly sand and gravel with densities typically ranging from very loose to medium dense, overlying
- Consolidated and unconsolidated calcareous sediments (mostly comprising sand and gravel) with densities typically ranging from medium dense to dense and weakly to moderately cemented carbonate rocks, overlying
- Extremely weathered to fresh metamorphosed crystalline and sedimentary rocks.

Due to client confidentiality requirements, only a summary of the ground conditions has been provided.

6 CONCLUSIONS

Three phases of nearshore geotechnical investigations comprising 160 boreholes (3,516 m of drilling), six EFCPT's, 17 jet probe holes, 235 km of seismic refraction survey, 164 km of seismic refraction survey, three hydrographic surveys and a comprehensive suite of laboratory tests were successfully completed within program and budget. This was achieved through:

- Careful planning of the fieldworks from a geotechnical and operational perspective
- Provision of full-time project management (office and site based) of the fieldwork operations
- Maintaining continuity of senior personnel from one phase of the project to the next
- Implementation of a continuous improvement process whereby lessons learnt from earlier phases of the project were applied to subsequent phases of the project.

This led to more efficient work practices with less standby time and better safety and environmental outcomes. In particular, by using a dedicated accommodation vessel moored close to the overwater drilling operations, an approximate reduction in personnel transfer times of 25% was achieved, leading to an overall increase in drilling productivity. Furthermore, by undertaking the nearshore geotechnical investigations in a phased approach, this provided flexibility in terms of being able to modify the fieldwork locations as the works proceeded based on the latest geotechnical information. This ultimately led to the optimisation of the concept design, resulting in a more cost effective solution. Overall the objectives of the nearshore geotechnical investigations were met and included:

- Completing a ±15% cost estimate for the marine infrastructure following the DFS
- Obtaining sufficient detailed geotechnical data for producing an execution strategy and preparing construction tender documentation.

This paper has outlined the benefit of a collaborative approach (by all parties involved) in planning the operational aspects of the nearshore geotechnical investigations during Hazard Identification Workshops conducted prior to undertaking the fieldworks. In addition to identifying key risks associated with health, safety and the environment,

these workshops also allowed integration of key operational issues such as team morale, fieldwork logistics, cyclone readiness, personnel rosters, vessel suitability, night operations and managing community expectations. This collaborative planning process was effective in "setting the tone" for the fieldworks campaigns and ensured all parties understood their role and responsibilities. Additionally, clear lines of communication were established to ensure key information was communicated efficiently to all parties.

This paper has highlighted the success of engaging full-time HSE advisors for the fieldwork operations. The key benefit from this approach was that a positive safety culture was developed from day one and carried throughout the project. This allowed key risks such as personnel fatigue, cyclone readiness, jack-up moves, personnel and equipment transfers and responding to environmental incidents to be effectively managed and facilitated by experienced HSE professionals through daily pre-start meetings, weekly tool box meetings, weekly safety drills and day-to-day interaction and oversight of the fieldworks.

This paper has demonstrated there can be clear benefits in employing a full-time geotechnician during large fieldworks campaigns to sub-sample rock core for laboratory testing. Careful wrapping and packaging of sub-sampled core into separate steel containers for overland transportation to the laboratory ensured samples remained intact for strength testing. This subsequently reduced core preparation time in the laboratory resulting in faster turn-around times for strength tests.

Finally this paper has shown that completing large laboratory testing programs within a tight program can be achieved if samples are routinely transported from site to the laboratories on a weekly basis. Additionally if preliminary laboratory schedules are completed on site this can significantly reduce the time required in preparing final schedules in the office. Regular liaison is essential with each laboratory to keep them accountable and ensure agreed timelines are met. Furthermore lessons learnt from earlier phases of the overwater investigations highlighted the need for developing an innovative computer based system for automatically tracking the status of each laboratory test.

7 ACKNOWLEDGMENTS

The authors wish to thank API for allowing this paper to be published and providing the opportunity to work on what has been a most challenging, yet rewarding project.

8 REFERENCES

Blake, T. S. (1993), Late Archaean crustal extension, sedimentary basin formation, flood basalt volcanism and continental rifting: the Nullagine and Mount Jope supersequences, *Precambrian Research*, vol. 60, pp. 185–241.

Hickman, A. H. (2002), 1:100,000 Geological Series Explanatory Notes, Geology of the Roebourne 1:100,000 sheet, *Western Australia Geological Survey*, Western Australia.

International Navigations Association (2000), Site Investigation Requirements for Dredging Works, *Permanent International Association of Navigation Congresses (PIANC)*.

Technical Committee 1 – International Society for Soil Mechanics and Geotechnical Engineering (2005), Geotechnical and Geophysical Investigations for Offshore and Nearshore Developments, *Swan Consultants*.

Thorne, A. M. & Trendall, A. F. (2001), Bulletin 144 - Geology of the Fortescue Group, Pilbara Craton, *Western Australia Geological Survey*, Western Australia.

PROBLEMS IN TESTING OF CARBONATE SEDIMENTS

H. Joer[1], S. Sharma[2] and Francis Lee[3]
[1]Director, [2]Principal Engineer, [3]Lab Testing Supervisor, Advanced Geomechanics, Perth, Australia.

ABSTRACT

Carbonate sediments are formed in marine environments, in the tropical and sub-tropical climate belts around the world, such as southern Africa, India, Indonesia, Brazil and Australia. These sediments are characterised by their high crushability potential and variability in composition, grain shape, fabric and mineralogy. The design of foundations for offshore structures to be installed in these areas requires engineering parameters, which are generally determined using offshore site investigation data combined with onshore laboratory tests. The reliability and robustness of the design criteria are heavily reliant on the accuracy of the field and laboratory data. The field testing methodologies are generally well understood and can be verified using the recovered samples. However, conventional laboratory testing procedures are generally inadequate for testing carbonate sediments. The results obtained using the standard testing procedures may result in the derivation of a wide range of engineering parameters, which could result in costly design of structures and in some cases may jeopardise the development of the field.

An audit was carried out by Advanced Geomechanics (AG) as part of their QA process. The audit was undertaken in two parts. The first part consisted of testing seven material types, three non-carbonate (Silica Sand, Silica Flour and Kaolin Clay) and four carbonate materials (one terrestrial and three offshore) at four different laboratories. The identity of the tested samples was kept from the laboratories (blind tests). The tests requested included classification, permeability and consolidation. The second part of the audit was to investigate the effect of the operator on the test results, which is currently being carried out at AG's laboratory (agLAB) and will be reported in a separate paper.

1 INTRODUCTION

Foundation problems associated with carbonate sediments, particularly those experienced by offshore hydrocarbon industry, are widely reported in the literature (Jewell and Andrews, 1988; Jewell and Khorshid, 1988; Al-Shafei 1999). In most cases, these problems were associated with the use of conventional wisdom in terms of soil characterisation and derivation of design parameters, which are not directly applicable for carbonate sediments. In recent years, increasing issues related to results of tests performed on carbonate sediments were encountered during AG's large testing programmes. In some cases these issues could not be explained using the current soil mechanics frame work. This prompted AG to perform a series of tests using various laboratories, some of which were previously used by AG and other were used occasionally. The laboratory identities are kept anonymous as agreed with the various laboratories used in this investigation.

Disparities between the results obtained from the different labs may be related to high turnaround of staff in commercial laboratories, "old-habit" performance, inexperience in testing carbonate soils, non-flexibility in changing testing standards to suit unusual soil types and in order to satisfy accreditation requirements, high volume of tests with tight deadlines and the lack of reference (data base) for checking the results as part of the QA process.

The tests performed are described in the following sections along with the findings from this investigation.

2 TESTING METHODOLOGY

2.1 SELECTED SEDIMENTS

The selected samples were delivered to each laboratory and were identified using a letter from the alphabet (A, B, C…). The three non-carbonate soils are Silica Flour (B), Kaolin Clay (C) and Silica Sand (D). They are widely used in research organisations around the world and their properties are well known. The four carbonate materials selected for this study are from different areas of Western Australia. Ledge Point Sand (A) was collected off the beach, about 100 km North of Perth, Rottnest Sand (E) was dredged off the west coast of Australia, near Rottnest Island. The other two carbonate sediments (F & G) are materials collected from the North West Shelf (NWS), Western Australia. Typical micrographs of carbonate and non-carbonate (silica) sands are shown on Figure 1. In general, the carbonate sands comprised mixtures of grains of different sizes, shapes and origin (both clastic and bio-clastic origins), while silica sand comprised spherical and uniform particles.

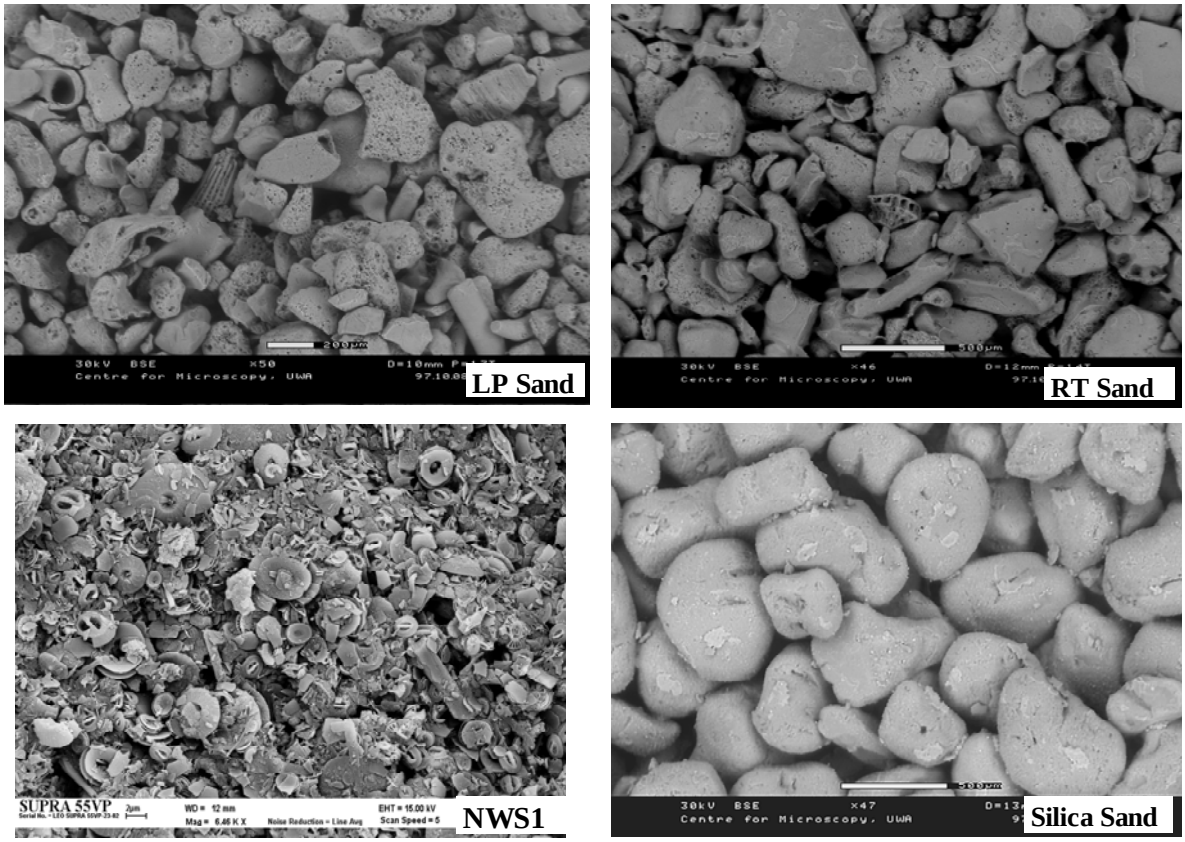

Figure 1: Typical Micrographs of Carbonate and Non-Carbonate Sands

Table 1 summarises the various sediments, sample ID used for testing and types of tests performed in this study.

Table 1: Summary of Tested Samples and Type of Tests.

Tested Samples	Sample ID used for testing	Type of Tests Performed
Ledge Point (LP)	A	Carbonate Content, (CO_3), Specific Gravity (G_s), Particle Size Distribution (PSD), Atterberg Limits (AL)
Silica Flour (SF)	B	
Kaolin Clay (KC)	C	
Silica Sand (SS)	D	
Rottnest (RT)	E	
Carbonate Sediment from NWS (NWS 1)	F	Specific Gravity (G_s), Particle Size Distribution (PSD), Oedometer and Permeability
Carbonate Sediment from NWS (NWS 2)	G	Oedometer

2.2 SELECTED TESTS AND LABORATORIES

The laboratory testing programme comprised classification tests, one-dimensional consolidation tests (oedometer) and permeability tests. The classification tests include carbonate content (CO_3), specific gravity (G_s) particle size distributions (PSD) and Atterberg limits (AL) measurements. The tests were performed at Advanced Geomechanics laboratories (agLab) and six other laboratories (referred as Lab 1 to Lab 6 in this paper). Table 2 summarised the types of tests performed at different laboratories.

Table 2: Summary of Testing Programme and Laboratories Used

Test Type	agLAB	Lab 1	Lab 2	Lab 3	Lab 4	Lab 5	Lab 6
Carbonate Content (CO_3)	✓	✓	✓	✓	✓		
Specific Gravity (G_s)	✓	✓	✓	✓	✓		
Particle Size Distribution (PSD)	✓	✓	✓	✓	✓		
Atterberg Limits (AL)	✓	✓	✓	✓	✓		
Oedometer Tests	✓	✓				✓	✓
Permeability Tests	✓	✓				✓	

3 TEST RESULTS AND DISCUSSION

3.1 CLASSIFICATION TEST RESULTS

3.1.1 Carbonate Content

The acid dilution method (standard WA915.1 – developed by Main Roads) was used by all laboratories to determine the carbonate content (CO_3) of the various materials. The test results are summarised in Table 3 and are generally as expected, i.e. high CO_3 for LP and RT Sands and low CO_3 for the SF, KC and SS. It should be noted that for the non-carbonate materials (SF, KC and SS), 0% CO_3 is expected. However, as can be noted from Table 3, except for SS tested at Lab 1, Lab 2 and Lab 3, where 0% CO_3 was obtained, variations in CO_3 ranging from 1 % to 4% were obtained for the other non-carbonate materials. Although these values are in absolute term very low, they are about 10 to 40 times the measurement uncertainty (0.1%).

For LP and RT Sands, the difference between the maximum and minimum values of CO_3 is 1.9% for LP Sand and 3.3% for RT Sand. These values correspond to 9.5 and 16.5 times the measurement uncertainty.

Table 3: Summary of Carbonate Content Test Results

Carbonate Content (%)					
Lab Used	**LP**	**SF**	**KC**	**SS**	**RT**
Lab 1	86.8	1.2	1.6	0.1	95.0
Lab 2	86.9	1.5	1.2	0.0	95.4
Lab 3	88.7	1.3	1.9	No Reaction	96.2
Lab 4	88.4	1.1	2.3	4.0	92.9

3.1.2 Specific Gravity

Specific gravity (G_s) was measured using the method described in the Australian Standard (AS 1289.3.5.1). The results obtained from different laboratories are summarised in Table 4.

The results obtained are generally consistent between the different laboratories, except for Lab 3 (all samples) and one sample (SS) for Lab 4, for which the reported G_s values were significantly different compared to other laboratories. It should be noted that according to AS 1289.3.5.1, repeated tests which differ by more than 0.03 g/cm^3 should be discarded. If the tests performed at the different laboratories on the same material are to be considered as repeated tests, then all the tests performed at Lab 3 and the test carried out at Lab 4 on the SS are to be discarded.

Table 4: Summary of Specific Gravity Test Results

Lab Used	Specific Gravity (g/cm^3)				
	LP	**SF**	**KC**	**SS**	**RT**
Lab 1	2.73	2.66	2.63	2.66	2.72
Lab 2	2.73	2.65	2.61	2.65	2.73
Lab 3	2.67	2.59	2.54	2.60	2.66
Lab 4	2.7	2.65	2.63	2.69	2.76
agLAB	-	-	-	2.66	-

3.1.3 Atterberg Limits

Atterberg Limit tests comprise measurement of the liquid limit (w_L) and plastic limit (w_P) of the soil. The liquid limit tests were carried out using the static cone penetrometer method (AS 1289 3.9), while the plastic limit tests were carried out by mixing the soil with water and rolling it until the soil showed signs of crumbling when the diameter is 3 mm (AS 1989 3.2.1). The comparison of the results obtained from different laboratories are summarised in Table 5.

Table 5: Summary of Atterberg Limit Test Results

Lab Used	Ledge Point Sand			Silica Flour			Kaolin Clay			Silica Sand			Rottnest Sand		
	w_L	w_P	I_P	w_L	w_P	I_P	w_L	w_P	I_P	w_L	w_P	I_P	w_L	w_P	I_P
Lab 1	39	NP	NP	N/O	NP	NP	58	28	30	N/O	NP	NP	37	NP	NP
Lab 2	39	N/O	NP	35	29	6	58	29	29	25	N/O	NP	37	N/O	NP
Lab 3	-	-	-	38	30	8	60	29	31	-	-	-	-	-	-
Lab 4	N/A	NP	NP	N/A	NP	NP	55	27	28	N/A	NP	NP	N/A	NP	NP

Notes: NP = Non-plastic, N/O = Not obtainable and N/A = Not Applicable

Atterberg limit testing is suitable for fine grained materials. The laboratory technician should be able to identify whether or not the selected sample is testable. However, on many occasions sand specimens were tested regardless of their suitability. This was also the case in this investigation, where the decision whether or not to perform the Atterberg Limit tests was left to the selected laboratories.

As can be noted from the results in Table 5, Lab 3 did not carry out the tests for all 3 Sands (LP, SS and RT), while Lab 1, Lab 2 and Lab 4 did perform the tests. In addition, it can be noted that Lab 1 reported w_L values for LP and RT sands and that w_L could not be obtained for SS, Lab 2 provided values of w_L for all 3 sands and no values for w_L or w_P were provided by Lab 4.

For the SF, Lab 1 and Lab 4 reported that this sample was non Plastic, while Lab 2 and Lab 3 reported values of w_L and w_P relatively similar and corresponding to plasticity index(I_P) of 6 (Lab 2) and 8 (Lab 3).

The results from all 4 laboratories for KC material were generally consistent with I_P ranging from 28 to 31.

3.1.4 Particle size distribution (PSD)

Particle size distribution (PSD) was determined using sieve analysis (for particles coarser than 75 μm) and hydrometer analysis (for particles finer than 75 μm) as per Australian standard (AS 1289 3.6.2). Figure 2 shows the PSD plot for all 3 Sands (LP, SS and RT), while the results obtained from Silica Flour (SF) and Kaolin Clay (KC) are presented on Figure 3. The results obtained from all the laboratories including agLAB are presented on these figures.

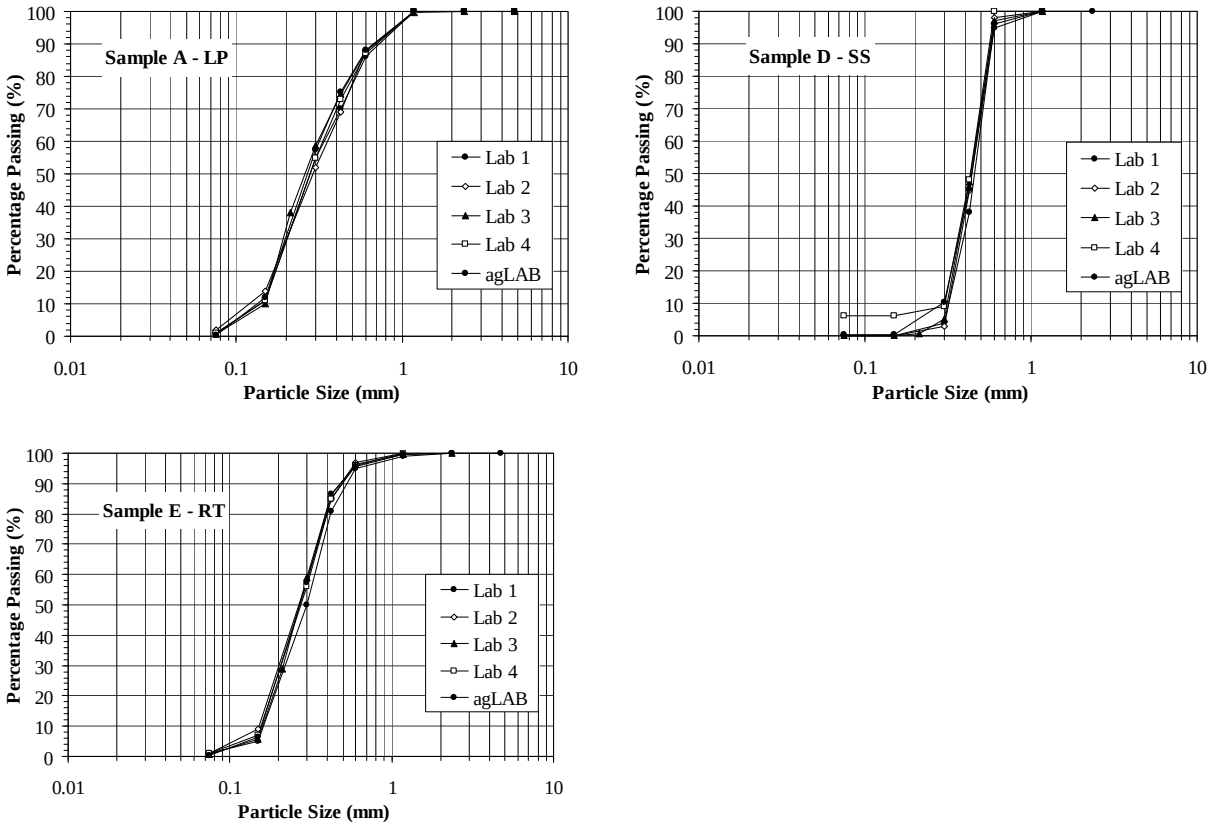

Figure 2: PSD Results – Sands (LP, SS & RT)

Figure 2 shows that the PSD results for the three sands obtained from different laboratories were generally consistent with each other and lie within a very narrow range, except for SS for which the PSD curve at particle size less than about 0.3 mm obtained by Lab 4 was slightly different compared to other laboratories. However, significant variation in the PSD curves were obtained for the fine grained materials (SF and KC) presented on Figure 3. These results clearly indicated that PSD curves obtained using sieve analysis are generally consistent between different laboratories and generally lie within the acceptable error limits. However, the PSD results obtained using hydrometer analysis are significantly different and the range of the PSD data obtained from different laboratories were well outside the expected measurement error generally associated with the resolution of the hydrometer reading (minimum of 1 division which may lead to an error up to about 2% in the values of percentage passing). The difference in the hydrometer analysis results obtained from different laboratories may be due to inadequate deflocculation of the particles during sample preparation using dispersing agent.

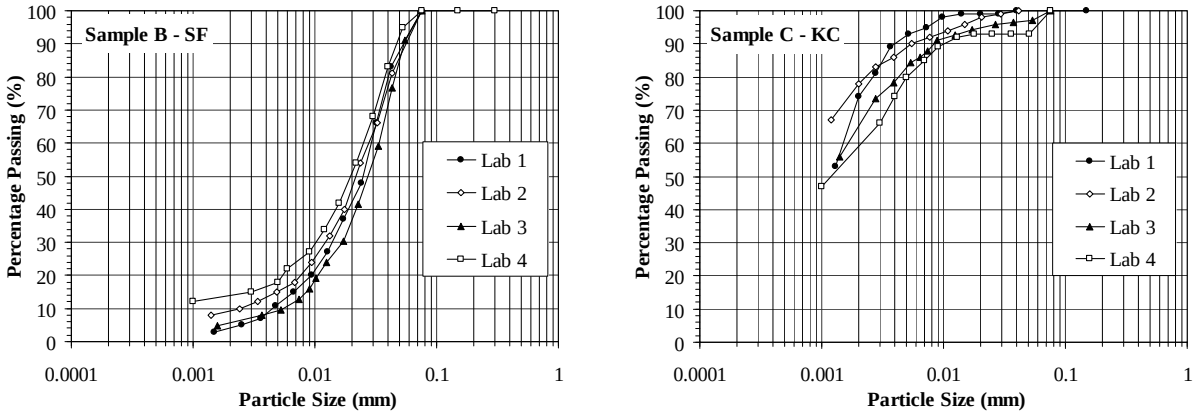

Figure 3: PSD Results – Silica Flour (SF) and Kaolin Clay (KC)

In order to investigate the effect of sample preparation on PSD curves, additional PSD tests were performed on carbonate sediment from NWS (NWS 1) at agLAB and Lab 1. Figure 4 shows the comparison of the PSD curves for three different samples from different depths (F1, F2 and F3) and from two boreholes (B1 and B2). The materials from these boreholes were expected to be similar, based on the field test results and other laboratory tests performed on these materials.

The results clearly indicated that the PSD curves obtained using the sieve analyses (for particles coarser than 75 μm) are generally consistent with each other. However, significant differences can be observed between the hydrometer analysis results obtained from agLAB and Lab 1. For the test performed at agLAB sudden change in PSD cure was observed for particle size ranging between about 10 μm and 5 μm, while similar change (albeit at a lesser degree) was observed for the tests performed at Lab 1 for particle size less than about 2 μm.

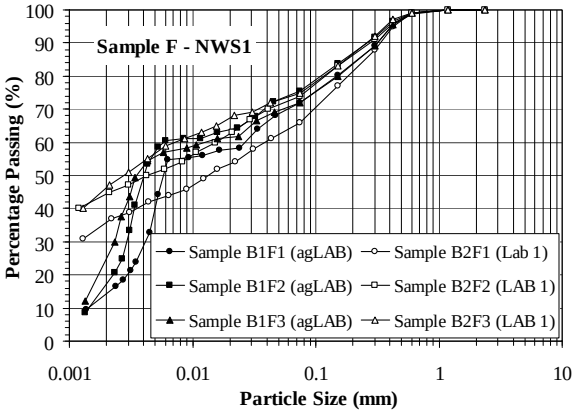

Figure 4: Comparison of the PSD results for North West Shelf Carbonate Sediments (NWS1)

The difference in the results between agLAB and Lab 1 is likely to be due to the difference in sample preparation method used for PSD analysis. For the tests performed at agLAB, the samples were tested using the 'wet method', i.e. the sample was soaked with dispersing agent to separate any lumps of materials and the analysis was performed on the wet samples. For the tests undertaken at Lab 1, the samples were prepared using the 'dry method', i.e. the samples were air-dried prior to sieving and any lumps of materials were broken using mortar and pestle. Although this is a standard sample preparation method widely used in the industry, this method generally leads to breakage of particles especially for the highly fragile carbonate sediments such as those found at the North West Shelf. Figure 5 shows the plot of PSD results obtained on the same sample, sieved 3 times, including twice after crushing the material using the mortar and pestle. The results clearly show the impact of the standard method on carbonate sediments, which lead to increase in fines due to particle crushing.

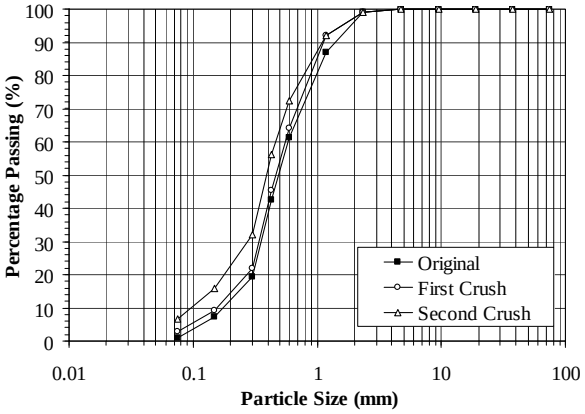

Figure 5: Comparison of the PSD results for Original and Crushed Samples

3.2 OEDOMETER TEST RESULTS

The oedometer tests were performed following the procedure described in the Australian Standard (AS 1289 6.6.1). The tests were performed on two samples from North West Shelf (NWS1) and were carried out at Lab 1 and Lab 5.

The results from these tests are presented on Figure 6a in terms of void ratio versus effective vertical stress, while a typical example for the determination of coefficient of consolidation using square root time method is presented on Figure 6b for σ'_v = 40 kPa. The results clearly show that the initial response (e.g. initial void ratio and consolidation response) of the samples tested at the two laboratories is generally similar at small stress level. However, significant difference on the consolidation curve can be noted with increasing stress level with the tests performed at Lab 5 consistently showing larger compression compared to the similar sample tested at Lab 1. In addition, it can be noted from Figure 6b that the rate of consolidation and the total duration of consolidation at each stress increment is different for the tests performed at different laboratories, which may have significant effect on the derived consolidation parameters such as coefficient of consolidation c_v.

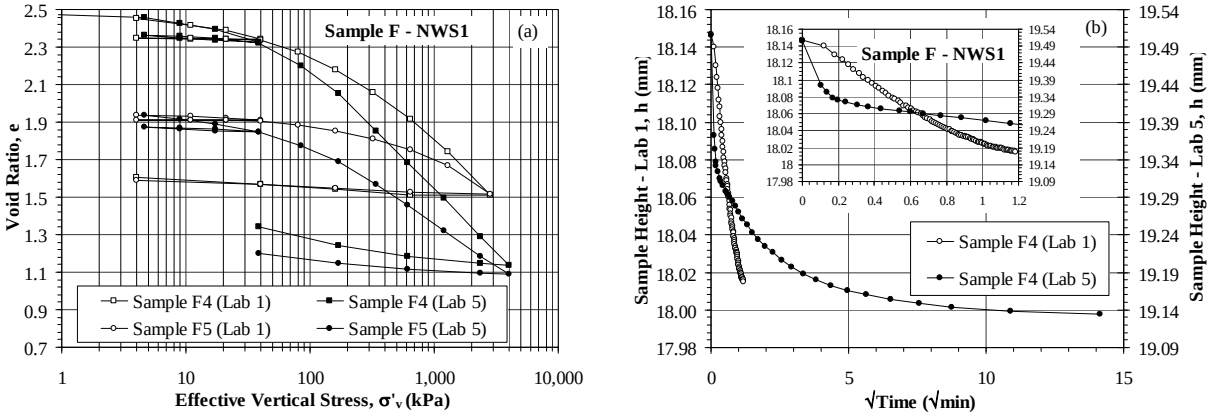

Figure 6: Oedometer Test Result for North West Shelf Carbonate Sediments (NWS1): (a) Void ratio – Effective Vertical Stress and (b) Typical Example for Determination of Coefficient of Consolidation using Square Root Time Method.

In order to further investigate the difference in the consolidation response obtained from different laboratories, additional consolidation tests were performed. The additional tests were performed on carbonate sediment from North West Shelf (referred to as NWS2 in this paper) and were carried out by four different laboratories including agLAB. The key consolidation parameters such as compression and swelling indices (c_c, c_s), coefficient of consolidation c_v, coefficient of compressibility (m_v) obtained from these tests are summarised in Table 6 and presented on Figure 7.

Table 6: Summary of Odeometer Test Results – NWS2

Lab Used	e_i	c_c	c_s	m_v (m^2/kN) (1)	$c_{v-measured}$ (m^2/year)(1)	$c_{v-calculated}$ (m^2/year) (2)	Settlement calculated using Elastic Formula (mm) (3)
agLAB	1.37	0.24	0.006	4.62E-04	586	9,046	4.1
Lab 1	1.32	0.27	0.009	2.66E-04	719	15,735	6.0
Lab 5	1.33	0.42	0.028	6.60E-04	383	6,332	18.8
Lab 6	1.37	0.41	0.014	7.14E-05	237	58,550	9.5

(1): m_v and c_v calculated using oedometer test results at σ'_v = 20 kPa (close to in situ stress level of the sample).
(2): c_v calculated using permeability value k of 1.3E -06 measured in the triaxial cell and in situ m_v measured using the oedometer test.
(3): Example elastic settlement calculated using compression parameters for a typical foundation of 10 m ×10 m subjected to 1,000 kN and uniform sediment profile.

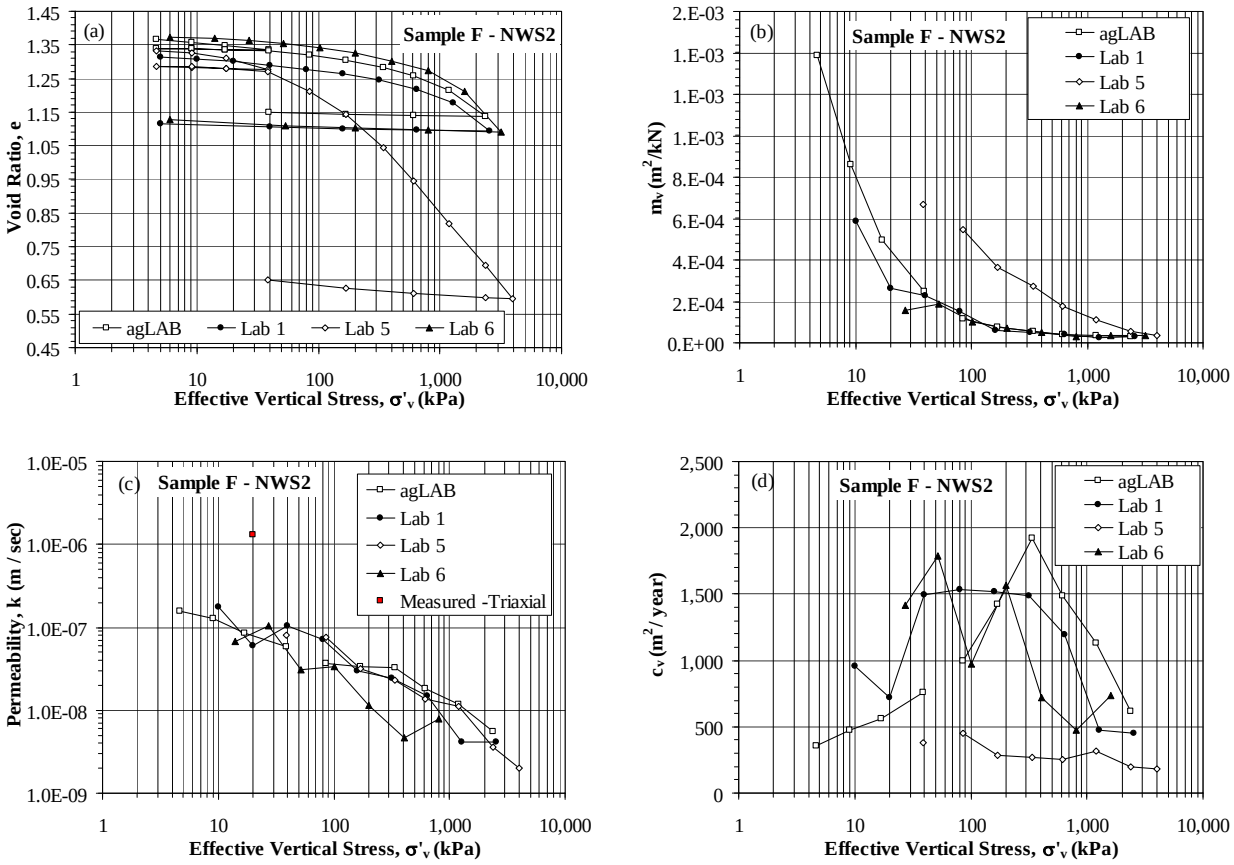

Figure 7: Oedometer Test Result for North West Shelf Carbonate Sediments (NWS2): (a) Void Ratio – Effective Vertical Stress, (b) Coefficient of Compressibility - Vertical Stress,(c) Permeability - Vertical Stress and (d) Coefficient of Consolidation - Vertical Stress.

The results clearly show that the initial void ratio of all the tested samples generally lie within a narrow range, between about 1.32 and 1.37. In addition, it can be noted from Figure 7a that the consolidation response obtained from different laboratories are generally similar and lie within acceptable range, except for the test performed at Lab 5, which shows very large compression compared to the results obtained from all other laboratories. As expected, the consolidation parameters such as m_v, k and c_v derived using the results from agLAB, Lab 1 and Lab 6 are generally similar and lie within a narrow range, while the results obtained from Lab 5 are significantly different compared to the results obtained from other laboratories as shown on Figures 7b to 7d.

3.3 PERMEABILITY TEST RESULTS

The permeability tests were performed using the triaxial setup while maintaining percolation under constant head conditions following the procedure described in the Australian Standard (AS 1289 6.7.3). The tests were carried out at Lab 1 and Lab 5 on two samples from NWS1. The results from these tests are summarised in Table 7.

The results clearly indicate that the permeability values measured at two different laboratories are different, with the permeability (k) values measured at Lab 1 about 143 and 2 times higher than the k value measured at Lab 5 for Sample 1 and Sample 2, respectively.

Table 7: Summary of Permeability Test Results – NWS1

Lab Used	Sample	p′ (kPa)	k (m/s)
Lab 1	Sample 1	7.5	7.9×10^{-7}
	Sample 2	22.5	8.6×10^{-9}
Lab 5	Sample 1	7.5	5.5×10^{-9}
	Sample 2	22.5	4.2×10^{-9}

It should be noted that triaxial permeability test was also performed on a sample from NWS2 at agLAB. The test was carried out at in situ stress level and the measured permeability value is also shown on Figure 7c. The results clearly indicate that the values of k interpreted from the oedometer tests were generally found to be lower by more than one order of magnitude compared to the measured value of k. This is consistent with our experience as the oedometer tests generally tend to provide consistent results for fine grained materials, while it tends to underestimate the permeability for coarse grained materials.

4 SUMMARY, CONCLUSIONS AND RECOMMENDATIONS

Foundation problems associated with carbonate sediments, particularly those experienced by offshore hydrocarbon industry, are widely reported in the literature. In most cases, the problems are associated with the use of conventional wisdom in terms of soil characterisation and derivation of design parameters, which are not directly applicable for carbonate sediments. In order to investigate the issues related to soil characterisation, a series of laboratory classification, consolidation and permeability tests was carried out at various laboratories on standard non-carbonate (e.g. Silica flour, Silica sand and Kaolin clay) and carbonate materials (e.g. Ledge Point and Rottnest sand) which are widely reported in the literature. Similar tests were also performed on carbonate sediments from North West Shelf (referred to as NWS1 and NWS2 in this paper).

The results from this study can be summarized as follows:

1. All the tests were performed following the Australian Standard, except for the CO_3 content test for which testing procedure is not available in the Australian Standard. The CO_3 content tests were carried out following acid dilution method developed by Main Roads.
2. The CO_3 content results obtained from different laboratories were generally consistent. However, CO_3 content up to about 4% were also reported for the other non-carbonate materials. Although these values are in absolute term very low and may not affect the soil characterisation, they are about 10 to 40 times the measurement uncertainty (0.1%)
3. The G_s values obtained from different laboratories were generally consistent except for Lab 3 (all samples) and one sample (SS) for Lab 4 for which the reported G_s values were significantly different compared to other laboratories.
4. The Atterberg limit test results obtained from different laboratories were generally consistent. However, in some cases these tests were also performed on sand samples, which indicate lack of experience of laboratory technicians to correctly identify the suitable sample for testing.
5. The PSD test results obtained from different laboratories are generally consistent for coarse grained materials (sieve analysis). However, significant variation in the PSD curves were obtained for the fine grained materials (hydrometer analysis), which is believed to be due to the difference in sample preparation method used for PSD analysis and inadequate deflocculation of the particles during sample preparation using dispersing agent.
6. The consolidation response and associated soil parameters derived using the results obtained from different laboratories are generally similar and lie within acceptable error range, except for the tests performed at Lab 5 for which significantly different results were obtained.
7. The permeability test results obtained from two different laboratories were different, with the permeability values measured at Lab 1 about 143 and 2 times higher than the k value measured at Lab 5 for Sample 1 and Sample 2, respectively.

The summary of the results and discussion presented above clearly indicate that some difference in results may be expected between different laboratories, which may leads to significant difference in the design parameters and therefore some variation in the final design outcome. For example the elastic settlement calculated using compression parameters presented in Table 6 for a typical foundation of 10 m ×10 m subjected to 1,000 kN and uniform soil profile

was found to vary between about 4.1 mm and 18.8 mm, which clearly indicates the implication of these results on the foundation design.

In addition, it should be noted that the differences in the results were found to be more evident for fine grained carbonate sediments such as those found on the North West Shelf. The problems may be associated with the lack of experience in testing carbonate soils, non-flexibility in changing testing standards to suit unusual soil types, high volume of tests with tight deadlines and the deficiency in QA process due to lack of references. The problems may also be related to high turnaround of staff in commercial laboratories, which is a separate topic for research. The effect of the operator on the test results is currently being investigated and will be reported in a separate paper.

5 REFERENCES

Al-Shafei, K. A. (editor). *Proceedings 2nd International Conference on Engineering for Calcareous Sediments*, Balkema, Rotterdam, The Netherlands, 1999

AS 1289 3.2.1. *Soil Classification Tests – Determination of the Plastic Limit of a Soil – Standard Method*, 1991

AS 1289 3.5.1. *Soil Classification Tests – Determination of Soil Particle Density of a Soil – Standard Method*, 1995.

AS 1289 3.6.2. *Soil Classification Tests – Determination of the Particle Size Distribution of a Soil – Analysis by Sieving in Combination with Hydrometer Analysis (Subsidiary Method*), 1995.

AS 1289 3.9. *Soil Classification Tests – Determination of the Cone Liquid Limit of a Soil*, 1991.

AS 1289 6.6.1. *Soil Strength and Consolidation Tests – Determination of the One-Dimensional Consolidation Properties of a Soil - Standard Method*, 1998.

AS 1289 6.7.3. *Soil Strength and Consolidation Tests – Determination of Permeability of a Soil – Constant Head Method using a Flexible Wall Permeameter*, 1999

Jewell, R. J., and Andrews, D. C. (editors), *Proceedings 1st International Conference on Engineering for Calcareous* Sediments, Vol. 1, Balkema, Rotterdam, The Netherlands, 1988

Jewell, R. J., and Khorshid, M. S. (editors), *Proceedings 1st International Conference on Engineering for Calcareous Sediments*, Vol. 2, Balkema, Rotterdam, The Netherlands, 1988.

WA 915.1. *Calcium Carbonate Content*, Main Roads Western Australia.

GEOTECHNICS OFFSHORE AUSTRALIA – BEYOND TRADITIONAL SOIL MECHANICS

D.J. White[1], N.P. Boylan[2]and N.H. Levy[3]
[1]*Shell EMI Chair of Offshore Engineering, Univ. of W. Australia (also, Principal Consultant, Advanced Geomechanics)*
[2]*Principal Engineer, Advanced Geomechanics (formerly Assistant Professor, Univ. of W. Australia)*
[3]*Principal Engineer, Advanced Geomechanics (formerly PhD student, Univ. of W. Australia)*

ABSTRACT

This paper provides an overview of current research into, and practice of, offshore geotechnics in Australia. Offshore geotechnics is a specialism within geotechnical engineering, and offshore geotechnics in Australia involves a further level of specialism, associated with the carbonate soil conditions found across our oil and gas development regions.

The geotechnical challenges faced by Australia's offshore developments are continually evolving as exploration moves from shallow to deep water and the types of offshore facilities evolve. Previous projects in shallow water have led to the development of new piled foundation design methods and construction technologies, and have generated new solutions suited to local soil conditions, such as shallow cemented layers. Current research is now mainly focused on deep water sediments, anchoring and shallow foundations (rather than piled foundations), long pipeline networks and the geohazards faced beyond the continental shelf. Examples of research and novel design practice show that much of this technology lies beyond traditional 'text book soil mechanics'. Defining characteristics of the deepwater frontiers include large deformations and transforming soil properties.

These challenges open up refreshing new avenues of research, and provide exciting challenges to the designer. Driven by these local needs, Australia is recognised globally as a leader in offshore geotechnics, and many of the technologies presented in this paper have become Australian exports into global practice.

1 INTRODUCTION

1.1 EVOLUTION OF AUSTRALIAN OFFSHORE GEOTECHNICS

This Special Issue provides an opportunity to reflect on research into, and practice of, offshore geotechnics in Australia. This paper describes recent observations, new analysis techniques and emerging engineering technologies, associated with previous and current challenges in offshore geotechnics. Many of these advances have been in support of oil and gas developments in Australian waters, and some have found application in other regions. The research and practice of offshore geotechnics in Australia is at the forefront of global practice and Australia punches far above its weight in terms of innovation and global influence.

The origin of this advantage can be traced to the foundation problems encountered during installation of the North Rankin A and Goodwyn platforms on the North West Shelf (Senders *et al.* 2013). At this time, a recognition of the unusual characteristics of the carbonate sediments offshore Australia led to an investment by government and local industry to support the growth of Perth-based expertise in the engineering of carbonate sediments and offshore geotechnics in general. This led to the formation of the Centre for Offshore Foundation Systems at the University of Western Australia (UWA) in 1997, with federal support as an Australian Research Council Special Research Centre. Meanwhile, the consulting firm Advanced Geomechanics was formed in 1994, principally employing graduates from UWA, and is now heavily involved in virtually all of Australia's offshore oil and gas developments.

In 2013, 30 years after the North Rankin A platform was installed, Australian offshore geotechnics is in rude health, and is generating solutions that are exported worldwide. UWA publishes more papers in the top geotechnical engineering journals than any other university worldwide, and these innovations across pile design, foundation engineering, anchoring and site investigation technology are finding adoption both in Australia and other offshore oil and gas development regions. Meanwhile, the offshore-onshore divide is crossed by partnerships such as the Australian Research Council Centre of Excellence in Geotechnical Science and Engineering[1] and the National Geotechnical Centrifuge Facility[1]. These networks are generating cross-pollination across the Nullabor between offshore geotechnical technology and the onshore sector in areas where this technology transfer can lead to improvements in practice.

[1] The ARC CGSE is a partnership between the Universities of Newcastle, Western Australia (UWA) and Woolongong. The NGCF is hosted at UWA in partnership with the Universities of Newcastle, Woolongong, Queensland, Monash and Adelaide.

1.2 GEOTECHNICAL CHALLENGES AT AUSTRALIAN OFFSHORE DEVELOPMENT FRONTIERS

The depletion of oil and gas reserves in shallow water and the development of technology to access reserves in deep water has resulted in offshore developments moving beyond the immediate continental shelf into deeper waters and new environments. This transition to deeper water has already occurred in other regions, and Australia is following suit. Deep water developments often consist of moored floating facilities that are tethered to the seabed via an anchoring system. Hydrocarbons are transported to and from the seabed through vertical or catenary risers connected to a flowline or pipeline system. The complex subsea infrastructure comprises an integrated network of wells, manifolds and pipelines, all of which are supported by foundations. Alternatively, there may be no facility at the sea surface, and the infrastructure may be entirely subsea. Pumping and separation may be performed by equipment located at the seabed, where the disadvantage of limited access is offset by the advantage of being sheltered from the surface waves and the associated environmental loading.

From a geotechnical perspective, the transition to deeper water increases the prevalence of certain design challenges (Figure 1):

- Characterisation of very soft sediments in depths where conventional drilling is inefficient
- Geohazardous terrain with mobile sediment, slides, shallow gas, gas hydrates and deepwater coral
- Anchoring systems for permanent moorings subjected to sustained vertical or inclined loading
- Pipeline networks that must accommodate cyclic thermal expansion – through controlled mobility
- Subsea foundations that must accommodate multi-dimensional cyclic operating loads, and satisfy demanding displacement tolerances due to the connected equipment and infrastructure such as spools and jumpers
- Export pipelines to shore, which must cross steep and unstable terrain at the shelf break and traverse mobile sediments in shallow water – protected, if required, by trenching, burial or anchoring.

In Australian waters, these engineering challenges can be exacerbated by the challenging constitutive behaviour of carbonate sediments. The brittle, liquefiable and sensitive nature of some carbonate soils – which leads to significant changes in operative strength – makes design more onerous. Also, the Australian region faces demanding environmental loadings – from seismic activity, wind, waves and currents.

Finally, the remoteness of the Australian region adds further challenges associated with vessel availability and high costs. There is a strong driver to minimise the size of subsea foundations and anchors to avoid the need to mobilise heavy lift vessels from other regions. Site investigation opportunities are also affected by the availability of specialist drillships.

Traditional soil mechanics is focused on ensuring the stability and serviceability of stationary foundations under working loads. However, in deep water applications the geotechnical infrastructure may be designed to allow movement, or the installation process may involve gross disturbance and deformation of the seabed. Examples include controlled lateral buckling of pipelines (due to operational temperature and pressure changes), trench development of steel catenary risers (SCRs) and the installation of drag and plate anchors. Even anchor piles may be permitted to displace by a distance of a metre or more under working loads. Design in these situations involves quantifying the changing soil resistance and kinematics for structural components moving distances that are comparable to or exceed their size. Structural failure can occur from both insufficient and also excessive geotechnical capacity. Structures that are designed to move may attract or impose unwanted loads if they are founded too well, with unexpectedly high soil resistance.

Given the mobility of much offshore infrastructure, and the episodic nature of offshore cyclic loading (from storms and tides), significant changes in soil strength and stiffness of more than an order of magnitude can occur, due to disturbance, remoulding, reconsolidation and water entrainment. The recovery of soil strength through reconsolidation can be as significant as the reduction in strength when remoulding is imposed.

A common thread through offshore geotechnical design is therefore careful characterisation of the appropriate soil strength from which to determine the design resistance. The effects of cyclic loading and consolidation episodes must be quantified. In addition, it is often necessary to bound the expected behaviour, rather than simply determine a safe cautious estimate of the foundation or anchor capacity.

In this paper, a central theme is the requirement to assess the transforming properties of soil beyond initial failure, often through cycles of remoulding and reconsolidation, and sometimes through gross movements of the associated infrastructure. We first describe examples of the analysis and investigation techniques that have emerged from research in order to provide improved methods to characterise the seabed. We then describe how these characteristics are applied

to the analysis and optimisation of foundations (piled and shallow), anchors and pipelines. Finally, we describe new techniques for modelling of submarine slide geohazards.

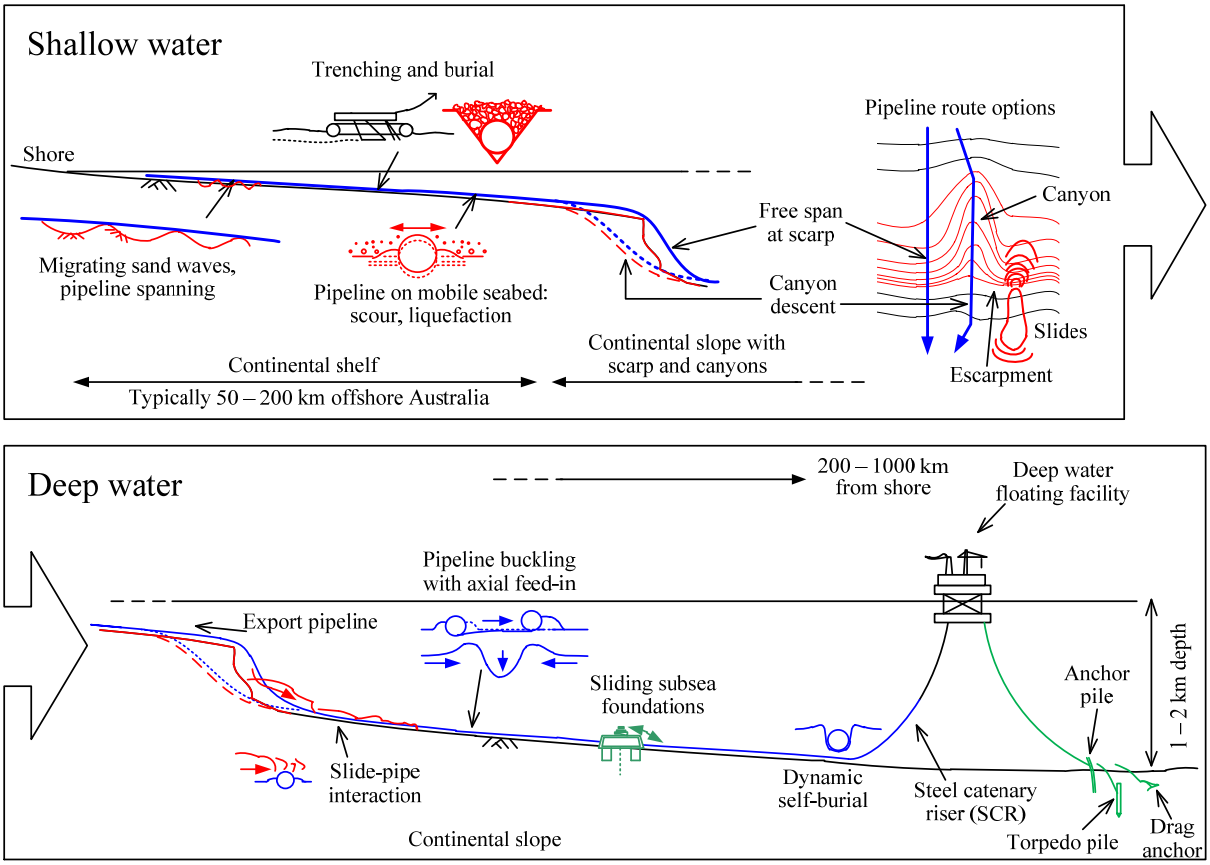

Figure 1: Geotechnical challenges at Australian offshore frontiers

2 OFFSHORE SITE INVESTIGATION TECHNOLOGY

2.1 SITE INVESTIGATION PLATFORMS

Australia has been a testing ground of several new site investigation technologies, partly because the developments have been pioneered by local organisations, and partly because of the particular requirements of local ground conditions.

In deep water conditions, a seabed-based platform is often favoured over a vessel-based drilling system in order to minimise the disturbance of the soft seabed sediments and to eliminate the laborious process of making and breaking a drillstring to the seabed. Seabed-based systems are also attractive from an HSE perspective since human involvement in the drilling is minimised. Seabed frames equipped with push sampling and *in situ* (CPT) systems have been widely used since the 1980s. In recent years, seabed-based drilling systems have increased the scope of activities that can be performed without the need for a drillstring from a vessel.

The first seabed drilling system developed for geotechnical surveys was an Australian innovation – the Portable Remotely Operated Drill (PROD), developed by Benthic Geotech Pty. Ltd., who were originally based in Sydney. Benthic Geotech had strong links to the University of Sydney during their embryonic phase, and they now operate several PROD tools throughout the world. Figure 2 shows a photograph of the second generation PROD, which has been in operation since 2010. These versatile systems are capable of drilling, sampling (storing samples onboard the device) and conducting *in situ* tests to depths approaching 150 m beneath the seabed.

For pipeline design and other applications where the characteristics of the upper one to two metres are of most interest, seabed frames equipped with miniature penetrometers and some form of sampling device have been designed, such as the SMARTSURF module (Borel *et al*., 2010). Also, the SMARTPIPE tool, which comprises a model pipe that can be

actuated in the vertical, axial and lateral directions, was developed by Fugro about 10 years ago, and has recently been deployed in Australian waters.

Figure 2: 2nd generation PROD (image: Benthic Geotech)

Figure 3: SMARTPIPE tool (image: Fugro)

2.2 NOVEL PENETROMETERS AND SAMPLING TOOLS

A new class of penetrometers, representing an evolution beyond the cone penetrometer, have been developed at UWA since 1990, and were first used in the field on surveys by the Australian Operator, Woodside. These so-called full-flow penetrometers involve an enlarged tip around which the soil flows, as compared to the cone shape which forces a form of cavity expansion mechanism. There are two principal motivations that have driven the development and application of full flow penetrometers. Firstly, the shape of these devices provides a more accurate theoretical link between the measured resistance and the mobilised soil strength. Secondly, the devices can be cycled vertically, allowing changes in strength through disturbance and remoulding to be examined.

The T-bar and ball full flow penetrometers are shown in Figure 4 and were initially developed from the miniature T-bar that was introduced at UWA for strength characterization of soft centrifuge samples (Stewart and Randolph, 1991). The T-bar consists of a cylindrical bar that is connected at right angles to the penetrometer rod. During penetration of the T-bar, the resistance generated by the flow of soil around the bar is measured continuously. The profile of penetration resistance can be converted to the shear strength of the soil using a suitable bearing capacity factor.

The T-bar was later scaled up for use in offshore site investigations and the first offshore tests were conducted by Fugro in the Timor Sea in 1996 for Woodside's Laminaria development (Randolph *et al*., 1998). The ball penetrometer was then developed to reduce the effect of the load cell being subjected to bending moments induced from non-symmetric resistances along the T-bar (Watson *et al*., 1998), and was first deployed in 2003 by Fugro for a Woodside site investigation off the coast of Mauritania (Peuchen *et al*., 2005).

Numerous studies have been carried out comparing the results of field tests with these devices to shear strength parameters determined *in situ* and in the laboratory (Boylan *et al*., 2007; Low *et al*., 2010; Lunne *et al*., 2005; Randolph, 2004; Yafrate and DeJong, 2005). These studies have shown that full flow penetrometers give a highly repeatable measure of resistance compared to the cone penetrometer while bearing capacity factors for these devices occupy a narrower range of values compared to the cone.

Sampling is always required in addition to *in situ* testing in order to provide material for a program of laboratory testing. In very soft soils, continuous samples of the seabed can be obtained to depths of 20 – 30 m beneath the mudline, with recovery rates greater than 90%, using devices such as the Jumbo Piston Corer (Young *et al*., 2000) or the STACOR sampler (Borel *et al*., 2002, 2005). In coarser materials, such as the silts and sands commonly found offshore Australia, conventional downhole sampling methods are generally required. For near surface samples, box coring has mixed success due to the difficulties in achieving penetration in harder soils, and the possible loss of fine material during recovery. In situations where sample disturbance can be tolerated, ROV-based samplers deployed by the manipulator tool have been used to achieve adequate sampling offshore Australia (and elsewhere).

3 SEDIMENT CHARACTERISATION

3.1 *IN SITU* TEST INTERPRETATION

The CPT, T-bar or ball penetrometers provide the basis for a continuous profile with depth of soil strength, but are usually ground truthed against laboratory test data at intervals. Figure 5 compares the first offshore T-bar profiles with

the corresponding CPT and laboratory test data. At this time, only a single in-out cycle was performed, and the resistance on extraction was referred to as a residual strength. More recently, it is usual to include episodes of cyclic movement during the penetration phase, with typically 10 cycles being performed, leading to a steady remoulded strength being mobilised. Figure 6 shows an example of a cyclic T-bar test conducted in carbonate site from offshore Australia. In this example, the soil resistance is ~20% of the initial resistance after being cyclically remoulded. The undrained strength gradient of more than 2 kPa/m is common – but not universal – in carbonate soils, and is higher than found in typical non-carbonate fine-grained soils. This is a reflection of the high internal angle of friction, and also the dilatancy under monotonic loading.

3.2 CARBONATE SOILS: *IN SITU* TESTING

Carbonate soils can also show particularly high sensitivity, leading to ultra-low levels of remoulded strength, as illustrated by the collated data from both carbonate and non-carbonate soils shown in Figure 7. It is also found that some recovery of strength can occur following reconsolidation. In the analysis of problems involving significant disturbance, it is necessary to identify the relevant soil strength, which may lie somewhere between the intact and remoulded values. Analysis techniques for design can capture the decaying soil strength by adopting a value that represents the relevant level of disturbance. The general approach is firstly to convert the penetrometer ductility parameter, N_{95}, to an equivalent strain level (e.g. Zhou and Randolph, 2009). The relevant strain level for the problem being considered is then used to deduce the operative undrained strength. Such techniques have been proposed for the penetration resistance of spudcan foundations (Erbrich, 2005; Hossain and Randolph, 2009). These methods utilise the type of strength degradation curves shown in Figure 7 to link the strains and operative strength around a spudcan to those around a T-bar. Similar approaches have been proposed for the laying of a pipeline, or the response in the touchdown zone of a catenary riser (Hodder *et al*., 2013, Cheuk and White, 2011).

3.3 CARBONATE SOILS: LABORATORY TESTING

Australia's carbonate soils also show unusual behaviour when tested in the laboratory to moderate strains, less than during cyclic penetrometers tests. The brief length of this paper cannot do justice to the complexity of the stress-strain response of these soils, and reference should be made to the comprehensive studies contained within Jewell and Khorshid (1988), Jewell and Andrews (1988) and more recent contributions (Al-shafei 1999, Randolph and Erbrich, 2000; Mao and Fahey, 2003)

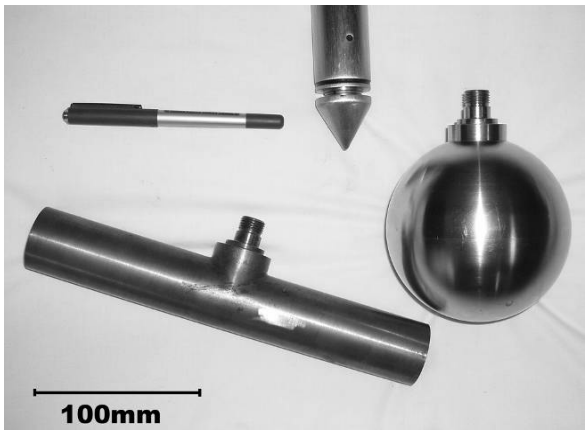

Figure 4: Cone, T-bar and ball penetrometers

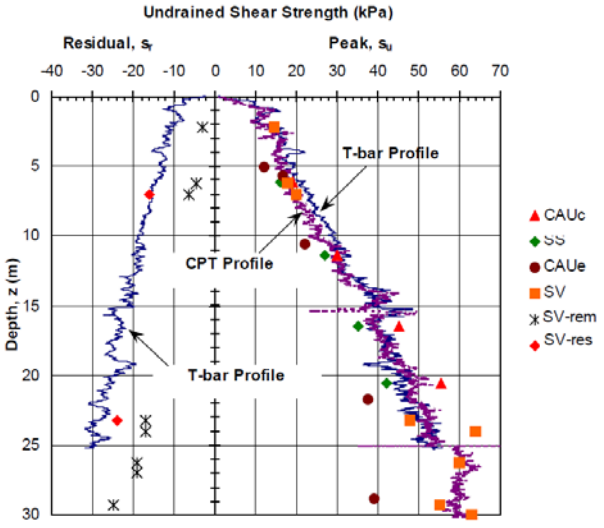

Figure 5: Offshore T-bar data (Erbrich & Hefer 2002)

The unusual stress-strain behaviour of carbonate soils arises from the angular, weak nature of the particles – whether sand-, silt- or clay-sized. The packing of these soils, and the potential for breakage, can lead to strong dilatancy under monotonic loading, accentuated by a high internal friction angle, but significant weakening under cyclic loading. In undrained conditions, this results in a potential for liquefaction but a ductile response with high strains to failure under monotonic loading. However, these trends are strongly dependent on the fabric and relative density of these soils. Examples results from simple shear tests performed at UWA illustrate these facets of behaviour (Figure 8).

Cementation is also widely present in regions that have been previously exposed at sea level lowstands. There are several paleoshorelines off Australia's North West Shelf and along each of these features there are coastal features such

as lagoons, reefs and dunes, often buried beneath only a shallow thickness of more recent sediments (Figure 9). This can lead to massive local variability in strength conditions, and requires intensive site investigations, integrating both geophysical and geotechnical data.

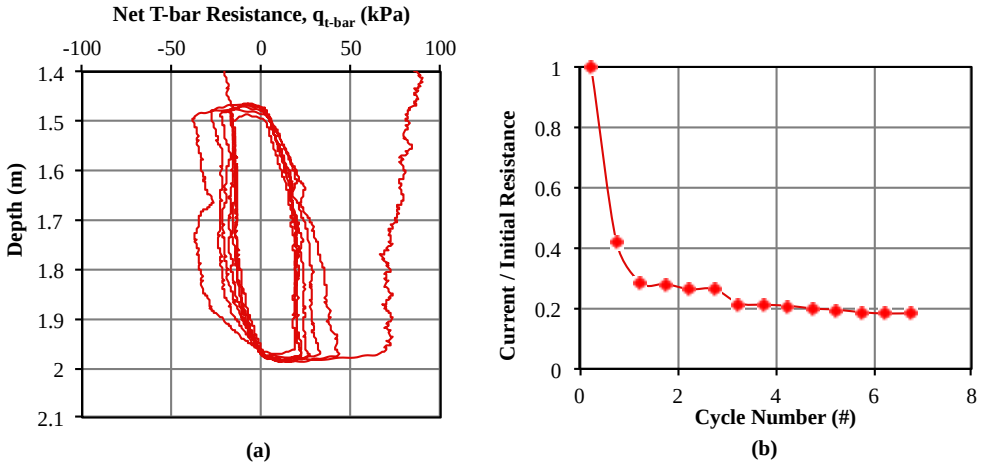

Figure 6: Cyclic T-bar penetrometer test (a) Net T-bar resistance (b) Degradation during cycling (Boylan *et al*., 2014)

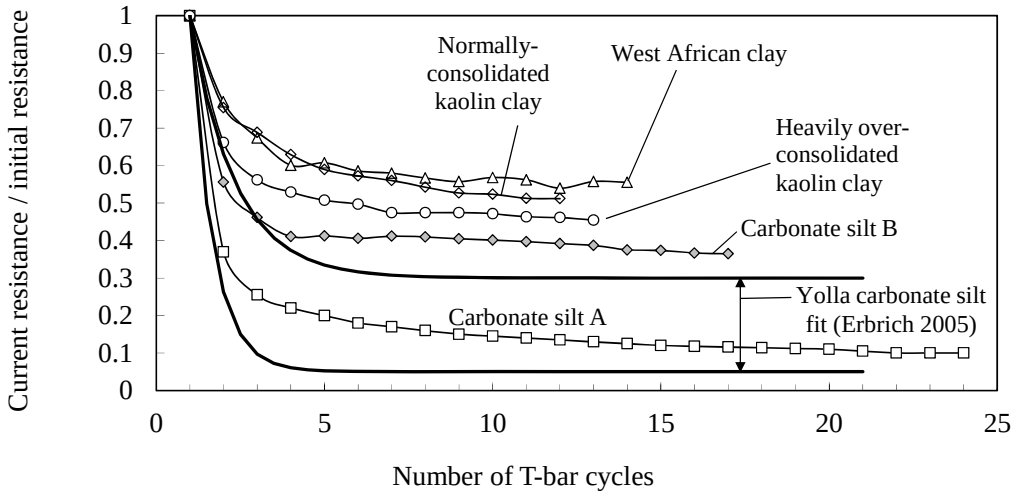

Figure 7: Changes in penetration resistance of fine-grained soils during cyclic T-bar tests (White and Cathie, 2010)

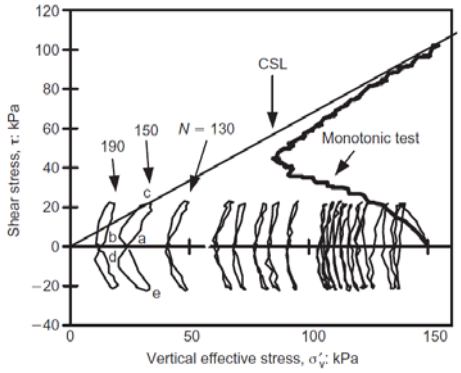

Figure 8: Simple shear tests of carbonate silt (Mao and Fahey 2003)

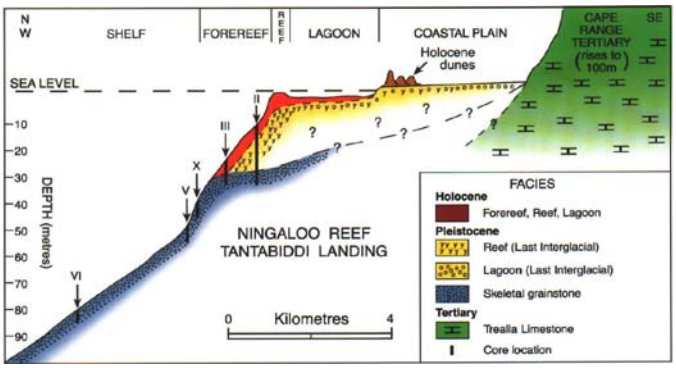

Figure 9: Ningaloo reef: typical Australian coastal geology (Collins 2002, in Hengesh *et al.* 2011)

4 PILED FOUNDATIONS

4.1 AXIAL RESPONSE IN CARBONATE SOILS

The most well-known piled foundations in carbonate soils are those beneath the North Rankin A (NRA) platform, operated by Woodside. The full story of the NRA piled foundations is set out in Jewell and Khorshid (1988), and is summarised elsewhere in the current volume (Senders *et al*., 2013). The low axial shaft capacity of driven piles in carbonate sands and silts has led to the development of new piling technologies that have been used for the subsequent platforms on the North West Shelf. These new technologies, including drilled and grouted, grouted driven and ribbed grouted piles, involve new technologies both for design and for construction.

The shaft capacity on driven piles in coarse-grained carbonate soils is very low, due to the contraction and loss of radial stress that accompanies the driving process (Randolph, 1988; White and Lehane, 2004; White, 2005). Driven piles remain used for laterally-loaded applications, in which case the potential risk from low axial resistance and unwanted free fall is significant. For axial-loaded applications, drilled and grouted piles are common, gaining capacity from a cemented layer with a primary driven pile being used to prevent hole collapse in shallower uncemented zone.

The axial t-z response of a grouted pile features dramatic softening if the displacement is sufficient to break the bond at the pile-grout-soil interface, and sophisticated cyclic t-z models have been developed to quantify this behaviour (Erbrich *et al*., 2010). Constant normal stiffness simple shear tests are used to calibrate this behaviour and an example t-z response from a program named CYCLOPS for the design of a drilled and grouted pile is shown in Figure 10. The brittleness and cyclic softening of the t-z response means that design analyses must be performed in the (pseudo-) time domain, with the wave-by-wave cyclic loading imposed explicitly. It is also necessary to impose a design storm in a suitably conservative manner. Neither of the traditional 'descending' or 'ascending' storm methods (in which the waves are ordered by increasing or decreasing size) are conservative relative to a more realistic building-then-falling random storm. Instead a form of 'ordered storm' is required, from which an example pile head response is shown in Figure 11.

4.2 LATERAL RESPONSE IN CARBONATE SOILS

For offshore piles under lateral loading, there are well-established p-y curves recommendations for design in non-carbonate sands and clays, although these have limited theoretical basis and are the subject of ongoing research (e.g. Doyle *et al*., 2004; Jeanjean, 2009; Kodikara *et al*., 2010). In carbonate soils, the p-y response is far softer, reflecting the compressibility of the soil (in drained conditions) and the high strain to failure (in undrained conditions). When it was recognised that the early Bass Strait platforms in carbonate sand required strengthening struts to be added, centrifuge and large-scale model tests were performed to determine suitable p-y curves for drained conditions (Wesselink *et al*., 1988; Wiltsie *et al*., 1988). Subsequent refinements have been reported by Novello (1999) and Dyson and Randolph (2001).

More recently, a methodology to generate p-y curves for undrained carbonate soils has been developed and applied to the design of piles in both Australian and other carbonate soils – including the Campos Basin. This approach, embodied in a program known as pCyCOS, uses the p-y curves derived from the soil stress-strain response, and incorporates the characteristic stress-strain profile of undrained carbonate soils as well as cyclic softening (Erbrich *et al*., 2010). For the design of laterally-loaded piles in cemented carbonate soils, the potential benefit of the cemented material can be safely incorporated by directly modelling breakage of shallow 'chips' (Erbrich 2004).

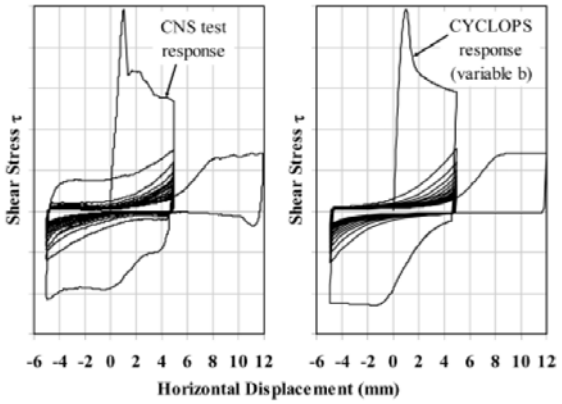

Figure 10: Axial t-z response for a drilled and grouted pile (Erbrich *et al*., 2010)

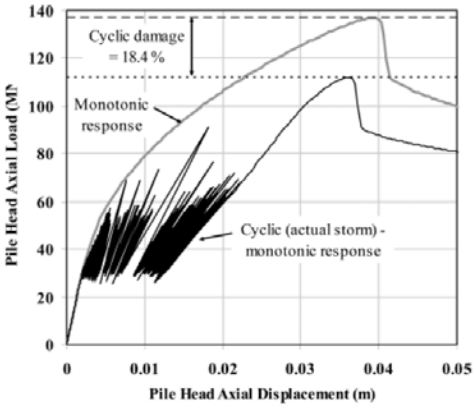

Figure 11: Pile head response due an 'ordered storm' (Erbrich *et al*., 2010)

5 SHALLOW FOUNDATIONS

5.1 SHALLOW FOUNDATIONS FOR PLATFORMS

Shallow foundations have been widely used offshore Australia as gravity bases for platforms or temporary foundations to provide support to steel jackets during piling. An early review of shallow foundation analysis on carbonate sediments is given by Randolph and Erbrich (2000).

Example applications of shallow foundations for platforms in Australian waters include the Wandoo B (Humpheson, 1998), Bayu-Undan (Neubecker and Erbrich, 2004), and the Yolla fields (Watson and Humpheson, 2007). Shallow foundations are particularly efficient in the presence of cemented layers. The example shown in Figure 12 is one of the two bridge-linked Bayu-Undan jacket structures, located in the Timor Sea, which is described by Neubecker and Erbrich (2004) and Sims *et al*. (2004). The site comprises a surficial layer of soft calcareous sandy silt over cemented calcarenite and limestone and the design was unusual in that the soft surficial materials were removed and shallow foundations rested directly on the cemented calcarenite. At each corner of the jacket, there is a shallow foundation made from steel plates, approximately 21 m × 6 m in plan dimensions. The factored foundation loads at all corners of these jackets are compressive, even during the most severe design storm. This is due to the heavy topsides and the relatively squat jacket shape. The only load case involving tension at any corner resulted from the low loads imposed during floatover deck installation. To resist these loads, a single short pile was installed at each corner of the jacket. This novel foundation design – the first shallow jacket foundation offshore Australia – led to significant cost savings through reduced installation time relative to a conventional drilled and grouted pile solution.

Figure 12: Bayu-Undan Jackets with permanent shallow foundations (Neubecker and Erbrich, 2004)

5.2 SHALLOW FOUNDATIONS FOR SUBSEA AND FLOATING INFRASTRUCTURE

Shallow foundations are also used to support large floating structures and the myriad of smaller seabed facilities involved in modern subsea developments, often on soft deep water sediments. Shallow foundations on soft sediments are typically designed to include skirts around their perimeter and, where necessary, internal skirts (Mana *et al*., 2013a). These skirts transmit foundation loads to deeper and stronger soil, and allow uplift loads to be sustained. Skirts also mitigate potential erosion of the soil around the foundation, as well as providing some compensation for seabed irregularity.

The inclusion of skirts introduces a new element to the design of a shallow foundation, that of ensuring that the skirts will penetrate to the target depth. Consequently, the design of a skirted foundation is multifaceted because the foundation weight must be sufficient for installation, whilst not jeopardising the capacity or causing excessive settlements. For light structures or those with relatively long skirts, suction assistance may be employed to fully install skirts.

Subsea shallow foundations are particularly challenging to design because the connected equipment (e.g. pipelines, spools (i.e. short connector pipes), wellheads) is often very intolerant of movements. The range of connections through which design loads are imposed is illustrated by the typical subsea pipeline end termination shown in Figure 13a. In addition to the complex geometry, the imposed loading is cyclical (varying with the pipeline and well operating conditions) and fully three-dimensional. Meanwhile, the strength of the surrounding soil may vary during the operating life due to consolidation.

5.3 THREE-DIMENSIONAL LOADING

Under three-dimensional loading, the resulting combination of bi-directional horizontal loads (H), bi-directional moments (M) as well as vertical (V) and torsional (T) loads, requires careful analysis. Bearing capacity under fully two-dimensional loading – i.e. co-planar vertical, horizontal and moment loads – is generally assessed using failure envelope concepts (e.g. Bransby and Randolph, 1998; Ukritchon *et al.* 1998; Taiebat and Carter, 2000; Gourvenec and Randolph, 2003; Gourvenec and Barnett, 2011). The use of failure envelopes to define bearing capacity under combined loading is gradually replacing the traditional methods involving inclination and eccentricity factors applied to the uniaxial vertical capacity. Failure envelopes provide a clearer presentation of the available foundation performance, and allow margins of safety and the influence of soil strength uncertainty to be more consistently quantified. In addition, the large body of recent research focused on failure envelope methods means that solutions for a range of design conditions – encompassing different shapes of foundation and profiles of soil strength – are readily available. This research, including contributions by UWA, has recently been adopted into a revised version of the global API RP2 GEO design standard (API, 2011) and the same approaches are on course for adoption in the corresponding ISO standard.

The failure envelope approaches can be extended to fully three-dimensional loading by scaling the 'deviatoric' capacities – i.e. the moments and horizontal loads – according to the levels of vertical and torsional loading. This allows the three-dimensional loading to be simplified to a two-dimensional interaction envelope of the resultant H and M loads (which may not be coplanar) that can be compared with the design loads (Feng *et al*., 2013). Figure 13b shows an H-M interaction diagram for a particular three-dimensional load case on a rectangular mudmat considered by Feng et al. (2013). The torque load component is 45% of the ultimate torsional capacity, and leads to a contraction of the resultant H-M envelope indicated by the red envelope relative to the black envelope.

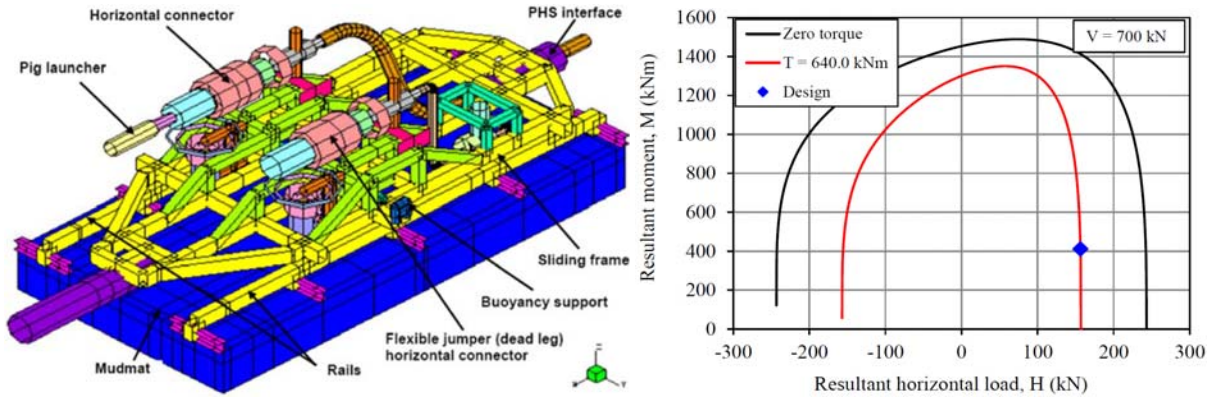

(a) Illustration of typical connections and equipment (Randolph 2012)

(b) Example failure envelope scaled to a design load case (Feng *et al*., 2013)

Figure 13: Three-dimensional loading of subsea foundations

Under fully three-dimensional loading, there are some important subtleties associated with the interacting load components. In the example of Figure 13b, the soil strength has been factored until the design load matches the envelope, to determine the design material factor. The design material factor cannot be determined from an envelope based on the unfactored soil strength and the vector through the design load to that envelope, as can be done for planar loading. This is because the mobilised level of vertical and torsional capacity affects the available normalised horizontal and moment capacity – so changes in soil strength have a double influence on the available resultant H and M (Feng *et al*., 2013).

5.4 CONSOLIDATION EFFECTS AND UPLIFT RESISTANCE

For structures founded on soft sediments under sustained compressive loads, the gain in soil strength due to consolidation of the soil over a given time is often crucial to provide improvement of the *in situ* soil strength, and even more so to counter the loss in strength experienced if cyclic loads are applied. The rate of consolidation of the soil beneath the foundation plate (i.e. including the soil confined within the skirts) can significantly influence the foundation sliding and bearing capacities (Gourvenec and Randolph 2010). Numerical analysis can be performed to calculate the increase in bearing capacity due to consolidation in the surrounding soil, although an appropriate model for the effect of the applied load on the soil strength is required. Such analyses can also be distilled into elegant simplified approaches that define the change in bearing capacity as a function of the duration and magnitude of the pre-load imposed by the foundation, and the *in situ* soil state (Bransby 2002; Gourvenec *et al*., 2013). Consolidation settlements also require careful assessment since these can induce additional loads into connected infrastructure such as spools.

The foundations of a floating structure may be subjected to uplift loading for brief or sustained periods – corresponding to a single wave, a full storm duration or a longer environmental event such as the loop current found in the Gulf of Mexico. The foundations of a tension leg platform or a top tensioned riser may be subject to uplift loading even in still water conditions. Piled foundations are often designed to resist a maintained uplift load, but shallow foundations are generally accompanied by ballast at foundation level to ensure that the still water geotechnical resistance is compressive.

If undrained conditions are assumed and the foundation top cap is sealed, the initial uplift resistance of a shallow skirted foundation is equal to the compressive resistance. However, slightly different failure mechanisms are observed experimentally in compression and uplift (Mana *et al*., 2012), and once finite movements occur then the effect of the overburden and the heave or settlement of the ground surface has a significant effect (Mana *et al*., 2013b).

However, under sustained uplift loading, consolidation and swelling of the surrounding soil leads to a reduction in the undrained strength and therefore the pullout resistance, as illustrated by the experimental results shown in Figure 14a (Gourvenec *et al.*, 2009). In addition, seepage flow into the skirts leads to progressive pullout of the foundation and a reduction in capacity due to the reduction in the embedded skirt length, as illustrated by the numerical results shown in Figure 14b (Mana *et al*., 2013c). The relative influence of swelling and seepage depends on the relative stiffness and permeability of the soil, and both mechanisms of capacity reduction must be considered in design.

If the uplift load is concurrent with a lateral component, there is the possibility of a gap forming along the side of the foundation skirts, which is a further threat to the uplift capacity. A gap can lead to a loss of suction at the foundation base, eliminating the reverse end bearing resistance. One strategy to mitigate gapping is to lay an impermeable membrane around the foundation to prevent water ingress into any gap (Keaveny *et al*., 1994; Mana *et al*., 2013d).

In some scenarios a reduction in uplift resistance can be desirable – for example when recovering a temporary foundation such as a piling support frame, or when lifting the legs of a jack-up unit. In these scenarios, strategies to minimise the uplift resistance include underbase water jets (Gaudin *et al*., 2011), perforations in the foundation (Martin and Hazell, 2005; White *et al*., 2005; Chen *et al*., 2012) or eccentric lifting.

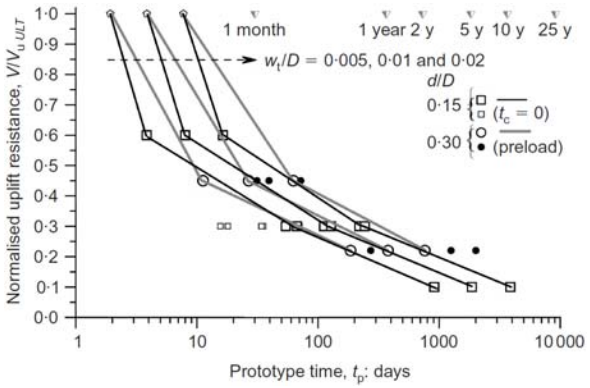

(a) Effect of uplift duration on pullout resistance (Gourvenec *et al*., 2009)

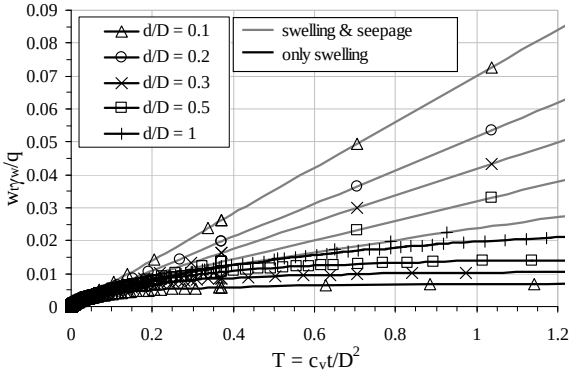

(b) Relative influence of swelling and seepage (Mana *et al*., 2013c)

Figure 14: Uplift response of skirted shallow foundations

5.5 WIDER DESIGN CONSIDERATIONS

In addition to finding the winning combination of foundation dimensions, structure weight and installation procedure to successfully install the skirts and achieve the required capacity and settlements for a structure, a wide range of other aspects require consideration in the design of an offshore shallow foundation. The interaction between these elements of design is summarised by Randolph and Gourvenec (2011), as shown in Figure 15. An additional influence on the shallow foundation design that is not included in the figure is the set of requirements from the client and installation contractor, i.e. the foundation must satisfy the given criteria for fabrication, transportation and lowering from the vessel. An understanding of logistics such as the proposed installation procedure and any size or weight limitations for the structure is essential to deliver a safe and optimised foundation design.

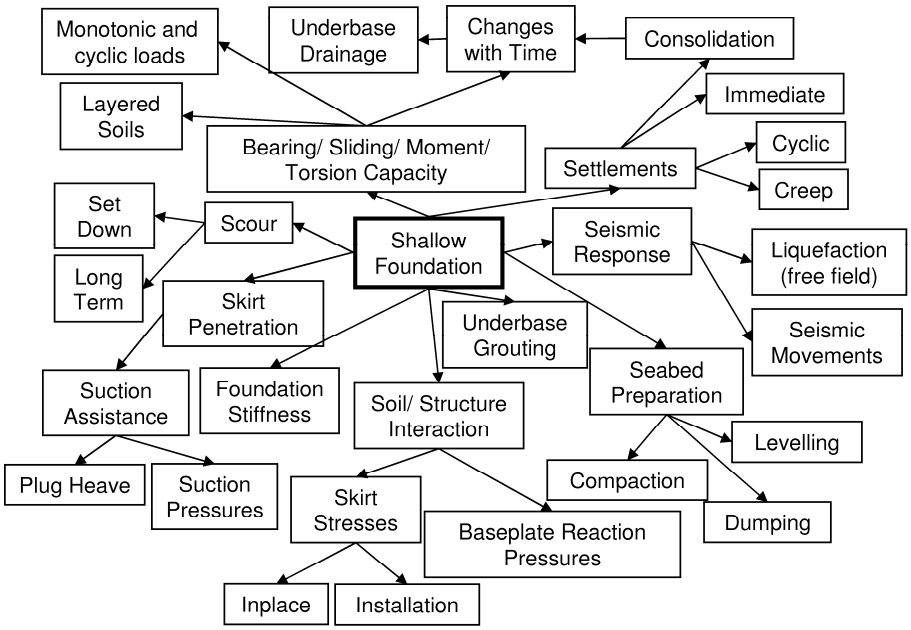

Figure 15: Considerations in the design of shallow foundations (Randolph and Gourvenec, 2011)

6 ANCHORING SYSTEMS

The early Floating Production, Storage and Offloading (FPSO) systems in Australian waters led to the development of new anchoring technology suited to the local seabed conditions, and the application of conventional anchors for the first time in carbonate soils.

The hard cemented seabed conditions found in some regions offshore Australia has led to different types of gravity anchors being deployed. The guys supporting the flare stack of the North Rankin A platform are anchored by 19 m × 18 m × 6 m deep steel boxes filled with iron ore (Figure 16a). An alternative to the gravity box is the grillage and berm anchor (Erbrich and Neubecker 1999), illustrated on Figure 16b. This requires a smaller lifting vessel and less steel fabrication compared to a gravity box, and was first used for the CALM buoy in the Stag field, offshore Australia.

As Australian developments have moved into deeper water, anchoring systems used in other regions have been adopted. The first large suction caissons installed offshore Australia were used on Woodside's Laminaria project to anchor an FPSO. In this case, the installation resistance was significantly lower than expected. The principal reason for this behaviour was the additional loss of axial resistance created by soil flow round the internal stiffeners of the caisson, as described by Erbrich and Hefer (2002).

There are currently no tension-leg or taut-leg moored structures anchored offshore Australia, although some are planned. These will be the first applications of long term uplift loading on Australian carbonate soils. Meanwhile, Shell's Prelude project – due for first production in 2017 – will bring the world's first giant FLNG vessel (488 m in length, 74 m in width) to Australia. Since the FLNG facility is larger than any FPSOs and will not be disconnectable during cyclones – unlike the majority of the FPSOs operating offshore Australia – this will represent a step out in anchoring system capacity.

These forthcoming applications have driven research into the performance of existing and novel anchoring systems for carbonate soils. Drag anchors have been widely utilised in Australian carbonate soils, but can be less efficient than assumed based on design experience in non-carbonate soils. The drag-in behaviour and subsequent operational response is affected by the sensitivity and consolidation response of the surrounding soil, and cyclic loading can lead to a degeneration of the anchor holding capacity (Neubecker *et al*., 2005; O'Neill *et al*., 2010). Careful design is required to explicitly account for these effects, rather than assuming a particular anchor efficiency based on weight in air.

Alternative shapes of drag anchor can be used to achieve a greater installed embedment, and a higher holding capacity. One example is the Delmar Omnimax anchor, which is now used in the Gulf of Mexico (Zimmerman *et al*., 2009). This anchor has recently been trialled in carbonate soils via centrifuge testing at UWA (Gaudin *et al*., 2013).

Alternatives to drag anchors that can be located in plan more accurately are the SEPLA and DEPLA anchors – Suction and Dynamically Embedded Plate Anchors, respectively. Torpedo anchors are a further alternative. None of these anchors has yet been used offshore Australia, but all have been researched extensively at UWA. The SEPLA is a plate anchor installed via a suction caisson (Wilde *et al*., 2001). The caisson pushes the plate in a vertical alignment to the target penetration, and is then retrieved. The plate is then keyed to an alignment perpendicular to the mooring line, yielding the design capacity.

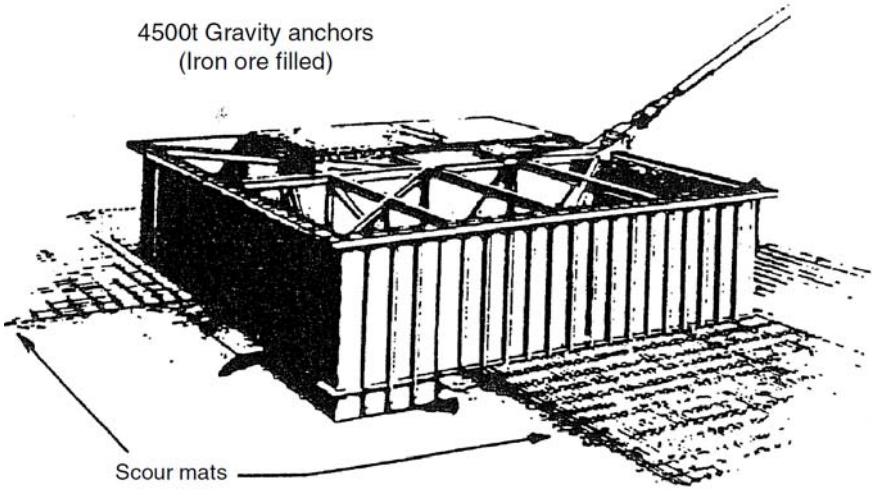

(a) Gravity box anchor (Woodside 1988)

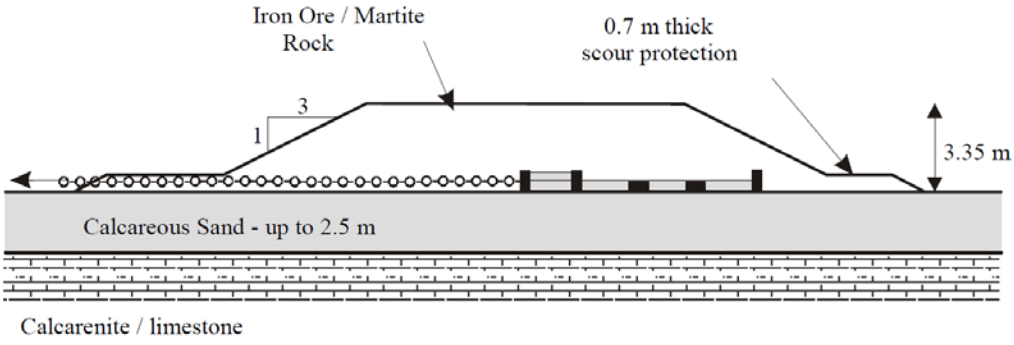

(b) Grillage and berm anchor for Stag CALM buoy (Erbrich and Neubecker 1999)

Figure 16: Novel anchors used offshore Australia

Torpedo anchors are released above the seabed and free fall to a penetration of typically 1-2 anchor lengths in soft soils. Pullout resistance, via a mooring line attached at the tail, is essentially comparable to the shaft resistance on a solid pile, augmented by the area of the fins. They are used in the Campos Basin by Petrobras (Madeiros 2001), and calculation methods for the dynamic embedment and subsequent pullout resistance, accounting for consolidation effects, are well-established (O'Loughlin *et al*., 2004). Richardson *et al.,* (2005) investigated the application of torpedo anchors in calcareous sand, and derived modified analysis methodologies for embedment and pullout.

The DEPLA is a UWA-patented technology which combines the plate anchor of a SEPLA with the dynamic installation method of a torpedo anchor (O'Loughlin *et al*., 2013). The plate anchor forms the flukes of the torpedo, and the main shaft is recovered after installation. The plate is released via a shear pin, and is then keyed via the mooring line. The DEPLA has been developed through numerical and centrifuge-scale modelling as well as and small scale field trials.

Both the SEPLA and DEPLA can achieve monotonic pullout resistances of typically 11-15 times the local undrained strength (Martin and Randolph, 2001; Gaudin *et al*., 2006; O'Loughlin *et al*., 2013). In soils with increasing strength with depth, the anchor shank and pad-eye must be designed to minimise the loss of embedment during keying (O'Loughlin *et al*., 2006; Song *et al*., 2009; Gaudin *et al*., 2010). For mooring design, cyclic and consolidation effects must be considered.

(a) Torpedo anchor (de Aguiar *et al*., 2009) (b) SEPLA (Brown *et al*., 2010) (c) DEPLA (O'Loughlin *et al*., 2013)

Figure 17: Novel anchors, researched in Australia but not yet used in this region

7 PIPELINES

The stability of seabed pipelines is affected by external loads from hydrodynamic forces and internal loads from thermal and pressure-induced expansions. In shallow water, hydrodynamic stability is the primary concern. In deeper water, and closer to the wellhead, design revolves around the control of thermal and pressure-induced expansions that cause lateral buckling and axial walking.

The gas platforms offshore Australia are connected back to onshore liquefaction plants that form LNG export terminals, as well as the domestic natural gas network. The large-diameter trunklines to shore are light and vulnerable to instability under hydrodynamic loading from cyclones or solitons. This has led to the use of various primary and secondary stabilisation solutions, including concrete weight coating, trenching, rockdumping and the use of intermittent gravity or pin pile anchors.

The first trunkline to shore – known as 1TL – was installed in 1983, linking the Burrup Peninsula to the North Rankin A platform. The majority of the pipeline was post-lay trenched by ploughing in the loose and variably cemented carbonate sands and silts. The as-built trench depth varied along the route and in some locations the pipe crown was not below the natural seabed level, although berms of ploughed soil provided additional shelter (Jas *et al*., 2012). After tropical cyclone Orson passed in April 1989, surveys showed that the v-shaped trench had disappeared. Recent analysis using the methodology outlined by Bonjean *et al*., (2008) determined that the sediment that would have naturally backfilled the trench would likely have liquefied during the cyclone. Due to the low SG of the pipeline, only partial liquefaction is needed to cause flotation, and for this reason 1TL is no longer at its original embedment, but is generally more exposed. Meanwhile, the nearby Goodwyn interfield trunkline has also experienced intermittent self-burial (Pinna *et al*., 2003).

The mobility of surficial sediment can both improve and reduce the stability of seabed pipelines. Processes of scour and liquefaction can lead to self-burial or exposure of pipelines, depending on the metocean environment, the soil characteristics and the weight and diameter of the pipeline. Carbonate soils with significant fines content typically show a higher resistance to scour and mobility compared to siliceous soils of the same grain size (Mohr *et al*., 2013). Extensive research is underway focused around the O-tube facilities at UWA, which can simulate the tripartite ocean-pipeline-seabed interaction (An *et al*., 2013). The O-tubes are recirculating water tunnels that can generate the cyclonic and tidal flow conditions that cannot be modelled in traditional wave flumes of similar dimensions (Figure 18). Figure 19 shows a sequence of images from a large O-tube test in which an irregular storm was imposed on a pipe initially at a very shallow embedment. The images show a sequence of (i) tunnel scour, (ii) propagation of the tunnel (away from the window), (iii) settlement of the model pipe and then (iv) breakout at the height of the storm.

To manage the thermal/pressure-induced expansions of a pipeline during operation, a common design solution is to incorporate engineered lateral buckles at intervals along the route, to safely and reliably accommodate the changes in pipe length. At the crown of an engineered buckle, the pipe might sweep laterally by a distance of several diameters across the seabed. A particularly challenging design condition is if engineered lateral buckles are required in a location where the hydrodynamic conditions also cause seabed mobility. Buckle reliability and tolerability can be adversely affected by a scour-induced self-burial process (Borges Rodrigues *et al.*, 2013). Westgate *et al.*, (2012) describe methods for predicting the as-laid embedment of pipelines on carbonate soils, but it is important to note that post-installation seabed mobility may alter this embedment significantly.

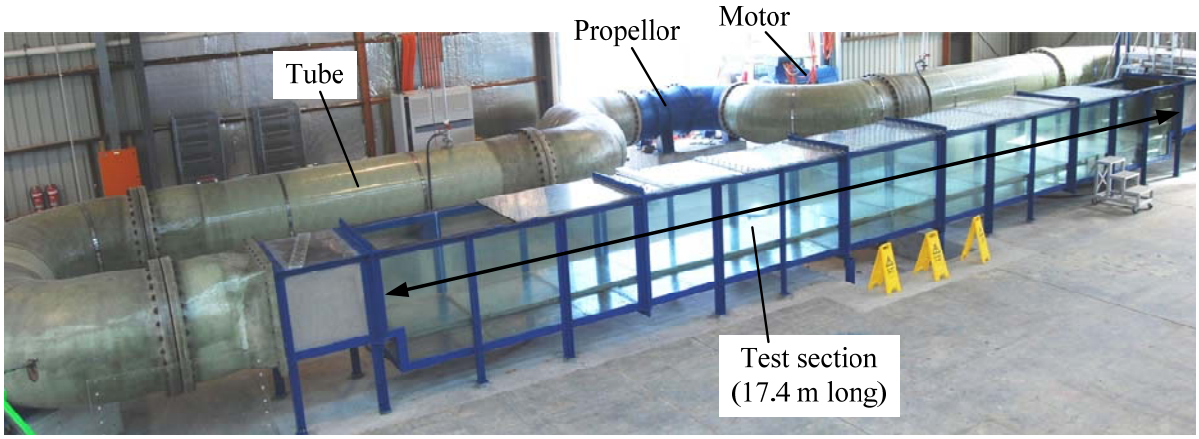

Figure 18: Large O-tube facility at UWA for modelling ocean-structure-seabed interaction (An *et al*., 2013)

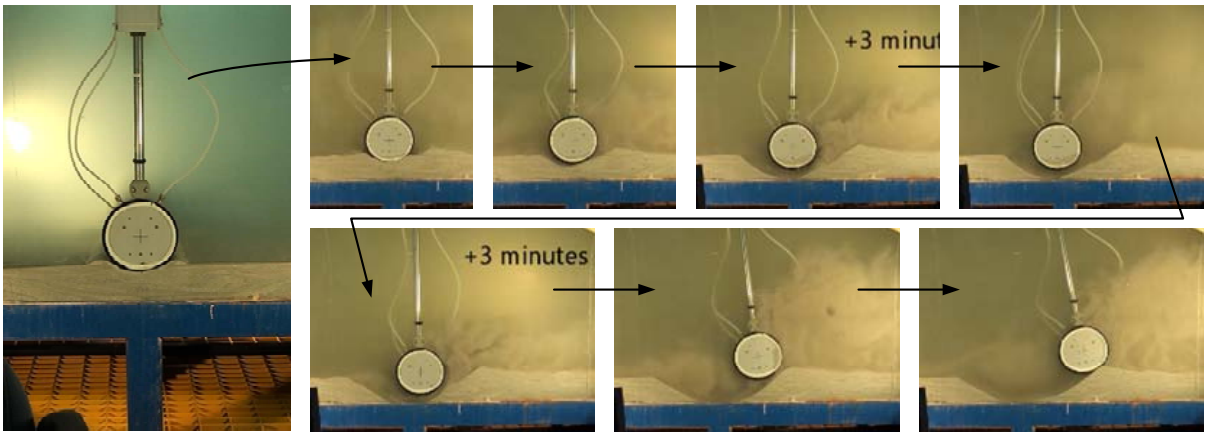

Figure 19: Images from a large O-tube test showing scouring and settlement of a pipeline, followed by breakout.

Pipe-soil interaction forces on carbonate soils can be determined using the same methods derived for non-carbonate soils, making allowance for the strength behaviour. In undrained conditions the monotonic penetration and lateral resistance can be determined using conventional plasticity-based approaches (Randolph & White, 2008). For large amplitude lateral movements, which are common in engineered buckles, the surrounding soil is significantly disturbed and remoulded. To simulate this accurately in a numerical model requires the changes in soil strength to be considered.

The RITSS method of large deformation finite element analysis (Hu and Randolph, 1998) has been applied to this problem by Wang *et al.* (2010), White *et al.* (2011) and Chatterjee *et al.* (2012a, b). By modelling the soil with a Tresca strength criterion, but with the strength reducing with accumulated plastic strain, it is possible to reproduce the centrifuge test results. This simple approach to model soil softening creates the same forms of failure mechanism as seen in the model tests, with failure rapidly localizing to a softened plane of soil at the base of the soil berms (Figure 20). The resistance is controlled not by the intact soil strength, but by a value closer to the remoulded strength.

The response of an engineered buckle is also affected by the axial pipe-soil resistance along the adjacent length of pipe that feeds into the buckle. The axial sliding resistance of rough pipes on carbonate soils can be significantly higher than on non-carbonate soils, reflecting the internal angle of friction (White *et al*., 2012). Consolidation-induced increases in the strength of the surrounding soil after pipe laying can also lead to enhanced sliding resistance (Krost *et al*., 2011).

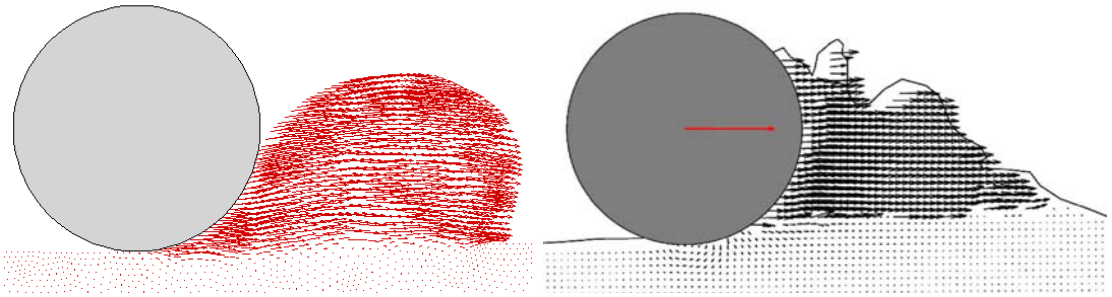

(i) Finite element analysis (Wang *et al*., 2010) (ii) Centrifuge model tests (Dingle *et al*., 2008)

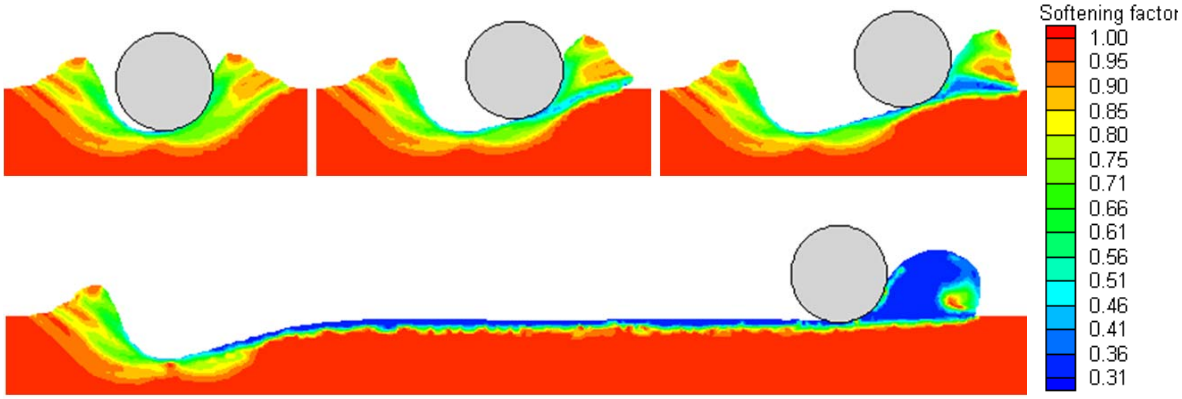

(iii) Contours of soil softening in large deformation finite element analysis (White *et al*., 2011)

Figure 20: Failure mechanisms and soil softening during lateral pipe movement

8 SUBMARINE MASS MOVEMENTS

In common with other oil and gas provinces around the world, current and future developments in Australian waters are moving further away from shore, beyond the continental margin into progressively deeper waters. This move is partly driven by the gradual depletion of nearshore resources in relatively shallow waters and the significant developments in technology that have made these frontier developments economically viable. A significant feature of the environment close to the continental margin and in the waters below is the presence of relic submarine mass movements and the potential for future events.

The Jansz field, which forms part of the Gorgon development and is currently in construction, is located in approximately 1300 m of water, downslope of the continental shelf break off Australia's north west coast (Figure 21, Equid, 2008). The gas field is located in the vicinity of relic slide run-out deposits and the export pipeline must past through these deposits before negotiating unstable regions of seabed around the steep scarp at the edge of the continental shelf on its way to landfall at Barrow Island. These challenging conditions expose pipelines to the risk of impact from a submarine mass movement. Also, the subsea facilities may also lie in the run-out paths of future potential events. Several recent gas discoveries have been made to the north and west of the Greater Gorgon project, so future projects are to be expected in the deeper water towards the Exmouth Plareau.

During the design of developments in these environments, a key consideration is whether the pipelines and subsea facilities can survive the impact of potential mass movements without being compromised. This risk is quantified via (i) an assessment of the routes of potential slides, via geological and geotechnical analysis, and (ii) modelling of the potential slide run-out behaviour. The latter provides information on the height, velocity and strength of the debris that can be used to assess the loading on and the response of impacted infrastructure.

Modelling of the run-out of mass movements is particularly challenging as the sediment may undergo gross changes in its engineering properties due to the progressive disturbance and the entrainment of water. At the initial stages of a slope failure, the sediment may have a strength and density that is similar to its *in situ* pre-failure state, before remoulding and reducing in strength as its runs out and entrains water. At the other extreme, the sediment may be transformed into a weak heavy fluid of suspended sediment. Modelling of these events has often not considered this transformation during run-out. As a consequence, the predicted run-out and slide behaviour may not be realistic or reliable.

As part of a Joint Industry Project (JIP) based at UWA, with the aim of improving methods for assessing the potential damage to pipelines from submarine slides, Boylan and White (2013) developed a program, entitled UWA-SM3 (University of Western Australia Submarine Mass Movement Modeller) that models slide run-out using a framework that captures the transformations described above. The model utilises a fluid mechanics approach, which is commonly used for modelling mass movement run-out, where the sediment rheology is described using either a linear viscoplastic Bingham model or a non-linear viscoplastic Herschel-Bulkley model. The run-out process is then modelled using a finite difference scheme based on depth-integrated equations of mass and momentum conservation, solved within a Lagrangian framework.

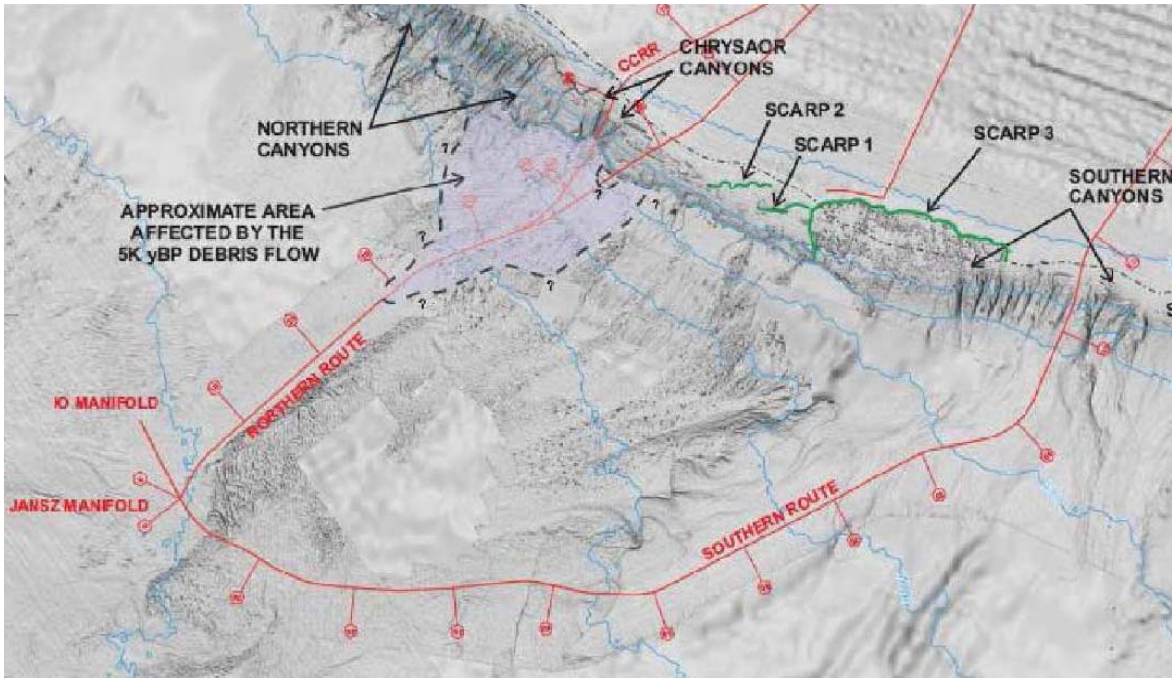

Figure 21: The Jansz field in deep water offshore Australia, close to previous submarine slide activity (Equid, 2008)

In lieu of established models of the combined soil disturbance and water entrainment process during run-out, this effect is taken into account empirically using a combination of hindcasting of relic mass movements, cyclic penetrometer testing to determine soil disturbance parameters and models of soil strength that span the solid-fluid boundary. Laboratory investigations (Figure 22) of the strength of soil over a wide range of moisture contents have shown that the strength decays steadily with increasing moisture content across the fluid-solid boundary (Boukpeti *et al*., 2009, 2012). This finding allows for a single model to describe the soil strength from the beginning to the end of the mass movement event. It is notable that of the soils investigated, the carbonate sediment showed a more dramatic loss of strength for a given change in moisture content (Figure 22a).

Figure 23(a) shows an example of the run-out of a slide block on a uniform slope with 5^o inclination, modelled using UWA-SM3. The first case uses a slide block with a shear strength that remains intact (or constant), $s_{u\text{-Intact}}$, during the run-out process. The second case ($s_{u\text{-With Softening}}$) includes softening so that the shear strength degrades towards the remoulded shear strength. In this case, inclusion of softening increased the run-out by a factor of 2.4. Figure 23(b) shows the evolution of the slide for the case with softening. The slide geometry is shown at increments of toe movement of approximately 10% of the final run-out distance.

The initial slide block collapses very early in the slide and the run-out stretches until the slide mass comes to a halt. As well as providing information on the run-out distance and the geometry of the debris, the program also provides information of the velocity of the slide mass, at the toe and internally. Figure 23(c) shows the time-velocity relationship for the front of the slide and at two fixed points relative to the toe of initial slide block – 40 m and 150 m ahead of the initial toe position. These results highlight how the time-velocity profile seen by an obstacle may differ depending on the location within the slide run-out path. For assessment of the impact loading from slides on infrastructure, the time-velocity profile at the position of the asset should be considered rather than the velocity at the toe of the slide – which may generate the highest load, but only momentarily at the asset position.

To model the run-out of debris flows in 3D terrain, the program has been further developed by the second author to explicitly consider mass and momentum conservation in both the x and y directions, while utilising depth averaging in the z direction. To avoid problems with mesh distortion that may arise due to the spreading and splitting of the run-out using a computational grid, the modelling uses a meshless technique developed from smoothed particle hydrodynamics (SPH) methods. Figure 24 shows an example of debris run-out in a canyon at a continental shelf break. This technology has been used to assess geohazards in the Gulf of Mexico and the Caspian region as well as offshore Australia.

More sophisticated numerical techniques that avoid the use of depth-averaged conditions provide an alternative, albeit computationally more demanding, approach to model slide run-out. Wang *et al*. (2013) describe a method based on the Abaqus continuum finite element analysis software that allows the extremely large deformations and long run-out distances of a submarine slide to be accommodated, with a reasonable level of computational robustness. Using this approach, outrunner blocks are observed to form for certain combinations of slide geometry and soil parameters. This is an aspect of slide behaviour that is difficult to replicate using depth-averaged methods. Although the continuum methods have overcome the computational difficulties with modelling long run-out processes, there is no widely-established approach to accommodate the water entrainment process within the rheological models used for the slide material.

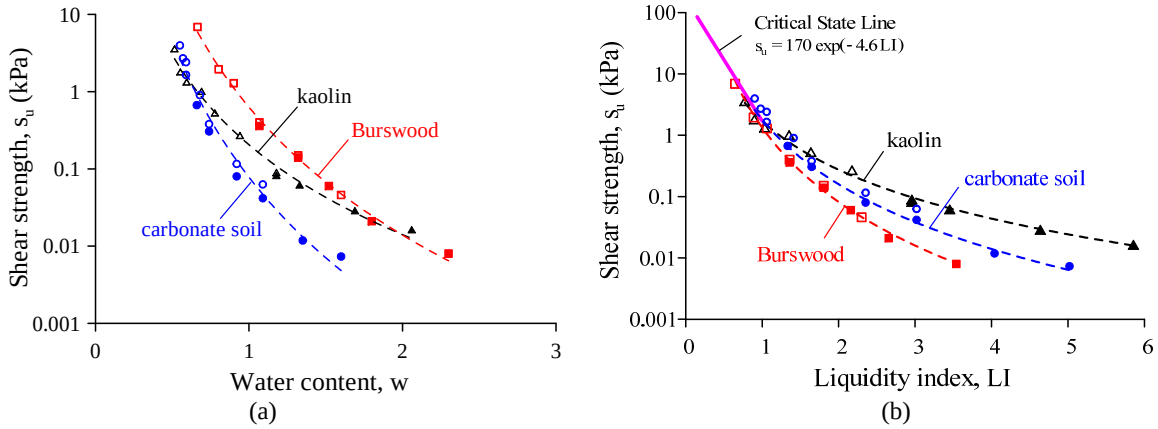

Figure 22: The solid-fluid strength 'boundary': effects of (a) moisture content, (b) liquidity index (Boukpeti *et al*., 2012)

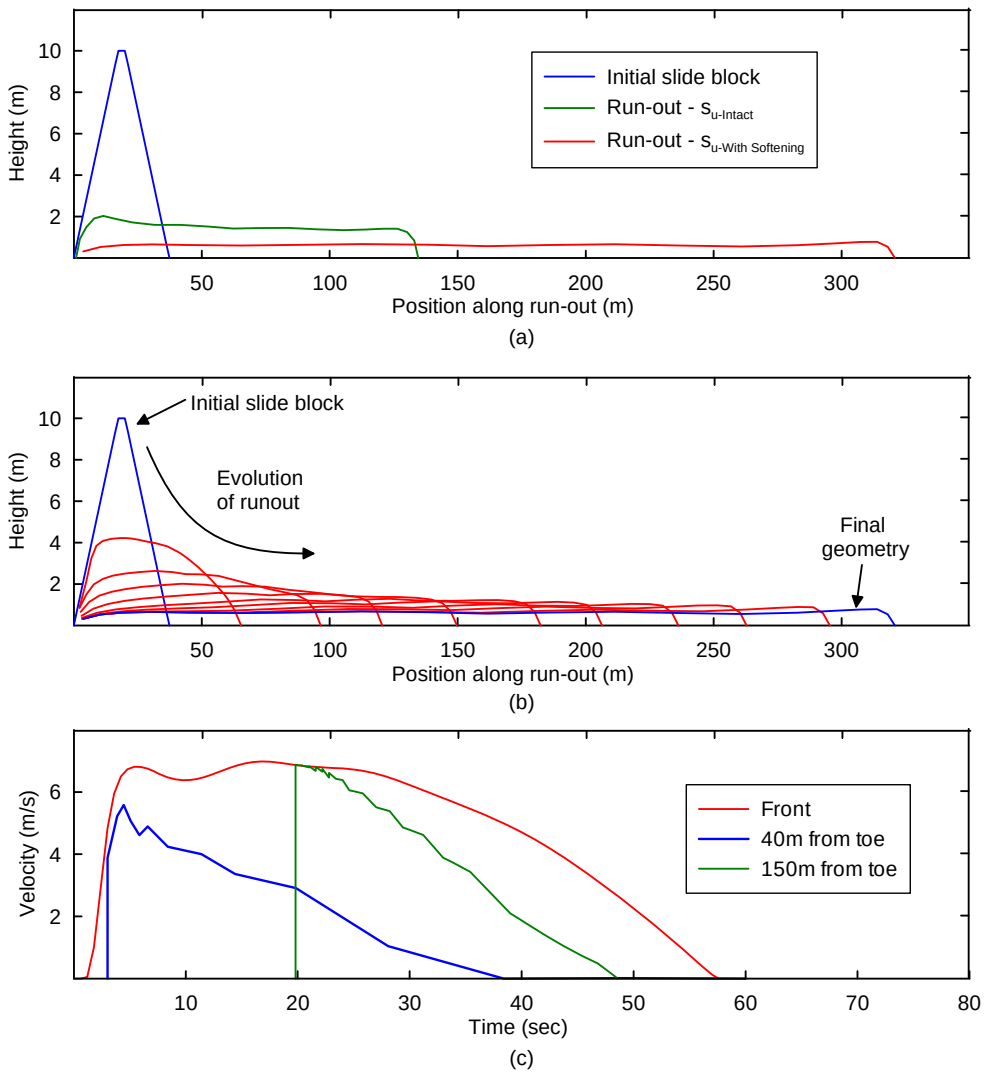

Figure 23: Example analyses of submarine slide run-out, using UWA-SM3 software (a) Comparison of runouts (b) Snapshots of softening case during runout (c) Time – Velocity profiles

9 CONCLUDING COMMENTS

This paper has provided a brief overview of current research into, and practice of, offshore geotechnics in Australia, with the selected content naturally being influenced by the authors' interests. Offshore geotechnics is a specialism within geotechnical engineering, and offshore geotechnics in Australia involves a further level of specialism, associated with the carbonate soil conditions found across our oil and gas development regions.

Australia has a strong tradition of offshore geotechnical engineering research, driven by the local needs. This growth has been supported by the establishment in Perth of a large research group based at the University of Western Australia – now known as the Centre for Offshore Foundation Systems (COFS). The associated testing facilities and the concentration of graduates within local industry has led to a local expertise base that is responsible for geotechnical design being retained as a major element of local content in an increasingly internationalised oil and gas industry supply chain.

Australian oil and gas developments have benefitted from many radical geotechnical solutions that have been pioneered to tackle the particular conditions in this region. New types of piled and shallow foundations have been deployed, relying on design methods that account for the unusual constitutive behaviour of our local carbonate materials. A new breed of *in situ* penetrometer test – based on the T-bar and ball 'full flow' devices – has been pioneered in this region, and is now seeing adoption worldwide.

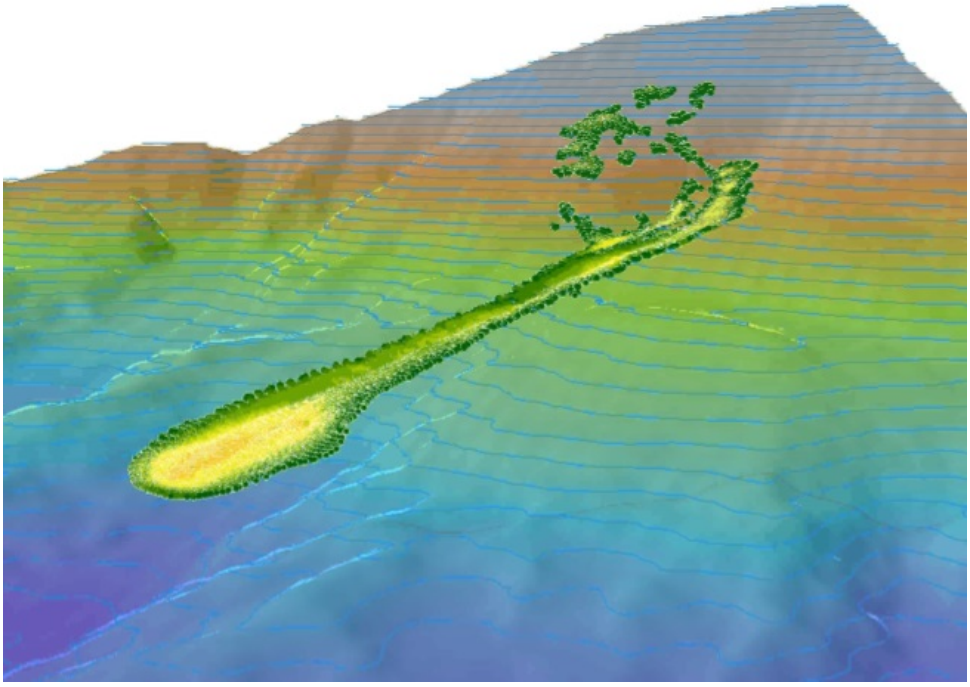

Figure 24: Example of submarine slide run-out modelled using SM3+1

The geotechnical challenges faced by Australia's offshore developments are continually evolving as exploration moves to deeper water and as facility solutions evolve. Research is now focused on deep water sediments, anchoring and shallow foundations (rather than piled foundations), long pipeline networks and the geohazards faced beyond the continental shelf. A theme that runs through this engineering is the mobility of the infrastructure and the seabed during installation and operation. For example, anchors are dragged to their operational position, pipelines sweep laterally and axially over the seabed during operation, risers dig deep trenches where they touch down on the seabed, and submarine mass movements transport and transform huge volumes of weak sediment.

The consequent disturbance and healing of the seabed soil leads to changes in topography and strength. Novel technologies to characterise the seabed through such episodes of disturbance are described, as well as tools to analyse and optimise the associated infrastructure. These examples draw attention to new areas of research and practice that lie beyond 'text book soil mechanics'. The defining characteristics are the changing geometry and the transforming soil properties, which can be particularly significant in the carbonate soils found offshore Australia. The gross seabed deformations around piles, penetrometers, anchors and pipelines, and during runout of submarine slides, require new numerical modelling techniques such as large deformation FE and SPH to capture the full process. These techniques can only provide realistic simulations if coupled with suitable soil models that account for the changing strength, including the effects of remoulding and reconsolidation. Such models in turn demand new *in situ* characterisation tests to provide site-specific input parameters.

These new regimes of geotechnical behaviour open up refreshing new avenues of research, and provide exciting challenges to the designer. Continued innovation in research and design practice is required, as Australia seeks to further exploit our offshore resources whilst preserving our ocean environment.

10 ACKNOWLEDGEMENTS

This paper forms part of the activities of the Centre for Offshore Foundation Systems (COFS) at UWA. COFS is supported by the Australian Research Council as a node of the ARC Centre of Excellence in Geotechnical Science and Engineering. The first author holds the Shell EMI Chair of Offshore Engineering at UWA and is supported by an Australian Research Council Future Fellowship (FT0991816).

We also gratefully acknowledge the contributions of many colleagues at COFS and Advanced Geomechanics to the work presented here.

11 REFERENCES

Al-Shafei, K. (ed.) (1999) Proc. 2nd Int. Conf. on Engineering for Calcareous Sediments, Volumes 1-2. Balkema

API (2011) "Recommended Practice 2GEO: Geotechnical and Foundation Design Considerations", 1st Edition, American Petroleum Institute, Washington.

An H., Luo C., Cheng L. and White D.J. (2013). "A new facility for studying ocean-structure-seabed interactions: the O-tube". Coastal Engineering. *In review*

Bonjean, D., Erbrich, C.T. and Zhang, J. (2008). "Pipeline flotation in liquefiable soil", Proc. Annual Offshore Tech. Conf., Houston, Paper OTC 19668.

Borel, D., Puech, A., Dendani, H. and de Ruijter, M. (2002). "High quality sampling for deep water geotechnical engineering: the STACOR® Experience", Proc. Symp on Ultra Deep Engineering and Technology, Brest, France.

Borel, D., Puech, A., Dendani, H. and Colliat, J-L. (2005). "Deep water geotechnical site investigation practice in the Gulf of Guinea", Proc. Int. Symp. on Frontiers in Offshore Geotechnics (ISFOG), Perth, 921-926.

Borel, D., Puech, A. and Po, S. (2010). "A site investigation strategy to obtain fast-track shear strength design parameters in deep water soils", Proc. 2nd Int. Symp. on Frontiers in Offshore Geotechnics, Perth, 253-258.

Boukpeti, N., White, D.J. and Randolph, M.F. (2009). "Characterization of the solid-liquid transition of fine-grained sediments", Proc. Conf. on Offshore Mechanics and Arctic Engineering, ASME, Honolulu, Paper OMAE2009-79738.

Boukpeti, N., White, D.J., Randolph, M.F. and Low, H.E. (2012). "The strength of fine-grained soils at the solid-fluid transition", Géotechnique, 62(3):213-226.

Boylan, N., Long, M., Ward, D., Barwise, A., and Georgious, B. (2007). "Full flow penetrometer testing in Bothkennar clay", Proc. 6th Int. Conf. on Offshore Site Investigation and Geotechnics, London. 177-186.

Boylan, N. and White, D. J. (2013). "Depth-averaged numerical modelling of submarine slide run-out in softening soil", In review.

Boylan, N. P., Brunning, P. and White, D.J. (2014) "Seabed friction on carbonate soils" OTC Asia 2014

Borges Rodriguez A., Bransby M.F., Finnie I.M., Low H.E. and White D.J. (2013). "Changes in pipeline embedment due to sediment mobility: observations and implications for design". Proc. Int. Conf. on Offshore Mech. and Arctic Engineering. Paper OMAE-2013-11425

Bransby, M. F. and Randolph, M. F. 1998. "Combined loading of skirted foundations". Géotechnique 48(5): 637–655.

Bransby, M.F. (2002). "The undrained inclined load capacity of shallow foundations after consolidation under vertical loads". Proc. 8th Numerical Models in Geomechanics (NUMOG), Rome, 431-437.

Brown, R., Wong, P. and Audibert, J.M. (2010). "SEPLA keying prediction method based on full-scale offshore tests". Proc. 2nd Int. Symp. On Frontiers in Offshore Geotechnics, Perth, Australia. Taylor and Francis. 717-722

Chatterjee S., Randolph M.F. and White D.J. (2012a). "The effect of penetration rate and strain softening on the vertical penetration resistance of pipelines on undrained soil". Géotechnique, 62(8):573-582

Chatterjee S., White D.J. and Randolph M.F. (2012b). "Numerical simulations of pipe-soil interaction during large lateral movements on clay". Géotechnique, 62(8):693-705

Chen R., Gaudin C., and Cassidy M.J. (2012). "An investigation of the vertical uplift capacity of deepwater mudmats in clay. Canadian Geotechnical Journal". 49(7): 853-865.

Cheuk, C.Y. and White D.J. (2011). "Modelling the dynamic embedment of seabed pipelines", Géotechnique, 61(1): 39-57.

Collins, L.B. (2002). "Tertiary foundations and Quaternary evolution of coral reef systems of Australia's North West Shelf", in Keep M. and Moss S. J. (Eds) 2002, The Sedimentary Basins of Western Australia 3: Proceedings of the Petroleum Exploration Society of Australia, Perth, pp. 129-152.

de Aguiar, C. S., de Sousa, J. R. M., Ellwanger, G. B.,Porto, E. C., de Medeiros Júnior, C. J., and Foppa, D. (2009). "Undrained load capacity of torpedo anchors in cohesive soils". Proc. 28th Int. Conf. Ocean, Offshore and Arctic Eng., OMAE 2009, ASME, Honolulu, USA, OMAE2009-79465.

Dingle H.R.C., White D.J., and Gaudin C. (2008). "Mechanisms of pipe embedment and lateral breakout on soft clay" Canadian Geotechnical Journal, 45(5):636-652

Doyle, E.H., Dean, E.T.R., Sharma, J.S., Bolton, M.D., Valsangkar, A.J. & Newlin, J.S. 2004. Centrifuge model tests on anchor piles for tension leg platforms. Proc. Offshore Technology Conference, Houston. Paper OTC16845.

Dyson G.J. and Randolph M.F. (2001). "Monotonic lateral loading of piles in calcareous sediments". J. Geotech Eng. Div, ASCE, 127(4), 346-352.

Equid, D. (2008). "Challenges of the Jansz deepwater tie-back", Proc. Deep Offshore Technology Conference (Asia-Pacific), Perth, Australia.

Erbrich, C.T. (2005). "Australian frontiers – spudcans on the edge", Proc. Int. Conf. on Frontiers in Offshore Geotechnics, Perth. 49-74.

Erbrich, C. and Hefer, P. (2002) "Installation of the Laminaria suction piles – a case history". Proc. Annual Offshore Technology Conf, Houston. Paper OTC 14240.

Erbrich, C.T. and Neubecker S.R. (1999) "Geotechnical design of a grillage and berm anchor". Proc. Annual Offshore Technology Conf., Houston, Paper OTC 10993.

Erbrich, C.T. (2004). "A new method for the design of laterally loaded anchor piles in soft rock". Proc. Annual Offshore Technology Conf., Houston, Paper OTC 16441.

Erbrich, C.T., O'Neill, M.P., Clancy, P. and Randolph, M.F. (2010). "Axial and lateral pipe design in carbonate soils". Proc. 2nd Int. Symp. On Frontiers in Offshore Geotechnics, Perth, Australia. Taylor and Francis. 125-154.

Feng, X., Randolph, M. F., Gourvenec, S. and R. Wallerand (2013). "Design approach for rectangular mudmats under fully three dimensional loading". Géotechnique. *In press, 10.1680/geot.13.P.051*.

Gaudin C. O'Loughlin C.D., Randolph M.F., Lowmass A.C. (2006). "Influence of the installation process on the behaviour of suction embedded plate anchors". Géotechnique, 56(6), 381-391.

Gaudin C., Simkin M., White D.J. and O'Loughlin, C.D. (2010). "Experimental investigation into the influence of a keying flap on the keying behaviour of plate anchors". Proc. 20th Int. Offshore and Polar Eng. Conf., Beijing, China.

Gaudin C., O'Loughlin, C.D., Hossain, M.S. and Zimmerman, E. (2013). "The performance of dynamically-embedded anchors in calcareous silt". Proc. Int. Conf. on Offshore Mechanics and Arctic Engineering, Nantes, France. Paper OMAE-2013-10115

Gaudin, C., Bienen, B. and Cassidy M.J. (2011). "Investigation of the potential of bottom water jetting to ease spudcan extraction in soft clay". Géotechnique, Vol. 61, No. 12, pp. 1043–1054

Gourvenec, S. and Barnett, S. (2011) "Undrained failure envelope for skirted foundations under general loading". Géotechnique, 61(3): 263 – 270.

Gourvenec, S. and Randolph, M.F. (2003). "Effect of strength non-homogeneity on the shape and failure envelopes for combined loading of strip and circular foundations on clay". Géotechnique 53(6), 575-586.

Gourvenec, S. and Randolph, M.F. (2010) "Consolidation beneath skirted foundations due to sustained loading". International Journal of Geomechanics. 10(1): 22-29.

Gourvenec, S., Acosta-Martinez, H.E. and Randolph, M.F. (2009) "Experimental study of uplift resistance of shallow skirted foundations in clay under concentric transient and sustained loading". Géotechnique, 59(6): 525-537.

Gourvenec S., Vulpe, C. and Murthy, T. (2013) "A method for predicting the consolidation undrained bearing capacity of shallow foundations on clay" Géotechnique. *In review*.

Hengesh J., Whitney B. and Royere A. (2011). "A tectonic influence on seafloor stability along Australia's North West Shelf", Proceedings of the International Offshore and Polar Engineering Conference (ISOPE), Maui, Hawaii, USA, pp. 596-604.

Hodder, M., White, D.J. and Cassidy M.J. (2013). "An effective stress framework for the variation in penetration resistance due to episodes of remoulding and reconsolidation", Géotechnique, 63(1):30-43

Hossain, M.S. and Randolph, M.F. (2009). "Effect of strain rate and strain softening on the penetration resistance of spudcan foundations on clay", ASCE Int. J. Geomech., 9(3):122-132.

Humpheson, C. (1998) "Foundation design of Wandoo B concrete gravity structure". Proc. Int. Conf. Offshore Site Investigation and Foundation Behaviour, Soc. For Underwater Technology, 353-367.

Hu, Y., and Randolph M.F. (1998). "A practical numerical approach for large deformation problems in soil". Int. J. Num. and Anal. Methods in Geomech., 22(5), 327-350

Jas, E, O'Brien, D, Fricke, D, Gillen, A, Cheng, L., White, D., and Palmer, A 2012, "Pipeline stability revisited". Journal of Pipeline Engineering, 4th Quarter, pp. 259-268.

Jeanjean, P. (2009) "Re-assessment of p-y curves for soft clays from centrifuge testing and finite element modeling." Proc., Offshore Technology Conference, Houston, America, 1-23. Paper OTC20158

Jewell, R.J. and Andrews, D.C. (eds.) (1988). Proc. Int. Conf. on Engineering for Calcareous Sediments, Volume 1, General Proceedings. Balkema.

Jewell, R.J. and Khorshid, M.S. (eds.) (1988). Proc. Int. Conf. on Engineering for Calcareous Sediments, Volume 2, North Rankin A Foundation Project and State of the Art Reports.

Keaveny, J.M., Hansen, S.B., Madshus, C. and Dyvik, R. (1994) "Horizontal capacity of large scale model anchors". Proc. XIII Int. Conf. Soil Mech. and Found. Engng (ISSMFE), New Delhi, 2: 677-680.

Kodikara, J., Haque, A., and Lee, K. (2010). "Theoretical p-y curves for laterally loaded single piles in undrained clay using bezier curves", Journal of Geotechnical and Geoenvironmental Engineering - ASCE 136(1):265-268.

Krost K., Gourvenec S. and White D.J. 2011. "Consolidation around partially-embedded submarine pipelines". Géotechnique, 61(2): 167-173.

Low, H.E., Lunne, T., Andersen, K.H., Sjursen, M.A., Li, X. and Randolph, M.F. (2010). "Estimation of intact and remoulded undrained shear strength from penetration tests in soft clays", Géotechnique, 60(11):843-859.

Lunne, T., Randolph, M. F., Chung, S. F., Andersen, K. H. and Sjursen, M. (2005). "Comparison of cone and T-bar factors in two onshore and one offshore clay sediments", Proc. Int. Symp. on Frontiers in Offshore Geotechnics (ISFOG), Perth, Australia, 981-989.

Mana, D.K.S, Gourvenec, S. and Martin, C.M. (2013a) "Critical skirt spacing for shallow foundations under general loading". *ASCE Journal of Geotechnical and Geoenvironmental Engineering*. doi: 10.1061/(ASCE)GT.1943-5606.0000882 (aop September issue).

Mana, D.K.S, Gourvenec, S. and Randolph, M.F. (2013b) "An experimental investigation of reverse end bearing of skirted foundations" Canadian Geotechnical Journal. *In press*

Mana, D.K.S, Gourvenec, S. and Randolph, M.F. (2013c) "Numerical modelling of consolidation and seepage beneath skirted foundation subjected to uplift loading". Computers in Geotechnics. *In press*

Mana, D.K.S, Gourvenec, S. and Randolph, M.F. (2013d) "A novel method to mitigate the effect of gapping on the uplift capacity of skirted foundations – Gap Arrestors". Géotechnique 10.1680/geot.12.P.173

Mana, D.K.S, Gourvenec, S., Randolph, M.F. and Hossain, M.S. (2012) Failure mechanisms of skirted foundations in uplift and compression. International Journal of Physical Modelling in Geotechnics, 12(2): 47-62.

Mao, X. and Fahey, M. (2003) "Behaviour of calcareous soils in undrained cyclic simple shear". Géotechnique, 53(8):715-727.

Martin, C.M. and Randolph, M.F. (2006). "Upper bound analysis of lateral pile capacity in cohesive soil". Géotechnique, 56(2), 141-145.

Martin, C.M. and Hazell, E.C.J. (2005). "Bearing capacity of parallel strip footings on non-homogenous clay", Proc. Int. Symp. on Frontiers in Offshore Geotechnics (ISFOG), Perth, 427-433.

Medeiros, C. J. (2001). "Torpedo anchor for deep water". Proc. Deepwater Offshore Technology Conf., Rio de Janeiro.

Mohr H., Draper S. and White D.J. (2013). "Seabed mobility on the North West Shelf of Australia: the free field instability of calcareous sediment". Proc. Int. Conf. on Offshore Mech. and Arctic Engineering. Paper OMAE-2013-11490

Neubecker, S.R. and Erbrich, C.T. (2004) "Bayu-Undan substructure foundations: Geotechnical design and analysis". Proc. Annual Offshore Tech. Conf., Houston, Paper OTC 16157.

Neubecker S.R., O' Neill M.P. and Erbrich C.T. (2005). "Preloading of drag anchors in carbonate sediments", Proc. International Symposium on Frontiers in Offshore Geotechnics (ISFOG), Perth, Western Australia, Balkema: Rotterdam

Novello, E. (1999). "From static to cyclic p-y data in calcareous sediments". Proc. 2nd Int. Conf. on Engineering for Calcareous Sediments, Bahrain, 1, 17-27.

O'Loughlin, C.D, Randolph, M.F. and Richardson, M. (2004). "Experimental and theoretical studies of deep penetrating anchors". Proc. Offshore Tech. Conf., Houston, Paper OTC 16841.

O'Loughlin, C.D., Lowmass, A., Gaudin, C. and Randolph, M. F., (2006). "Physical modelling to assess keying characteristics of plate anchors", Proc. Int. Conf. on Physical Modelling in Geotech., Hong Kong, 1, 659-665.

O'Loughlin, C.D., Blake, A.P., Wang, D., Gaudin, C. and Randolph, M. F., (2013). "The dynamically-embedded plate anchor: results from field studies and numerical analysis". Proc. Int. Conf. on Offshore Mechanics and Arctic Engineering, Nantes, France. Paper OMAE-2013-11571

O' Neill M.P., Neubecker S.R., and Erbrich C.T. (2010). "Installation and in-place assessment of drag anchors in carbonate soils." Proc. 2nd International Symposium on Frontiers in Offshore Geotechnics (ISFOG), Perth, Western Australia, Balkema: Rotterdam 747-752

Peuchen, J., Adrichem, J. and Hefer, P. A. (2005). "Practice notes on push-in penetrometers for offshore geotechnical investigation", Proc. Int. Symp. on Frontiers in Offshore Geotechnics (ISFOG), Perth, 973-979.

Pinna, R., Wehterald, A., Grulich, J., Ronalds, B.F., (2003). "Field observations and modelling of the self-burial of a North West Shelf pipeline", ASME 2003 22nd International Conference on Offshore Mechanics and Arctic Engineering (OMAE2003) June 8–13, 2003, Cancun.

Randolph, M.F. (1988) "The axial capacity of deep foundations in calcareous soil". Proc. Int. Conf. on Engineering for Calcareous Sediments, Perth, Vol. 2, 837-857

Randolph, M. F. (2004). "Characterisation of soft sediments for offshore applications", Proc. of 2nd Int. Conf. on Geotechnical and Geophysical Site Characterization, ISC'2, Porto, 1: 209-232.

Randolph, M.F. (2012), "Offshore Geotechnics - The Challenges of Deepwater Soft Sediments", GeoCongress 2012 Geotechnical Engineering State of the Art and Practice, Keynote Lectures from GeoCongress 2012, USA, ASCE Geotechnical Special Publication No. 226, pp. 241-271.

Randolph M.F. and White D.J. (2008). "Upper bound yield envelopes for pipelines at shallow embedment in clay" Géotechnique, 58(4):297-301

Randolph, M. F., Hefer, P. A., Geise, J. M. and Watson, P. G. (1998). "Improved seabed strength profiling using T-bar penetrometer", Proc. Int. Conf. Offshore Site Investigation and Foundation Behaviour - "New Frontiers", Society for Underwater Technology, London. 221-235.

Randolph, M.F and Erbrich, C.T. (2000) "Design of shallow foundations for calcareous sediments". Proc. Engineering for Calcareous Sediments. Ed. Al-Shafei, Balkema (2): 361-378.

Randolph, M.F. and Gourvenec, S. (2011) Offshore Geotechnical Engineering. Spon Press/ Taylor and Francis. ISBN: 978-0-415-47744-4. pp 528.

Richardson, M. D., O'Loughlin, C. D. and Randolph, M. F., (2005). "The geotechnical performance of deep penetrating anchors in calcareous sand". Proc. Int. Symp. on Frontiers in Offshore Geotechnics (ISFOG), Perth, 357-363.

Senders, M., Banimahd, M., Zhang, T. and Lane, A. (2013). "Piled foundations on the North West Shelf". Australian Geomechanics (this issue)

Sims, M.A., Smith, B.J.A and Reed, T. (2004). "Bayu-Undan substructure foundations: Conception, design and installation aspects". Proc. Annual Offshore Technology Conf., Houston, Paper OTC 16158.

Song, Z., Hu, Y, O'Loughlin, C.D., Randolph, M.F. (2009). "Loss in anchor embedment during plate anchor keying in clay". J. of Geot. and Geoenv. Eng., ASCE, 135(10), 1475-1485.

Stewart, D. P. and Randolph, M. F. (1991). "A new site investigation tool for the centrifuge", Proc. Int. Conf. on Centrifuge Modelling, Centrifuge '91, Boulder, Colarado. 531-538.

Taiebat, H.A., and Carter, J.P. (2000). "Numerical studies of the bearing capacity of shallow foundations on cohesive soil subjected to combined loading". Géotechnique, 50(4): 409–418.

Ukritchon, B. Whittle, A.J. and Sloan, S.W. (1988). "Undrained limit analysis for combined loading of strip footings on clay". J. Geot. and Geoenv. Eng., ASCE 124(3): 265-276.

Wang D., White D.J. & Randolph M.F. (2010). "Large deformation finite element analysis of pipe penetration and large-amplitude lateral displacement". Canadian Geotechnical Journal. 47:842-856

Wang, D., Randolph M.F. and White, D.J. (2013). "A dynamic large deformation finite element method based on mesh regeneration", Computers and Geotechnics. *In press*

Watson, P.G., Humpheson, C., (2007) "Foundation design and installation of the Yolla A platform" Proc. SUT Conf. on Offshore Site Investigation and Geotechnics. London, UK.

Watson, P. G., Newson, T. A. and Randolph, M. F. (1998). "Strength profiling in soft offshore soils", Proc. 1st Int. Conf. On Site Characterisation - ISC '98, Atlanta, 2: 1389-1394.

Wesselink, B.D., Murff, J.D., Randolph, M.F., Nunez, I.L., and Hyden, A.M. (1988). "Analysis of centrifuge model test data from laterally loaded piles in calcareous sand". Proc. Int. Conf. Calcareous Sediments, Balkema, 1, 261-270.

Westgate, Z., White, D.J. and Randolph, M.F. (2012). "Field observations of pipeline embedment in carbonate sediments". Géotechnique, 62(9):787-798

White D.J. (2005). "A general framework for shaft resistance on displacement piles in sand". Proc. International Symposium on Frontiers in Offshore Geotechnics, Perth. 697-703

White D.J. and Lehane B.M. (2004). "Friction fatigue on displacement piles in sand." Géotechnique 54(10):645-658

White D.J., Maconochie A.J., Cheuk C.Y., Bolton M.D., Joray D. & Springman S.M. 2005. "An investigation into the vertical bearing capacity of perforated mudmats". Proc. International Symposium on Frontiers in Offshore Geotechnics, Perth. 459-465

White D.J. and Cathie D.N. (2010). "Geotechnics for subsea pipelines", Proc. 2nd Int. Symp. on Frontiers in Offshore Geotechnics, Perth, 87-123.

White D.J., Chatterjee S. and Randolph M.F. (2011). "The use of large deformation finite element analysis to investigate pipe-soil interaction during lateral buckling". Proc. SUT Symp. on Lateral Buckling of Subsea Pipelines, Perth. Feb. 2011 15pp.

White D.J., Campbell M.E., Boylan, N.P. and Bransby, M.F. (2012). "A new framework for axial pipe-soil interaction illustrated by shear box tests on carbonate soils", Proc. Int. Conf. on Offshore Site Investigation and Geotechnics, SUT, London.

Wiltsie, E.A., Hulett, J.M., Murff, J.D. Hyden, A.M. and Abbs, A.F. (1988). "Foundation design for external strut strengthening system for Bass Strait first generation platforms." Proc. Conf. on Engineering for Calcareous Sediments, Perth, Balkema, 2, 321-330.

Wilde, B., Treu, H. and Fulton, T. (2001). "Field testing of suction embedded plate anchors". Proc. 11th Int. Offshore and Polar Eng. Conf., 544-551.

Woodside Offshore Petroleum (1988). "General information on the North Rankin A platform: Proc. Int. Conf. Engineering of Calcareous Sediments Perth, Australia, 2:761-773

Yafrate, N. J. and DeJong, J. T. (2005). "Considerations in evaluating the remoulded undrained shear strength from full flow penetrometer cycling", Proc. Int. Symp. on Frontiers in Offshore Geotechnics (ISFOG), Perth, Australia, 991-997.

Young, A.G., Honganen, C.D., Silva, A.J. and Bryant, W.R. (2000). "Comparison of geotechnical properties from large diameter long cores and borings in deep water Gulf of Mexico", Proc. Offshore Technology Conference, Houston, Paper 12089.

Zhou, H. and Randolph, M. F. (2009). "Penetration resistance of cylindrical and spherical penetrometers in rate-dependent and strain-softening clay", Géotechnique, 59(2):79–86.

Zimmerman, E.H., Smith, M.W., Shelton J.T., (2009). "Efficient gravity installed anchor for deep water mooring". In: Proc. Offshore Technology Conference, Houston, Paper OTC 20117.

MARINE GEOPHYSICAL INVESTIGATIONS OF PALAEO-DRAINAGE SYSTEMS IN THE HAWKESBURY RIVER ESTUARY, NEW SOUTH WALES, AUSTRALIA.

R. J. Whiteley[1] and S. B. Stewart[2]
[1]Senior Principal, [2]Principal, Coffey Geotechnics, Sydney, Australia

ABSTRACT

The Hawkesbury River is a key element in a major river system in eastern Australia. The river and its tributaries virtually encircle Sydney's metropolitan area, extending northward to the Pittwater and Brisbane Water embayments and entering the Tasman Sea at Broken Bay, some 35 km north of Sydney Harbour. Since the 1960's marine geophysical techniques, principally seismic reflection, supported by land gravity surveys have revealed extensive and deep palaeodrainage systems incising the underlying sedimentary rocks mainly beneath the River and its tributaries. These are masked by considerable thicknesses of recently deposited sandy sediments.

Case studies from three recent infrastructure and research projects, completed near the mouth of the Hawkesbury River system demonstrate the application of marine seismic and gravity technologies in the mapping parts of this palaeodrainage system. These projects are within the maritime zone of the Hawkesbury River. In this zone the Hawkesbury River estuary is a drowned river valley within steeply incised gorges surrounded by dissected plateaus. The terrain is dominated by the sandstone geology with an extensively dissected and generally rugged landscape.

Installation of a wastewater transfer main beneath the Hawkesbury River between the then unsewered Dangar Island and Brooklyn on the mainland was required. This involved a 1400 m long directional bore beneath tidal mud flats and a deep tidal channel. The marine geophysics mapped the bedrock profile, identified a fault and strong seismic reflectors within the bedrock near the centre of the palaeochannel at about 45 m depth. These were interpreted as regions of stress concentration in the Newport Formation created by valley bulging processes following rapid erosion. The geotechnical model inferred from these investigations was applied in the design of the directional drilling operation that was successfully completed in rock. This upgraded sewer system is now in operation and has removed a significant pollution source from the Hawkesbury River.

Upgrading of the electricity supply from Wagstaffe to Booker Bay required installation of an 11kV power cable across Brisbane Water, a distance of 630 m. Previous regional gravity surveys in this area had identified a deep palaeodrainage system beneath the Woy Woy and Ettalong peninsulas. A marine seismic reflection and refraction survey along the proposed crossing confirmed the presence of a palaeochannel margin extending to about 25 m below the seabed. The conduit was subsequently successfully installed by horizontal directional boring up to 30 m below sea bed.

Development of an airborne electromagnetic system for bathymetric mapping and sea-floor characterisation required independent calibration using marine geophysics within Broken Bay. A broad and deep channel representing a high energy palaeo-fluvial drainage system in the Hawkesbury River outreaches was identified. This extended to approximately 80 m depth below river level and was somewhat shallower than indicated by previous studies suggesting that there may be some uncertainty in seismic bedrock depth possibly due to the dense basal sediments. Also in another nearby area a dendritic fluvial pattern extending to approximately 70 m depth was observed. A moderately narrow palaeochannel extending to 90 m depth either side of the Palm Beach tombolo was also clearly identified.

1 INTRODUCTION

The Hawkesbury River system is a major river system in eastern Australia that drains about 22,000 km^2 of the eastern highlands of New South Wales (Martens, 1999). This River and its tributaries virtually encircle Sydney's metropolitan area, extending north to Pittwater and Brisbane Water and entering the Tasman Sea at Broken Bay about 35 km north of Sydney Harbour. Pittwater and Brisbane Water are major embayments north and south of Broken Bay. This system has maintained virtually the same drainage pattern that developed in the Early Tertiary, some 40 million years ago. During the Pliocene, about 5 million years ago, the river system was rejuvenated initiating intensive erosion of the Triassic sedimentary rocks deepening and widening the drainage system. This process was repeated at the start of the Quaternary about 2.6 million years ago and was followed extensive infilling mainly during the Pleistocene about 1.6 million years ago. This infilling effectively masked the pre-existing drainage system. This was little known until the 1960's when marine geophysical techniques, principally seismic reflection, supported by land gravity surveys mapped parts of an extensive and deep palaeo-drainage system beneath the Hawkesbury River.

Case studies from three recent projects, demonstrate the results of marine seismic and gravity investigations over parts of this palaeo-drainage system. These projects are located in Figure 1 (labelled 1, 2 and 3) and are within the estuarine zone of the Hawkesbury River that extends roughly 15 km inland from the coastline. In this region the Hawkesbury River estuary is a drowned river valley bordered by steeply incised gorges and surrounded by dissected plateaus. The terrain is dominated by the sandstone geology with the landscape being unrelentingly dissected and generally rugged. In its current condition the Hawkesbury River estuary is best described as a micro-tidal estuary with a very low discharge rate delivering a very low sediment supply to the estuary head except during infrequent short-lived, large magnitude fluvial flood events (Hughes *et al*., 1998).

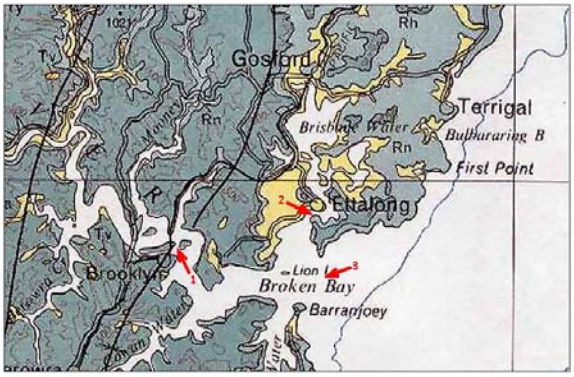

Figure 1: Location of Case Studies Areas in the Hawkesbury River Estuary: 1 - Waste Water Pipeline, Brooklyn to Dangar Island; 2 - Electrical Conduit, Wagstaffe to Booker Bay; 3 - Bedrock Mapping, Broken Bay and Pittwater.

2 CASE STUDIES

2.1 CASE STUDY 1: WASTE WATER PIPELINE INSTALLATION, BROOKLYN TO DANGAR ISLAND

In order to reduce potential contamination of the Hawkesbury River from wastewater overflows and leaks a 150 mm diameter transfer main beneath the River and within a conduit created by Horizontal Directional Drilling (HDD) was proposed. This main linked the reticulation system on Dangar Island with a transfer main to a sanitary treatment plant (STP) in the Seymour Creek valley (Figure 2). Two preferred HDD alignments about 650 m in length were initially considered as shown in Figure 2.

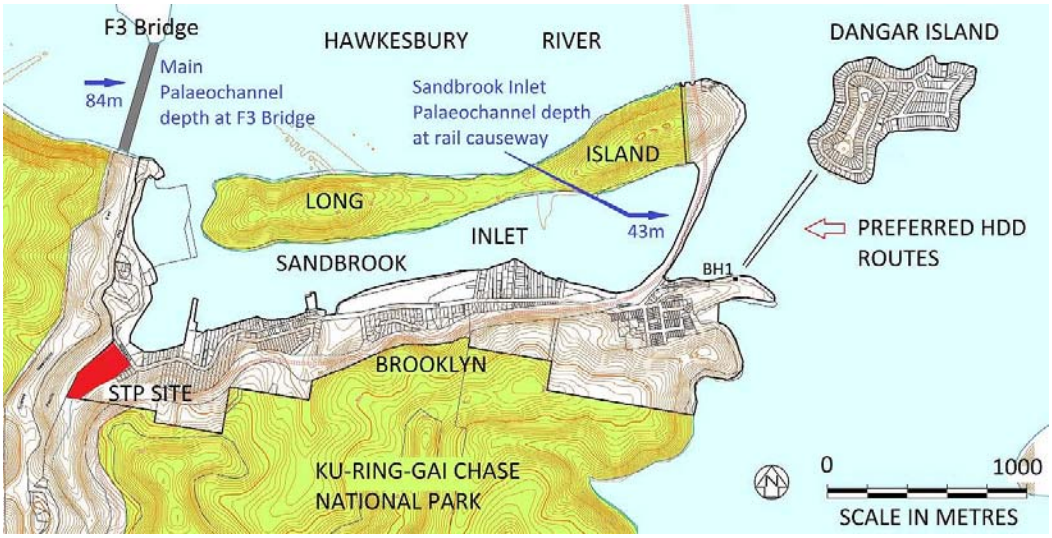

Figure 2: Site Plan with proposed Waste Water Transfer Main Crossings from Brooklyn to Dangar Island.

Details of the geotechnical aspects of this project are provided by Waddell *et. al*. (2011). Test holes and piling records for the F3 Freeway (now the M1 Motorway) bridge over the main Hawkesbury River channel to the west of the site (Figure 2) shows the palaeochannel infilled with alluvium to at least 84 m below river level with the current channel floor about 20 m below river level. The presence of Long Island (Figure 2), being parallel to the southern shoreline of the Hawkesbury River and forming a barrier to the main river channel, suggests a separate watercourse (possibly originally Seymours Creek) may have incised into the bedrock to form Sandbrook Inlet. The depth of the palaeochannel beneath the 750 m wide Sandbrook Inlet appears to be shallower than, and separate from, the palaeochannel beneath the Hawkesbury River at the bridge.

On the Brooklyn shoreline a single deep borehole (BH1, Figure 2) was drilled to 80 m depth near the preferred HDD entry for both alignments. This intersected approximately 2.5 m of fill and residual soil overlying a relatively thin layer (~1.5 m thick) of Hawkesbury Sandstone and interbedded laminite, shale and sandstone from the Newport Formation of the Narrabeen Group. The Newport Formation is predominantly quartz-lithic sandstone interbedded with siltstones, mudstones and laminite. This ranges from low and medium strength to about 20 m depth, medium and high strength to about 25 m and high strength with bands of medium strength and very high strength rock to the borehole depth at 80 m.

Marine seismic reflection using single channel continuous seismic profiling (CSP) was completed in the area of the proposed crossings (Figure 2) with the objectives of mapping the bedrock profile, locating any possible impediments to the proposed HHD and testing whether the Sandbrook Inlet palaeochannel extends beneath the preferred alignments or whether a deeper palaeochannel associated with the main Hawkesbury River palaeochannel was present. The marine reflection survey was completed along both of the proposed alignments with shorter cross-lines at 50 m intervals. Bathymetric data was also acquired. This showed that the river floor levels along the proposed HDD alignments varied from about RL-3 m AHD to RL-12 m AHD. Levels rise abruptly on the Dangar Island side of the HDD alignments which is consistent with the outcropping rock on Dangar Island.

Figure 3 shows the interpreted bedrock contour plan based on all the marine seismic data with an interpreted fault and the approximate extent of a region where there was a strong sub-bottom reflector at depth. The bedrock rises abruptly to the north-east close to the landfall on Dangar Island and it is likely that this side of the palaeochannel is also faulted.

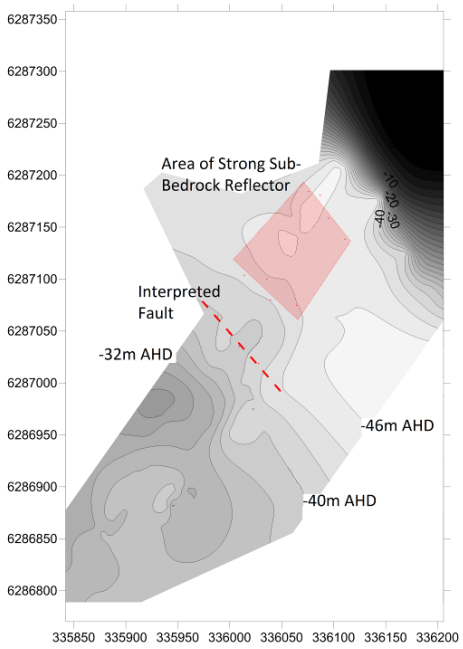

Figure 3: Interpreted bedrock contour plan from Brooklyn to Dangar Island.

Figure 4 shows the interpreted seismic section (not tidally corrected) acquired with an air-gun source along one of the HDD alignments.

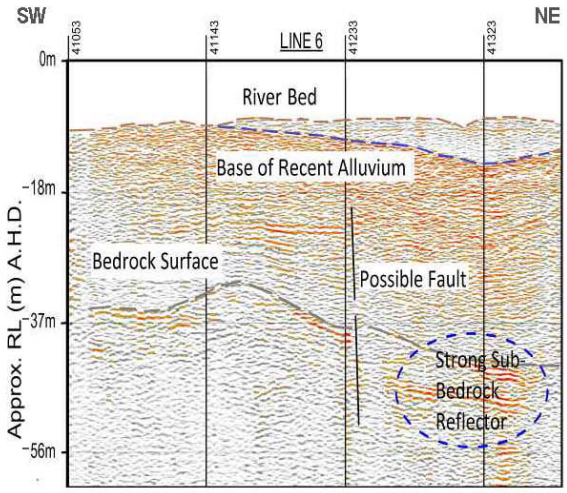

Figure 4: Sample marine seismic reflection section along HDD alignment

The river floor, base of recent sediments and the bedrock reflector are marked with dashed lines. There are other reflectors that are evident on this section including younger palaeochannels within inferred bedded sandy sediments but these have not been marked. The bedrock reflector marked on Figure 4 is complex in shape and deepens to the north-east from about RL-37 m AHD to about RL-45 m AHD. This could be due to a combination of erosion and tectonic activity. A fault with possible shear zone from 5 m to 22 m wide near Station 41233 has displaced the bedrock surface and the overlying sediment reflectors. To the north-east of this fault, in the rectangular area shown on Figure 4, bands of strong sub-bedrock reflectors demonstrate an increased acoustic impedance (density x seismic velocity) that often indicates stress-concentrations that have been observed in earlier tunnelling operations in Sydney Harbour beneath palaeochannels (Whiteley, 2005).

Based on the rock levels predicted from the geotechnical investigation, the HDD was bored with 25 m to 35 m of rock cover. Figure 5 shows the 'as-built' HDD vertical section.

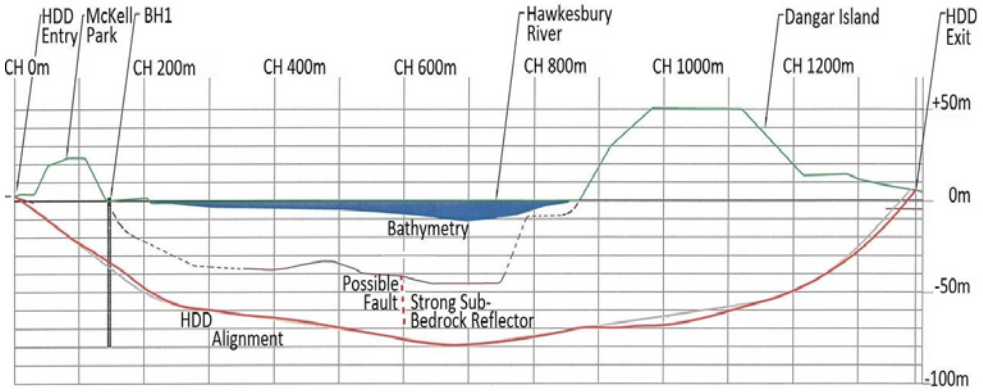

Figure 5: 'As-built' HDD vertical section from Brooklyn to Dangar Island

Allowing 25 m to 35 m of rock cover was considered prudent, given the inferred likely faulting and the potential high rock stress zone in the base of the palaeochannel shown in Figure 5. Such features increase both the risks to drilling and to drilling fluid breakout if the HDD encounters poor quality rock or there is insufficient rock cover. Anecdotal information from the HDD contractor indicated that the HDD may indeed have passed through a fault zone as indicated by the seismic survey, but was drilled without incident. The HDD was successfully constructed entirely in rock.

2.2 CASE STUDY 2: ELECTRICAL CONDUIT INSTALLATION, WAGSTAFFE TO BOOKER BAY

Brisbane Water forms the northern arm of Broken Bay (Figure 1). It was originally an inland lake system that only became a tributary of the Hawkesbury River in recent times. A proposed energy supply upgrade for residents of the south-eastern shores of Broken Bay required HDD installation of a 630 m length power cable across the waterway from Booker Bay on the Ettalong Peninsula to Wagstaffe. Recent sand deposits cover the Ettalong Peninsula while

sandstones and siltstones outcrop at Wagstaffe. The proposed HDD crossing lies near the southern border of an area where a previous regional gravity survey had been completed (Qureshi, 1981). This survey involved gravity measurements, at a nominal 100 m spacing, along the road network on both sides of Brisbane Water but no overwater gravity data was gathered. Gravity has previously proved to be useful in mapping palaeochannels incising bedrock in connection with major tunnel projects in the Sydney region (Whiteley, 2005). These are typically observed as linear gravity lows produced by the increased thicknesses of lower density (relative to rock) sandy sediments within the palaeochannels.

Figure 7 shows the regional gravity contour plan (the contour interval is 5 Gravity Units from Qureshi, 1981, 1 GU = 10^{-3} ms^{-2} SI) with a qualitative interpretation of the palaeo-drainage pattern. This shows a highly irregular bedrock profile with many deeply incised palaeochannels. The approximate location of interpreted palaeochannel axes are marked in Figure 7. The major north-south palaeochannel appears to extend from Woy-Woy Creek to Ocean Beach and is intersected by another interpreted large east-west trending paleochannel that extends beneath St. Huberts Island to Davistown. A number of palaeo-tributary channels are interpreted to join both these major channels at various locations. A palaeo-tributary or bedrock depression is also interpreted in the vicinity of the HDD crossing.

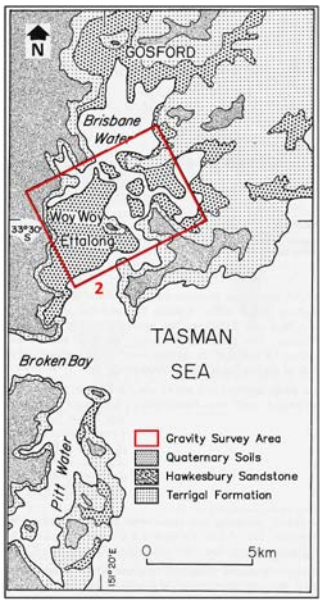

Figure 6: Site plan, Booker Bay and location of regional gravity survey area.

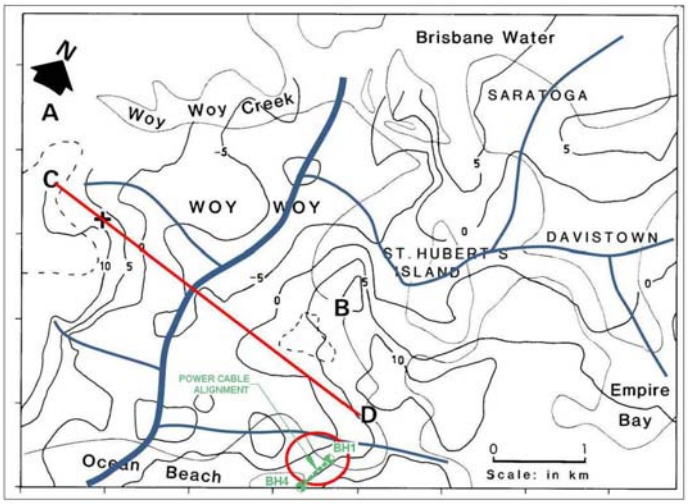

Figure 7: Interpreted gravity contour map, Brisbane Water. The conduit crossing is shown within the red circle.

Qureshi (1981) also provided an interpreted gravity along a 4 km length Line CD (Figure 7) that crosses the major north-south palaeochannel. This interpreted section is shown in Figure 8. The eastern end of this profile is only about 500 m north of the HDD crossing. A density contrast of -0.5 T/m^3 between the infilling sandy sediments and the sandstone/siltstone bedrock has been used to provide this interpreted bedrock profile. This density contrast is close to that used previously by Whiteley (2005) near Sydney Harbour and Botany Bay. Two palaeochannels are interpreted on Line CD. The major north-south trending channel is about 2 km wide and extends to a depth of about 70 m. Its eastern margin is marked by an interpreted bedrock high near Ch. 3 km that is inferred to represent a southern extension of Blackwall Mountain (marked by the dashed line in Figure 6) beneath the sands at Woy Woy. From Ch. 3 km to 4 km Line CD crosses near the northern margin of an interpreted palaeo-tributary (Figure 7) with bedrock at a maximum depth of about 40 m. This gravity interpretation suggested that a significant deepening of the bedrock from Wagstaffe to Booker Bay could be expected as the HDD crossing enters the palaeo-tributary from the southern side.

Figure 7 shows the approximate location of the two land boreholes BH1 and BH2 that were drilled for this project near the proposed landfalls of the HDD crossing. BH4 at Wagstaffe encountered extremely weathered sandstone beneath fill at about 2 m depth and BH1 at Booker Bay was drilled through mainly sandy sediments to about 23 m depth but did not encounter rock. This is consistent with the decreasing gravity values in the direction of BH1 towards the interpreted gutter of the east-west trending palaeo-tributary to the north of BH1.

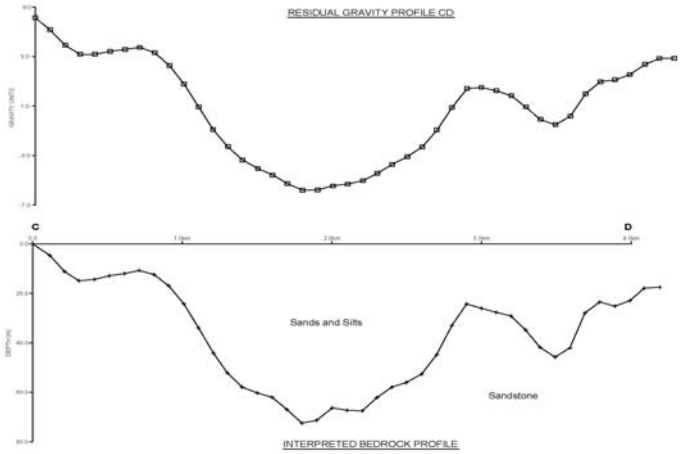

Figure 8: Interpreted gravity section on Line CD.

This interpretation led to the drilling of two additional overwater boreholes (BH2 & 3) along the HDD alignment and to a marine geophysical survey using both seismic reflection and underwater seismic refraction (USR, Whiteley and Stewart, 2008) methods.

Figure 9 shows the cable alignment with the borehole locations and trackplots for one of the reflection lines (CSP 1) and refraction lines (USR 3). CSP1 is adjacent to Wagstaffe and approximately orthogonal to the alignment while USR 3 follows the alignment near Wagstaffe but was deviated southward because of a shallow water shoal.

Figure 9 Marine reflection (CSP 1) and underwater seismic refraction (USR 3) trackplots with borehole locations.

The interpreted seismic record obtained along CSP1 is shown on Figure 10. A simplified borehole log for BH4 has been projected onto this record and the depth to rock correlates closely with the interpretation. The bedrock deepens rapidly to the north and south of the alignment.

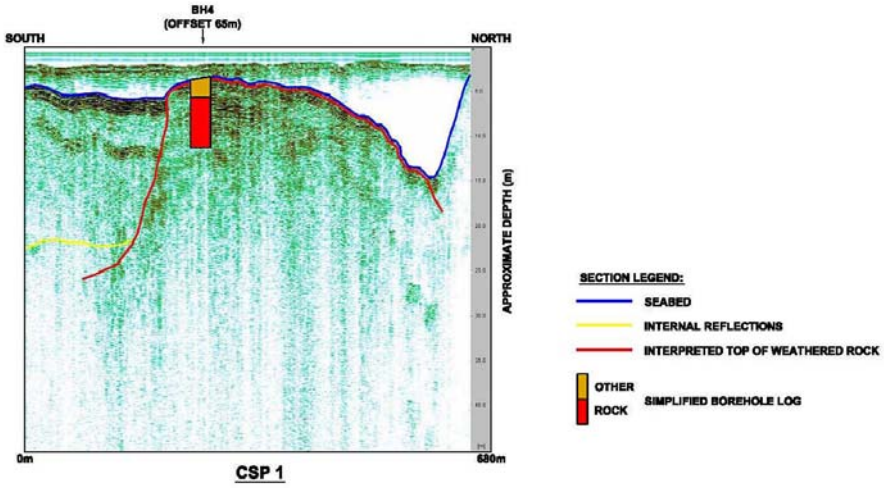

Figure 10 Interpreted seismic reflection record along CSP 1

The interpreted refraction section for USR 3 is shown on Figure 11 with simplified boreholes for the two overwater boreholes (BH 1 and BH 2) projected onto the line. The top of the weathered bedrock has been associated with seismic velocities greater than about 1900 m/s and is marked by the dashed line while the deeper base of the weathering has been associated with velocities in excess of 3000 m/s. The deeper interface has not been mapped along the entire line, however, the weathered rock extends along the alignment from at about 15m depth near the Wagstaffe shoreline then deepens rapidly to about 20 m to 25 m depth near BH 3, maintaining this level along most of the alignment.

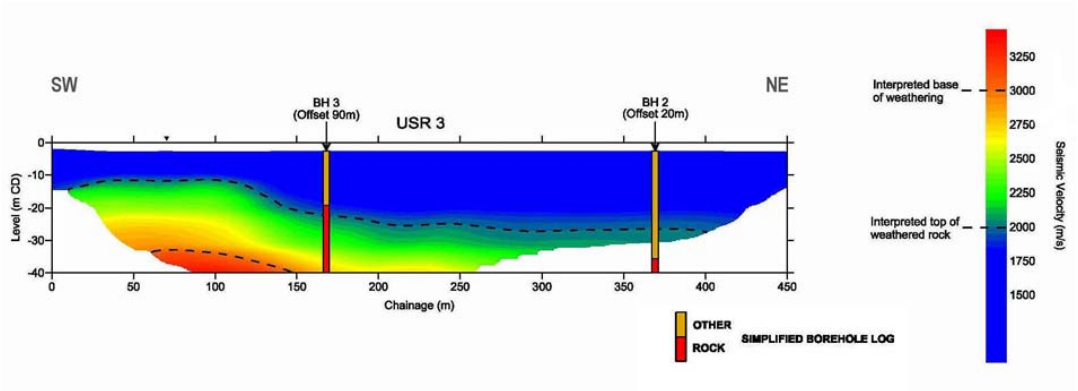

Figure 11 Interpreted underwater seismic refraction section along USR 3 with simplified borehole logs (see Figure 10.)

Using this information the power cable was recently installed in three welded sections from Wagstaffe to Booker Bay within in the HDD conduit that was created in rock 30 m below the floor of the river channel.

2.3 CASE STUDY 3: BEDROCK MAPPING, BROKEN BAY AND PITTWATER

Pittwater forms the southern arm of Broken Bay (Figure 1). Previous studies in this region by Albani and Johnson (1974), Albani *et al.* (1988) and Albani *et al.* (1991) have shown that Broken Bay was formed by fluvial erosion of Triassic sandstone during marine regressions with further erosion of the palaeochannels by coastal streams during the Pleistocene. Subsequent sea-level rise drowned this drainage system, forming the estuary and reworking the offshore sediments that presently fill the seaward section of the drowned palaeochannels. As part of a project to test an new airborne bathymetric and sub-seafloor mapping system (Vrbanchich *et al*., 2011) geophysical studies in Broken Bay were undertaken using continuous marine seismic reflection profiling supported by shallow vibrocoring. The objectives were to map the bedrock and to provide shallow sediment information to assist calibration of the airborne system.

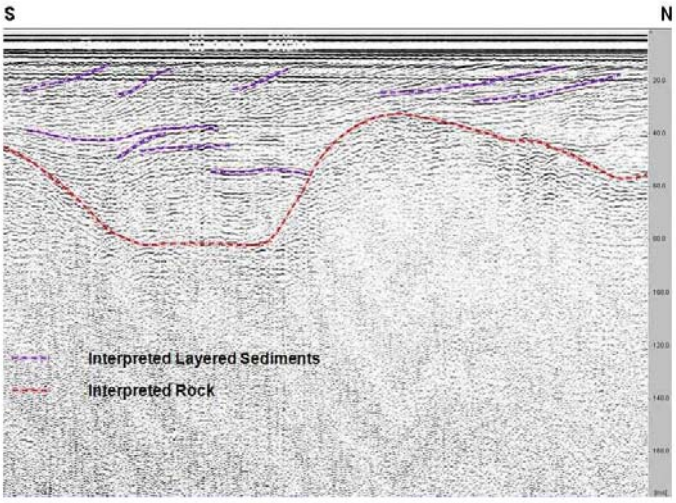

Figure 12: Interpreted seismic record near West Head (8, Figure 13).

Figure 12 shows an interpreted seismic record obtained along a transect near West Head (8, Figure 13). The southern end of this transect is on the left side Figure 12. This section is about 1 km long and uncorrected for tidal variations. Reflection travel time was converted to depth assuming average seismic velocities of 1550 m/s and 1700 m/s for sea water and marine sands respectively (Whiteley and Stewart, 2008). Coherent seismic reflectors, interpreted as representing sea floor, planar and steeply dipping sediment layers and an irregular bedrock interface were identified from the seismic records. The interpreted bedrock topography is highly irregular. Uncertainties could exist in the interpreted bedrock levels, especially where these levels are deep and/or steeply dipping.

Figure 13 shows the sediment sample locations and a contour plan of interpreted bedrock depths along the various seismic transects that were completed. The term 'bedrock' in this context implies a graduation rather than an abrupt interface as the boundary between sediments, partially weathered bedrock and fresh bedrock are not always clearly or unambiguously observed. The presence of indurated sediments (due to regression/transgression of sea level) can reduce the depth of penetration of the seismic signal at some locations. The acoustic impedance contrast between deeper sediments and the anticipated sandstone bedrock was variable suggesting the presence of very dense sands (i.e. tighter packing) and variably weathered sandstones.

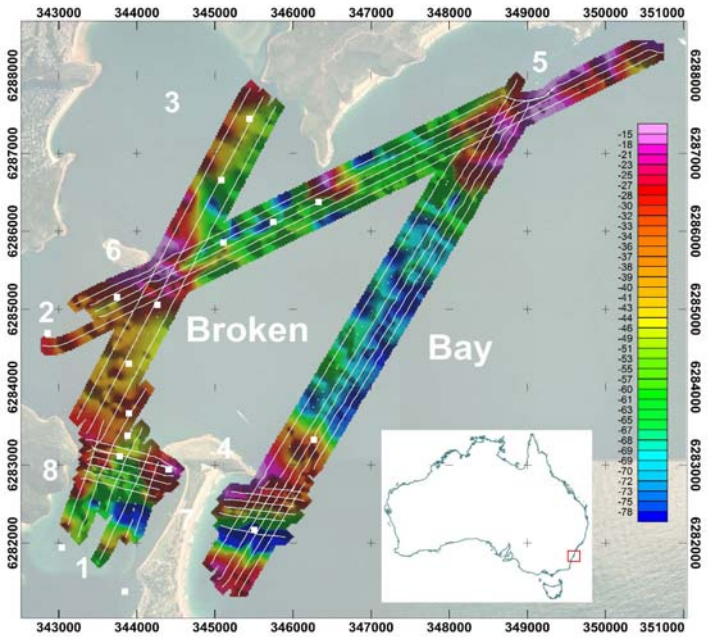

Figure 13: Contour plan of interpreted rock level in Broken Bay and the entrance to Pittwater.

Between West Head, 8 in Figure 13 and Barrenjoey Head (4, Figure 13) at the current entrance to Pittwater a relatively shallow rocky saddle linking these locations has also been mapped. To the south of this, in the area on the eastern and western sides of the Palm Beach tombolo a moderately narrow channel extends to levels down to approximately –90 m AHD with steep banks on either side. This may represent an earlier entrance to Pittwater and this interpretation is in good agreement with palaeochannel levels of approximately –100 m AHD beneath the Palm Beach tombolo obtained from an earlier seismic refraction study by Merrick and Greenhalgh (1990). These features were also detected by Albani *et al.* (1988) at similar depths. However, at some locations, between Lion Island (6, Figure 13) and West Head and in the main Hawkesbury River outlet in Broken Bay our interpreted bedrock levels differ from those presented by Albani and co-workers and are considerably shallower. In these areas, Albani *et al*. (1988) present bedrock contours with maximum depths of ~100 m and 140–180 m, respectively. Vrbanchich *et al*. (2011) provide additional discussion.

3 CONCLUSIONS

Case studies from recent infrastructure and research projects that were completed within the maritime zone near the mouth of the Hawkesbury River system clearly demonstrate the usefulness of marine seismic reflection, underwater seismic refraction and gravity technologies in mapping this extensive palaeodrainage system. These technologies support overwater geotechnical and geological investigations in this and similar environments.

4 REFERENCES

Albani, A. D., and Johnson, B. D., *The bedrock topography and origin of Broken Bay, NSW*: Journal of the Geological Society of Australia, 1974, **21**: p. 209–214.

Albani, A. D., Tayton, J. W., Rickwood, P. C., Gordon, A. D., and Hoffman, J. G., *Cainozoic morphology of the inner continental shelf near Sydney, NSW*: Journal and Proceedings of the Royal Society of New South Wales, 1988, **121**, p. 11–28.

Albani, A. D., Rickwood, P. C., Nielson, L., and Lord, D., 1991, *Geological and hydrodynamic conditions in Broken Bay, New South Wales*: Technical Contribution, No. 1, Centre for Marine Science, University of New South Wales, 1991, 88p.

Hughes, M. G., Harris, P. T., and Hubble, T. C. T., *Dynamics of the turbidity maximum zone in a micro-tidal estuary: Hawkesbury River, Australia*: Sedimentology, 1998, **45**, 397–410.

Martens D., editor, *Geomorphology of the Hawkesbury-Nepean River System*: Hawkesbury-Nepean Catchment Management Trust 1999.

Merrick, N. P., and Greenhalgh, S. A., *The use of anomaly offset in solving hidden layer refraction problems*: Geoexploration, 1990, **26**, 181–190.

Qureshi, I. R., *A gravity survey of Woy Woy district, New South Wales*: Exploration Geophysics, 1981, **12**, 4, 101-109.

Vrbanchich, J., Whiteley, R. J. , Caffi, P., and Emerson, D. W., *Marine seismic profiling and shallow marine sand resistivity investigations in Broken Bay, NSW, Australia*. Exploration Geophysics, 2011, **42**, 227-238.

Waddell. P. J., Whiteley, R. J. and Gilchrist, D., *Geotechnical and marine geophysical investigations of near-shore directional drilling alignments: a case study from the Hawkesbury River, Sydney*. ANZ 2012 Conference Proceedings, Melbourne 15-18 July 2012, 734-739.

Whiteley, R. J., *Gravity mapping and seismic imaging of large tunnel routes in Sydney, Australia:* in Near Surface Geophysics, D. W. Butler, ed., Investigations in Geophysics 13, Society of Exploration Geophysicists Tulsa, 2005, Ch. 15, 503-512.

Whiteley, R. J., and Stewart, S. B., *Case studies of shallow marine investigations in Australia with advanced underwater seismic refraction (USR)*: Exploration Geophysics, 2008, **39**, 34–40.

EQUIVALENT ABSOLUTE LATERAL STATIC STABILITY OF ON-BOTTOM OFFSHORE PIPELINES

Y. Tian[1] and M.J. Cassidy[2]
[1]Assistant Professor, [2]Professor, Centre for Offshore Foundation Systems and ARC Centre of Excellence for Geotechnical Science and Engineering, University of Western Australia, Perth, Australia

ABSTRACT

Although Dynamic Lateral Stability Analysis (DLS) is highly recommended for analysing offshore pipeline stability by authoritative recommended practice, namely DNV (2007) and PRCI (2002), it is still limited in its practical applications due to its complexity and because the software required is not widely available. In contrast, Absolute Lateral Static Stability (ALSS) analysis, in which the critical state is that the hydrodynamic loads on a pipe segment do not exceed the soil resistance, is still widely used in industry design. It is usual for ALSS analysis still to be based on the concepts of simplistic Coulomb friction model and the Morrison equation to account for soil resistance and hydrodynamic loading, although both are criticized for their conservatism and less theoretical basis. This paper presents a suite of new design charts with tabulated data using the Fourier method and pipe-soil models based within a plasticity framework for evaluating hydrodynamic loads and soil resistance, respectively. The results are presented as equivalent soil friction factors and hydrodynamic coefficients using the ALSS framework. These can be consulted by pipeline designers to give extra insight into an offshore on-bottom analysis without running the numerically complex DLS.

1 INTRODUCTION

One of the most fundamental engineering tasks in pipeline design is to secure on-bottom stability under the action of hydrodynamic wave and current loads. Offshore Australia, in regions such as the North West Shelf, the Capital Expenditure (CAPEX) cost of stabilization can reach 30% of the total pipeline (Brown *et al*., 2002). For shallow water case, light gas pipes, complex calcareous soil characteristics and harsh tropical storm loading can cause considerable challenges to the pipe stability design. Therefore, advanced stability analysis models and approaches are required.

Three approaches to the design of offshore pipelines for on-bottom stability are recommended in DNV-RP-F109 (DNV, 2007). In order of increasing complexity these methodologies are Absolute Lateral Static Stability (ALSS), Generalized Lateral Stability (GLS) and Dynamic Lateral Stability Analysis (DLS). These are summarized in Table 1.

Table 1 Comparison of the three pipeline stability analysis methods.

Analysis method	Stability criterion	Advantages	Disadvantages
ALSS	Static equilibrium	• Simple • Industry experience already accumulated • Quick and easy estimation	• Conservative • Lacking fundamental basis in fluid-pipe-soil interaction mechanisms (Coulomb friction and Morison Eq.)
GLS	Break-out (0.5D) or allow accumulated displacement (10D)	• Balance between ALSS and DLS • Relatively easy to use	• Empirical in nature • Not able to calculate the exact lateral displacement if weight and seastate are known • Limited flexibility and applicability
DLS	Lateral displacement can be set by operator	• Time domain dynamic analysis • Capable of modelling the entire sea state history, with a full displacement history provided • Can accommodate three-dimensional analysis of a long pipe • Incorporates modelling based on physical processes	• Requires experience to conduct • Few software packages available • Require complex soil-pipe models

ALSS is based on the static equilibrium of the forces acting on the pipeline, usually using the simplistic Coulomb friction and the traditional Morison equation to account for the soil resistance and hydrodynamic loading. This absolutely static criterion often leads to a heavy pipeline design and thus ALSS is frequently criticized as being conservative and lacking a fundamental understanding of fluid-pipe-soil interaction. Nevertheless, a large amount of

practical experience in the use of ALSS has been accumulated and it remains the most established and the computationally easiest approach.

The GLS approach suggested by DNV (2007) is a balance between the simplistic ALSS and more complicated DLS and is calibrated from DLS by using half or ten diameters as the allowable lateral displacement criterion. However, it is still empirical in nature and has limited flexibility.

DLS is considered to be the most comprehensive method as a complete calculation is performed in the time domain analysis. Unfortunately, DLS has not been widely used. Tørnes *et al*. (2009) ascribed the reason to limited software availability and also limitations within those available. With only two DLS packages available in literature, i.e., the American Gas Association (AGA) software package and PONDUS (Holthe *et al*., 1987; PRCI, 2002), the publication of Zeitoun *et al*. (2009) demonstrates the industry desire to develop applicable DLS package. In their DLS package SimStab, Morison equation and empirical soil model (Verley and Sotberg, 1992) are used.

The authors of this paper have developed a DLS package by implementing available force-resultant pipe-soil models and the Danish Hydraulic Institute (DHI) Fourier model into commercial finite element program ABAQUS (Dassault Systèmes, 2010). Force-resultant pipe-soil models relate the resultant vertical and horizontal forces on a segment of pipe to the corresponding displacement and represent a more fundamental understanding of the pipe-soil behaviour (Cathie *et al*., 2005; Zeitoun *et al*., 2008). Two models were employed to describe the pipe behaviour sitting on calcareous sand and clayey soil, respectively. Both developed from centrifuge tests in the University of Western Australia, the calcareous sand model was proposed by Zhang (2001) and Zhang *et al*. (2002) under drained condition while the clay model was presented by Hodder and Cassidy (2010) under undrained condition. These models were written as in-house code in Fortran 95 and further integrated into commercial finite element program ABAQUS through the UEL user subroutine. The Fourier hydrodynamic model developed from the DHI was reviewed and written in Fortran 95 program by Youssef *et al*. (2010). The implementation of this in-house code was verified to be correct by validating its prediction results against the DHI results in Sorenson *et al*. (1986). The details about the developing the DLS package are not shown and can be referred to Tian and Cassidy (2008, 2010) and Tian *et al.* (2011) as this paper does not intend to demonstrate developing process.

However, this paper does not conduct any full time-domain dynamic analysis in the DLS mode. On the contrary, this paper aims to develop a suite of reference charts and tables from two of its components, the hydrodynamic module and the pipe-soil interaction module, acting independently. These charts and tables provide a fast and preliminary estimation of pipeline stability. The paper aims to give pipeline engineers an additional assessment tool which has been developed using a new Fourier wave model and a novel plasticity approach for pipe-soil modelling.

2 DESIGN OF A PIPELINE USING THE WEIGHT PARAMETER *L*

The criterion for ALSS analysis is whether soil resistance is greater than the peak hydrodynamic load. If the concept of Coulomb friction and the Morison equation framework are used, the following formulation can be used to evaluate the absolute static stability:

$$\mu(W_s - F_Z) \geq \gamma_{sc} F_Y \quad \textbf{(1)}$$

where μ is the friction factor or soil resistance factor, W_s is the pipeline submerged weight, F_Y and F_Z are the in-line (horizontal) and lift (vertical) hydrodynamic forces (see Figure1 for illustration) and γ_{sc} is the safety factor. The following equations hold if F_Y, F_Z F_Y and F_Z are calculated using the Morison equation concept:

$$F_Y = \frac{1}{2} C_Y \rho_w D (U_w + U_c)^2$$

$$F_Z = \frac{1}{2} C_Z \rho_w D (U_w + U_c)^2 \quad \textbf{(2)}$$

where ρ_w is the water density, D is the pipe diameter and U_w and U_c are the wave and current induced water velocities, respectively. C_Y and C_Z are the horizontal and vertical coefficients, respectively.

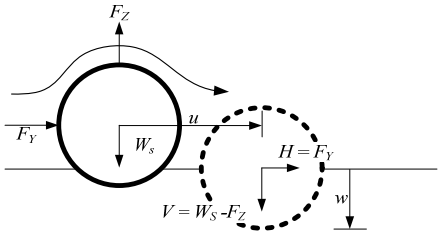

Figure 1: Symbol convention.

Following the DNV (2007), the weight parameter L can be defined as:

$$L = \frac{W_s}{\frac{1}{2}\rho_w D(U_w + U_c)^2} \quad \textbf{(3)}$$

By substituting Eq. 2 and 3 into Eq.1, the pipeline weight parameter L is:

$$L = \frac{\gamma_{sc} C_Y}{\mu} + C_Z \quad \textbf{(4)}$$

From Eq.4 we can see the pipe weight parameter L represents a direct and quick assessment of pipe weight design by counter balancing the two effects of hydrodynamic loading and the soil resistance. In this paper, equivalent hydrodynamic coefficients C_Y, C_Z and soil resistance factor μ are independently derived (as reference tables and charts) from the DHI Fourier model and the force-resultant pipe-soil models, respectively. These are not a function of the safety factor γ_{sc}. Further, the pipe weight can be evaluated from these charts for any specific sea state (later in the paper the pipe weight parameter L is presented for the most simplistic assumption of a safety factor γ_{sc} of 1, though it is noted that this may require recalculation for the most relevant safety factor for a location).

A large amount of analysis examples were conducted using the Fourier model. The peak hydrodynamic load (F_Y^*, F_Z^*) is converted into the equivalent peak hydrodynamic coefficients C_Y* and C_Z* as shown in the following equation in the sense of the traditional Morison equation:

$$C_Y^* = \frac{F_Y^*}{\frac{1}{2}\rho_w(U_w^* + U_c)^2}$$

$$C_Z^* = \frac{F_Z^*}{\frac{1}{2}\rho_w(U_w^* + U_c)^2} \quad \textbf{(5)}$$

where U_w* is the peak wave induced water velocity. As the force-resultant pipe-soil models are based on the "critical state" framework, there exists a "parallel point" on the yield surface where plastic flow is purely lateral sliding (i.e. no change in pipe penetration). At the parallel point, the model predicts the ultimate lateral resistance and the equivalent soil resistance factor μ^* can be calculated by normalizing the ultimate horizontal resistance with the vertical load.

The process of achieving the equivalent hydrodynamic coefficients and soil resistance factor is detailed in the following sections.

3 PEAK LOAD FROM FOURIER MODELS OF HYDRODYNAMIC CALCULATION

The basic idea of the traditional Morison equation is to calculate hydrodynamics loads using the ambient flow velocity and time invariant coefficients. Despite its extensive applications, it has been proven to give poor predictions of the hydrodynamic load acting on a pipe that is sitting on the seabed. This is especially true when a current velocity is superimposed on an irregular wave velocity, because the force coefficients are highly dependent on the current-to-wave ratio (M) and the Keulegan-Carpenter number (K) (Zeitoun *et al*., 2009; Verley *et al*., 1989; Verley and Reed, 1989; DNV, 2007). In fact, the ambient velocity approaching the pipe is modified by the wake sweeping back and forth over the pipe, and the force in one half-cycle is coupled by the previous half-cycle. To account for these facts, the Danish Hydraulic Institute carried out experimental tests, which was further employed to develop the Fourier model i.e. Sorenson *et al.* (1986). The concept of the Fourier model is fundamentally based on the fact that a periodic variation with a certain period T can be reproduced by superposition of a number of sine waves with periods of T/i (i=1,2,3…). A composition of nine harmonic sine waves can be used to calculate the drag force F_D and lift F_L on a pipeline:

$$F_{D,L}(t) = \frac{1}{2}\rho_w D U_w^2 \left[C_0 + \sum_{i=1}^{9} C_i \cos i(\omega t - \varphi_i) \right] \quad \textbf{(6)}$$

where ω is the angular frequency, t denotes time, U_w is the wave induced water velocity, and C_i and φ_i are the Fourier coefficients, which are functions of K and M. The Fourier models calculate the inertia force F_I using the same expression as the traditional Morison formulation but with a fixed inertia coefficient value of 3.29.

$$F_I(t) = 3.29\frac{\pi}{4}\rho_w D^2 a \quad \textbf{(7)}$$

where a is the water particle acceleration.

It should be noted that the DHI Fourier model rather than the DHI experimental test data were employed in this study, which was written in in-house Fortran 95 code and rigorously verified against the DHI report (i.e. Sorenson et al. 1986)

by Youssef *et al*. (2010). Suites of regular waves together with steady current with varying K and M were input into the in-house program and the peak in-line and lift forces $F_Y^*= F_D^*+ F_I^*$ and $F_Z^*=F_L^*$ were extracted. Consequently, the equivalent hydrodynamic coefficients C_Y^* and C_Z^* were calculated from the peak F_Y^* and F_Z^* using Eq.5. The calculated results of C_Y^* and C_Z^* are tabulated in in Tables 2-4 and are visually illustrated in Figures 2-4 accounting for fine, medium and rough pipeline surface condition.

It should be noted that the calculation results are valid in a certain range, i.e. K=10~70, M=0~1.2 because the Fourier model developed in Sorenson *et al*. (1986) is limited to this range. DNV RP-F109 (DNV 2007) is believed to be directly derived from the measured experimental data of the DHI tests (which were used to develop the Fourier model). Ideally, the DNV RP-F109 and this paper should have the same predictions if the Fourier model retrospectively predicts the experimental tests perfectly. As the Fourier model was believed to be verified in previous work (Jacobsen and Bryndum 1984; Sorenson et al. 1986; Fyfe et al. 1987; Bryndum et al. 1988), this paper assume the Fourier model can adequately predict the physical experiments. However, the discrepancy between the Fourier model and the experimental tests (if any) may lead to the disagreement between this paper's C_Y^*, C_Z^* and DNV's.

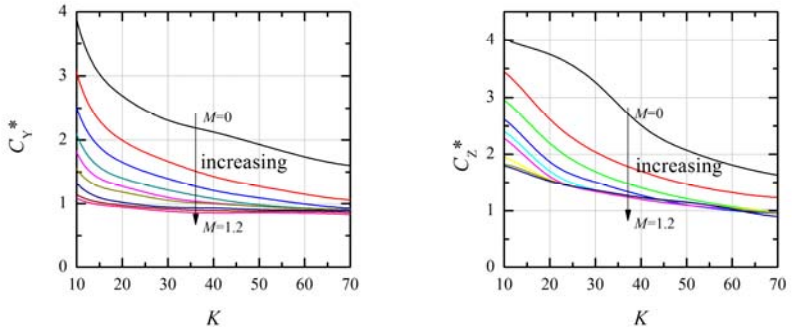

Figure 2: Peak load coefficients for fine pipe surface.

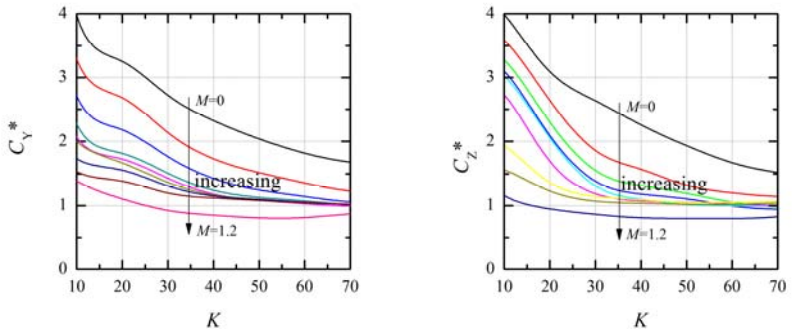

Figure 3: Peak load coefficients for medium pipe surface.

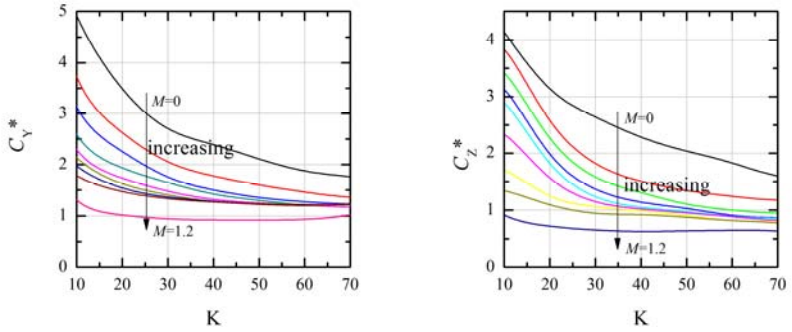

Figure 4: Peak load coefficients for rough pipe surface.

Table 2 Peak load coefficients of fine pipeline surface roughness

C_Y*		K							C_Z*		K						
		10	20	30	40	50	60	70			10	20	30	40	50	60	70
M	0	3.28	2.65	2.27	2.14	1.93	1.73	1.57	M	0	3.96	3.81	3.34	2.42	2.05	1.8	1.61
	0.1	2.56	1.94	1.66	1.41	1.27	1.15	1.03		0.1	3.56	2.54	2	1.69	1.45	1.32	1.2
	0.2	2.08	1.61	1.39	1.19	1.09	0.99	0.91		0.2	3.06	2.11	1.66	1.4	1.2	1.07	0.96
	0.3	1.69	1.38	1.21	1.07	0.97	0.93	0.90		0.3	2.73	1.74	1.51	1.26	1.09	0.93	0.94
	0.4	1.45	1.28	1.07	1.01	0.95	0.92	0.91		0.4	2.51	1.59	1.28	1.15	1.11	1.04	1
	0.6	1.30	1.19	1.03	1.00	0.95	0.92	0.91		0.6	2.38	1.48	1.28	1.25	1.21	1.18	1.02
	0.8	1.14	1.01	0.93	0.94	0.90	0.90	0.89		0.8	2.01	1.52	1.41	1.29	1.24	1.3	0.98
	1	1.05	0.97	0.91	0.89	0.88	0.88	0.87		1	1.76	1.63	1.43	1.33	1.26	1.34	0.92
	1.2	1.00	0.95	0.87	0.85	0.86	0.85	0.84		1.2	1.84	1.61	1.37	1.32	1.2	1.38	0.84

Table 3 Peak load coefficients of medium pipeline surface roughness

C_Y*		K							C_Z*		K						
		10	20	30	40	50	60	70			10	20	30	40	50	60	70
M	0	3.37	2.66	2.31	2.03	1.81	1.65	1.49	M	0	4.06	2.96	2.65	2.24	1.93	1.65	1.50
	0.1	2.80	2.08	1.70	1.51	1.36	1.19	1.11		0.1	3.71	2.60	1.74	1.60	1.28	1.20	1.12
	0.2	2.27	1.73	1.40	1.23	1.15	1.03	0.99		0.2	3.41	2.24	1.44	1.31	1.20	1.04	0.96
	0.3	1.88	1.49	1.21	1.12	1.08	1.00	0.98		0.3	3.24	2.01	1.28	1.17	1.12	0.98	0.93
	0.4	1.79	1.41	1.15	1.08	1.03	0.98	0.97		0.4	3.16	2.00	1.19	1.10	1.00	1.00	0.99
	0.6	1.70	1.34	1.14	1.10	1.05	1.01	1.00		0.6	2.88	1.54	1.13	1.06	1.06	1.02	1.00
	0.8	1.61	1.28	1.13	1.10	1.05	1.01	1.00		0.8	2.02	1.26	1.13	1.09	1.04	1.05	1.07
	1	1.43	1.16	1.12	1.08	1.04	1.02	1.01		1	1.61	1.18	1.05	1.04	1.02	1.01	1.05
	1.2	1.10	0.90	0.85	0.80	0.80	0.88	1.00		1.2	1.08	0.94	0.86	0.80	0.80	0.80	0.80

Table 4 Peak load coefficients of rough pipeline surface roughness

C_Y*		K							C_Z*		K						
		10	20	30	40	50	60	70			10	20	30	40	50	60	70
M	0	4.77	3.39	2.61	2.41	2.10	1.85	1.76	M	0	4.14	3.02	2.64	2.26	2.03	1.85	1.54
	0.1	3.37	2.60	1.99	1.77	1.59	1.46	1.33		0.1	4.02	2.43	1.75	1.49	1.33	1.24	1.15
	0.2	2.84	2.25	1.70	1.49	1.34	1.27	1.22		0.2	3.59	2.13	1.51	1.31	1.08	1.00	0.93
	0.3	2.33	1.91	1.64	1.40	1.30	1.20	1.17		0.3	3.30	1.83	1.31	1.12	1.04	0.89	0.86
	0.4	2.07	1.72	1.46	1.30	1.25	1.21	1.16		0.4	3.05	1.68	1.17	1.04	0.98	0.88	0.85
	0.6	2.03	1.58	1.40	1.26	1.24	1.22	1.21		0.6	2.45	1.46	1.10	1.02	0.95	0.89	0.80
	0.8	1.89	1.50	1.35	1.28	1.22	1.20	1.22		0.8	1.77	1.17	1.05	0.99	0.91	0.80	0.81
	1	1.71	1.45	1.32	1.27	1.22	1.19	1.22		1	1.37	1.07	0.92	0.93	0.88	0.81	0.80
	1.2	1.13	1.01	0.93	0.92	0.92	0.92	0.99		1.2	0.84	0.71	0.65	0.62	0.64	0.65	0.66

4 EQUIVALENT SOIL RESISTANCE FACTOR FROM THE FORCE-RESULTANT PIPE-SOIL INTERACTION MODELS

A key issue for pipeline on-bottom analysis is employing a realistic pipe-soil interaction model. In the past decades, various empirical models have been presented (most, if not all, were based on the simplistic Coulomb friction model), including those of Wantland *et al*. (1979), Brennodden *et al*. (1989), Wagner *et al*. (1989), Verley and Sotberg (1992) and Verley and Lund (1995). Recently, force-resultant models, such as those presented in Schotman and Stork (1987), Zhang (2001), Calvetti *et al*. (2004), Di Prisco *et al*. (2004), Hodder and Cassidy (2010) and Tian *et al*. (2010), have been increasingly used as an alternative. As preferred by Cathie *et al*. (2005) and Zeitou *et al*. (2008), these force-resultant models are based on a more fundamental understanding of the pipe-soil behaviour within the plasticity framework. Among these, the drained model developed by Zhang (2001) and Zhang *et al*. (2002) and the undrained model developed by Hodder and Cassidy (2010) are employed in this study. The former represent the drained pipe-soil behavior in calcareous sand while the latter describes the undrained behaviour in clayey soil. These models are briefly reviewed in the following sub-sections with the typical values of the parameters tabulated in Table 5. Full details of the models can refer to Zhang (2001), Zhang *et al*. (2002), Tian and Cassidy (2008) and Hodder and Cassidy (2010).

4.1 DRAINED MODEL FOR PIPES IN CALCAREOUS SAND

4.1.1 Bounding surface

The equation for the bounding surface is written directly in terms of the load (V, H) on the model (see Figure. 1 for the convention and Figure. 5 for an illustration):

$$F = |H| - \mu_D\left(\frac{V}{V_0} + \beta\right)(V_0 - V) = 0 \qquad \textbf{(8)}$$

where μ_D, β are the aspect ratios defining the surface shape and V_0 is the size of the yield surface representing the bearing capacity of the pipe under a purely vertical load at the current embedment (and noting that the parameter μ_D is not

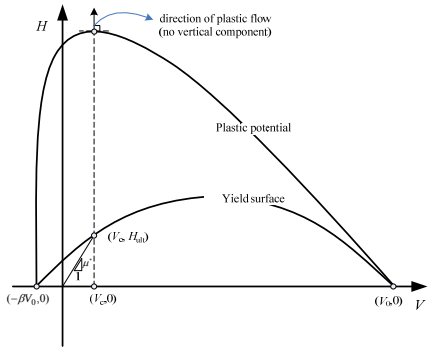

Figure 5: Illustration of drained model surfaces and definition of friction factor

4.1.2 Hardening law

The hardening of the bounding and yield surfaces is directly correlated with the vertical plastic displacement increment Δw^p as a change in surface size, as follows:

$$\Delta V_0 = \frac{k_{ve} k_{vp}}{k_{ve} - k_{vp}} \Delta w^p \qquad \textbf{(9)}$$

$$\mu_D = \mu_{D0} + \kappa \frac{w}{D} \qquad \textbf{(10)}$$

where the superscript p denotes a plastic component, κ is the slope of μ_D to w^p, and k_{ve} and k_{vp} are the elastic and plastic vertical stiffness.

4.1.3 Non-associated flow rule

The plastic potential surface maintains a similar shape and position as the inner yield surface (see Tian and Cassidy, 2008 for details).

$$g = |H - H_N| - \mu_t\left(\frac{V}{V_0} + \beta\right)^m (V_0 - V) = 0 \qquad \textbf{(11)}$$

where μ_t and m are aspect ratios controlling the shape of the plastic potential surface and H_N is the ordinate of the inner yield surface centre.

Table 5 Model parameters

parameters	*Model*	*Description*	*Dimension*	*Value*	*Unit*
k_{ve}	Drained	Elastic stiffness (horizontal)	F/L/L	8000	kN/m/m
	Undrained			$k_v s_{u0}$	
k_{he}	Drained	Elastic stiffness (vertical)	F/L/L	8000	kN/m/m
	Undrained			$0.925k_{ve}$	
V_0	Drained	Yield surface size	F/L/L	$\frac{k_{ve}k_{vp}}{k_{ve}-k_{vp}}w^p$	
	Undrained			$N_c s_{u0} D$	
k_{vp}	Drained	Plastic stiffness (vertical)	F/L/L	400	kN/m/
κ	Drained	Increase of yield surface size with normalized depth		0.65	
β	Drained	Aspect ratio of the yield surface (tensile capacity ratio)	-	0.06	-
μ_D	Drained	Aspect ratio of the yield surface	-	$\mu_{DS}+\kappa\frac{w}{D}$	-
μ_t	Drained	Aspect ratio of the plastic potential	-	0.65	-
m	Drained	Aspect ratio of the plastic potential	-	0.18	-
$h_{0,surface}$	Undrained	Dimension of yield surface (horizontal: no penetration)	-	0.147	-
η	Undrained	Tensile capacity (yield surface apex)	-	$\phi_{uplift}\eta_{deep}$	-
β_1	Undrained	Curvature factor for yield surface (low stress)	-	0.75	-
β_2	Undrained	Curvature factor for yield surface (high stress)	-	0.75	-
β_3	Undrained	Curvature factor for plastic potential (low stress)	-	0.65	-
β_4	Undrained	Curvature factor for plastic potential (high stress)	-	0.65	-
h_0	Undrained	Aspect ratio of the yield surface	-	$h_{0,surface}+\phi_b\left(h_{0,deep}-h_{0,surface}\right)$	-

4.2 UNDRAINED MODEL FOR PIPES IN CLAYS

4.2.1 Yield surface

The equation for the yield surface is shown as follows (referring to Fig. 7):

$$F=\frac{|H|}{h_0V_0}-\beta_f\left(\frac{V}{V_0}+\eta\right)^{\beta_1}\left(1-\frac{V}{V_0}\right)^{\beta_2}=0 \qquad \textbf{(12)}$$

where β_1,β_2,h_0 are aspect ratios defining the surface shape, η is the ratio of the intersection of the yield surface and V axis of V_0 and $\beta=\left(\beta_1+\beta 2\right)^{\beta_1+\beta_2}/\beta_1^{\beta_1}\beta_2^{\beta_2}\left(1+\eta\right)^{\beta_1+\beta_2}$ $\beta=\frac{(\beta_1+\beta_2)^{\beta_1+\beta_2}}{\beta_1^{\beta_1}\beta_2^{\beta_2}(1+\eta)^{\beta_1+\beta_2}}$.

4.2.2 Hardening law

The hardening of the yield surface is directly correlated to the vertical plastic displacement w^p as follows:

$$V_0=N_c s_{u0} D$$
$$\eta=\phi_{uplift}\eta_{deep}$$

$$h_0 = h_{0,surface} + \phi_h\left(h_{0,deep} - h_{0,surface}\right) \quad (13)$$

where N_c is a bearing capacity factor, s_{u0} is the undrained shear strength of the soil at the pipe invert, ϕ_{uplift} is a transition factor, η_{deep} is the tensile capacity at deep pipe embedment, $h_{0,surface}$ is the value of h_0 at zero embedment, $h_{0,deep}$ is the limiting value of h_0 and ϕ_h is a transition factor.

4.2.3 Flow rule

A slightly non-associated flow rule is used as the following:

$$g = \frac{|H|}{h_0 V_0'} - \beta'\left(\frac{V}{V_0'} - \eta\right)^{\beta_3}\left(1 - \frac{V}{V_0'}\right)^{\beta_4} = 0 \quad (14)$$

where V_0' is a dummy parameter defining the intersection of the plastic potential surface that passes through the current load point with the vertical load axis, β_3, β_4 are aspect ratios defining the plastic potential and $\beta' = \left(\beta_3 + \beta_4\right)^{\beta_3+\beta_4} / \beta_3^{\beta_3}\beta_4^{\beta_4}\left(1+\eta\right)^{\beta_3+\beta_4}$.

4.3 THE EQUIVALENT ULTIMATE SOIL RESISTANCE FACTOR μ^*

The force-resultant models used in this study are all based on the critical state concept, which assumes a parallel point exists on the yield surface. At the parallel point, the plastic flow continues while the size of the yield surface does not change. Physically, it represents the state that the pipe reaches the ultimate lateral resistance while it is sliding laterally (noting that this may not represent the largest horizontal load, but the final load causing sliding). As the hardening parameter is the vertical plastic penetration, the parallel points on the points are where the vertical plastic displacement increment becomes zero:

$$\frac{\partial g}{\partial V} = 0 \quad (15)$$

Substituting the flow rules into the above equation, the abscissa value of the parallel point can be derived:

$$V_c = \frac{m-\beta}{1+m}V_0 \qquad \text{drained calcareous sand model}$$

$$V_c = \frac{1+\eta}{2}V_0 \qquad \text{undrained clay model} \quad (16)$$

Physically, the ordinate value of the parallel point implies the ultimate lateral resistance, which can be evaluated as the following equations referring to Figure 5, Figure 6 and Figure 7:

$$H_{ult} = \mu_D m\left(\frac{1+\beta}{1+m}\right)^2 V_0 \qquad \text{drained model}$$

$$H_{ult} = \beta_f h_0 V_0\left(\frac{1+\eta}{2}\right)^{\beta_1+\beta_2} \qquad \text{undrained model} \quad (17)$$

Consequently, the ultimate equivalent soil resistance factor can be calculated as the slope of the parallel point (Figure 5 and Figure 6):

$$\mu^* = \frac{H_{ult}}{V_c} = \frac{\mu_D m(1+\beta)^2}{(1+m)(m-\beta)} \qquad \text{drained calcareous sand model}$$

$$\mu^* = \frac{H_{ult}}{V_c} = \beta_f h_0\left(\frac{1+\eta}{2}\right)^{\beta_1+\beta_2-1} \qquad \text{undrained clay model} \quad (18)$$

In the above equations, μ_D and h_0 are dependent on the pipe embedment. Therefore, μ^* is also related to the pipe embedment. Referring to Table 5, the μ^* can be evaluated from the above equations and the results are tabulated in Table 6. It is noted that although the relative pipe roughness will contribute to the soil resistance factor, it was not a parameter included in the plasticity models used in the derivation here. Equation 18 is therefore not a function of pipe roughness.

It is important to note that the physical tests used to develop the plasticity models sometimes required significant lateral displacements to mobilse the model's resistance to the parrallel point. For instance, recent centrifuge testing of Tian *et al.* (2010) showed some tests allowed a displacements of 2.5 diameters for drained calcaerous soils to reach the stabilised resistance. Therefore, this needs to be considered when employing the results of this paper, especially if smaller pipe displacements are required.

Cathie *et al*. (2005) summarized the soil friction factors from the existing literature, which is employed here to compare with this study's results. As shown in Figure 7, this paper's soil resistance factor is reasonably bounded by the existing data. The DNV RP-F109 recommended friction factors of 0.6 and 0.2 for sand and clay for the pipe without embedment effect. Lower bounding the data in Figure 7, this tends to result in a safe and conservative assessment of these available data.

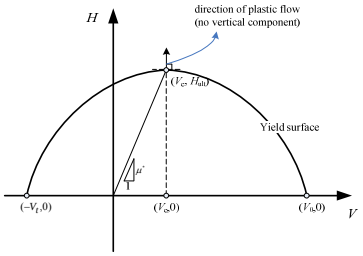

Figure 6: Illustration of undrained model surfaces and definition of friction factor.

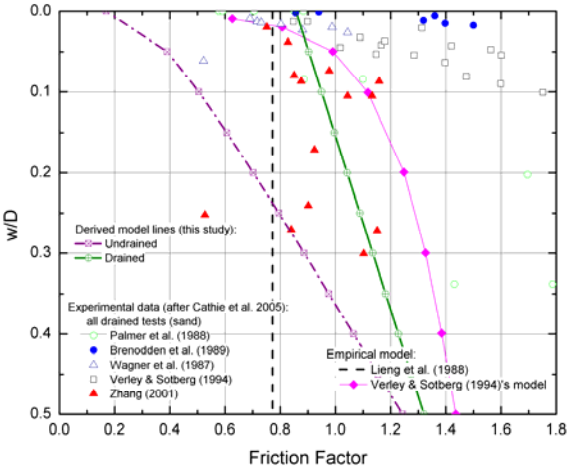

Figure 7: Friction factor.

5 DESIGN PIPELINE WEIGHT PARAMETER *L**

Following the derived equivalent hydrodynamic coefficients (Tables 2-4) and soil resistance factors (Tables 6 and Eq.18), it is straightforward to calculate the corresponding pipeline weight parameter *L** using Eq.4 (assuming a safety factor γ_{sc} of 1, though it is noted that different safety factors may be more relevant). As an example, Table 7 shows the weight parameter *L** with zero embedment and medium pipe roughness, which is further illustrated in Figure 8. As a comparison, the DNV RP-F109 hydrodynamic coefficients from Table 3-9 of DNV RP-F109 and friction factor of 0.6 are used to calculate the pipeline weight parameter *L** using Eq.4 and the results are shown in Figure 9. We can see that the DNV predicts a heavier pipe than this paper. For example, a weight parameter of 6.4 is obtained using the DNV code with *K*=20, *M*=0.2. In contrast, a value of 4.3 is predicted from this paper. Obviously, this discrepancy is mainly due to the difference soil resistance factor between DNV and this paper.

Table 6 Equivalent ultimate friction factor μ^*

w/*D*	0	0.05	0.1	0.15	0.2	0.25	0.3	0.35	0.4	0.45	0.5
Drained model	0.86	0.9	0.95	1	1.04	1.09	1.14	1.18	1.23	1.27	1.32
Undrained model	0.17	0.39	0.5	0.61	0.7	0.8	0.89	0.98	1.07	1.15	1.24

Table 7 Weight parameter *L** for medium pipe roughness with 0 embedment

*L**	*K*	*L**	*K*

(Drained)		10	20	30	40	50	60	70
M	0	7.98	6.05	5.34	4.60	4.03	3.57	3.23
	0.1	6.97	5.02	3.72	3.36	2.86	2.58	2.41
	0.2	6.05	4.25	3.07	2.74	2.54	2.24	2.11
	0.3	5.43	3.74	2.69	2.47	2.38	2.14	2.07
	0.4	5.24	3.64	2.53	2.36	2.20	2.14	2.12
	0.6	4.86	3.10	2.46	2.34	2.28	2.19	2.16
	0.8	3.89	2.75	2.44	2.37	2.26	2.22	2.23
	1	3.27	2.53	2.35	2.30	2.23	2.20	2.22
	1.2	2.36	1.99	1.85	1.73	1.73	1.82	1.96

(Undrained		10	20	30	40	50	60	70
M	0	23.8	18.6	16.2	14.1	12.5	11.3	10.2
	0.1	20.1	14.8	11.7	10.4	9.28	8.20	7.65
	0.2	16.7	12.4	9.68	8.55	7.96	7.10	6.78
	0.3	14.3	10.7	8.40	7.76	7.47	6.86	6.69
	0.4	13.6	10.2	7.95	7.45	7.06	6.76	6.70
	0.6	12.8	9.42	7.84	7.53	7.24	6.96	6.88
	0.8	11.4	8.79	7.78	7.56	7.22	6.99	6.95
	1	10.0	8.00	7.64	7.39	7.14	7.01	6.99
	1.2	7.55	6.23	5.86	5.51	5.51	5.98	6.68

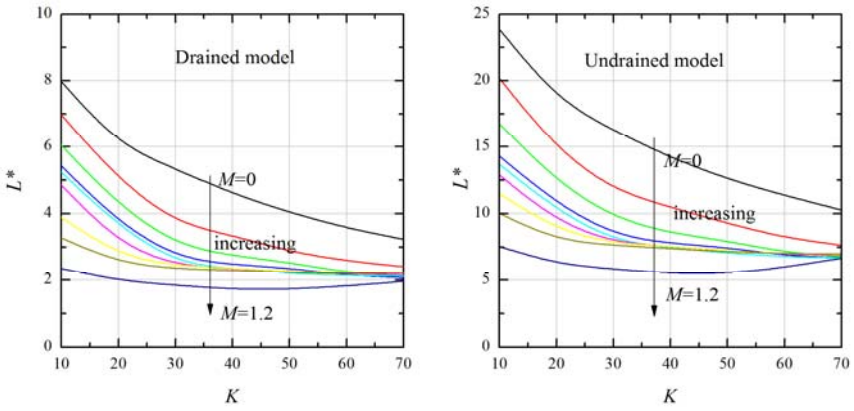

Figure 8: Weight parameter L^* for medium pipe roughness with 0 embedment

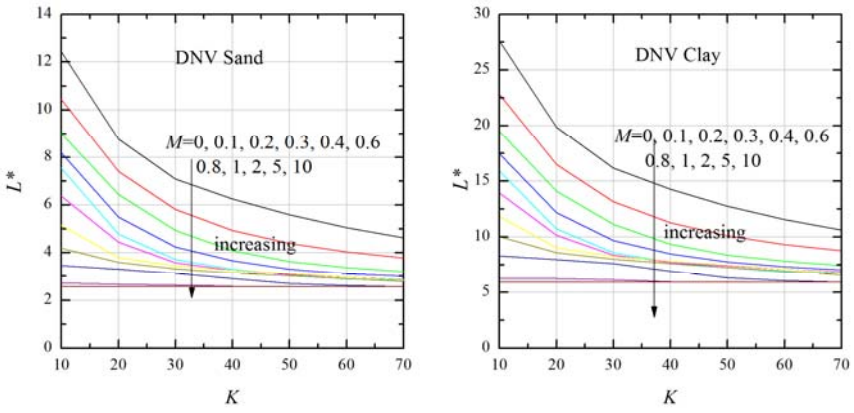

Figure 9: Weight parameter L^* from DNV

6 CONCLUSIONS

This paper achieved the equivalent hydrodynamic coefficients and soil resistance factors from independent Fourier wave and force-resultant pipe-soil models. Furthermore, the pipeline weight parameter design tables and curves were derived within an ALSS framework, which can provide a quick reference for and a preliminary assessment of a pipeline's on-bottom stability. The result of this paper does not intend to challenge the authoritative design practice DNV RP-F109. On the contrary, it aims to provide pipeline engineers extra insight into the stability design with alternative analysis approaches. Furthermore, it should not replace a detailed DSLA analysis with realistic pipe-soil and hydrodynamic modeling as this provides the more accurate and comprehensive prediction of pipeline displacement and penetration behaviour for a sea state's loading history.

7 ACKNOWLEDGEMENT

This research was undertaken within the CSIRO Wealth from Oceans Flagship Cluster on Subsea Pipelines with funding from the CSIRO Flagship Collaboration Fund and the Australia-China Natural Gas Technology Partnership Fund. The second author is the recipient of an Australian Research Council Future Fellowship and holds the Chair of

Offshore Foundations from the Lloyd's Register Foundation (LRF). LRF a UK registered charity and sole shareholder of Lloyd's Register Group Ltd, invests in science, engineering and technology for public benefit, worldwide.

8 REFERENCES

Brennodden, H., Lieng, J. T. and Sotberg, T. (1989). "An Energy-Based Pipe-Soil Interaction Model". *OTC*, Houston, Texas.

Brown, N. B., Fogliani, A. G. and Thurstan, B. (2002). "Pipeline Lateral Stabilisation Using Strategic Anchors". *Pro. of the Society of Petroleum Engineers (SPE) Asia Pacific Oil and Gas Conference*, Melbourne, Australia.

Bryndum, M. B., Jacobsen, V. and Tsahalis, D. T. (1988). "Hydrodynamic Forces on Pipelines: Model Tests". *Proc. 7th Offshore Mech. and Arctic Eng. Conf.*

Calvetti, F., Di Prisco, C. and Nova, R. (2004). "Experimental and Numerical Analysis of Soil-Pipe Interaction." *Journal of Geotechnical and Geoenvironmental Engineering ASCE* 130(12): 1292-1299.

Cathie, D. N., Jaeck, C., Ballard, J.-C. and Wintgens, J.-F. (2005). "Pipeline Geotechnics – State-of-the-Art". *Proc. of the Int. Symp. on the Frontiers in Offshore Geotechnics: ISFOG 2005*, Perth, Australia, pp 95-114, Taylor and Francis Group.

Dassault Systèmes. (2010). Abaqus analysis user's manual.

Di Prisco, C., Nova, R. and Corengia, A. (2004). "A Model for Landslide-Pipe Interaction Analysis." *Soils and Foundations* 44(3): 1-12.

DNV (2007). "On-Bottom Stability Design of Submarine Pipelines", DNV-RP-F109.

Fyfe, A. J., Myrhaug, D. and Reed, K. (1987). "Hydrodynamic Forces on Seabed Pipelines: Large Scale Laboratory Experiments". *Proc. 19th Offshore Tech. Conf.*

Hodder, M. S. and Cassidy, M. J. (2010). "A Plasticity Model for Predicting the Vertical and Lateral Behaviour of Pipelines in Clay Soils." *Geotechnique* 60(4): 247-263.

Holthe, K., Sotberg, T. and Chao, J. C. (1987). "An Efficient Computer Program for Predicting Submarine Pipeline Response to Waves and Current". *Proceedings of the 19thOffshore Technology Conference*, Houston, Texas.

Jacobsen, V. and Bryndum, M. B. (1984). "Determination of Flow Kinematics Close to Marine Pipelines and Their Use in Stability Calculations". *OTC*, Houston, Dexas.

PRCI (2002). "Submarine Pipeline on-Bottom Stability". PRCI. Project Number PR-178-01132

Schotman, G. J. M. and Stork, F. G. (1987). "Pipe-Soil Interaction: A Model for Laterally Loaded Pipelines in Clay". *OTC*, Houston, Texas.

Sorenson, T., Bryndum, M. and Jacobsen, V. (1986). "Hydrodynamic Forces on Pipelines- Model Tests". Danish hydraulic Institute (DHI). Contract PR-170-185. Pipeline Research Council International Catalog No. L51522e

Tian, Y. and Cassidy, M. J. (2008). "Modelling of Pipe-Soil Interaction and Its Application in Numerical Simulation." *Int. J. Geom. ASCE* 8(4): 213-229.

Tian, Y. and Cassidy, M. J. (2010). "The Challenge of Numerically Implementing Numerous Force-Resultant Models in the Stability Analysis of Long on-Bottom Pipelines." *Computers and Geotechnics* 37: 216-312.

Tian, Y., Cassidy, M. J. and Gaudin, C. (2010). "Advancing Pipe-Soil Interaction Models through Geotechnical Centrifuge Testing in Calcareous Sand." *Applied Ocean Research* 32(3): 294-297.

Tian, Y., Cassidy, M. J. and Youssef, B. S. (2011). "Consideration for on-Bottom Stability of Unburied Pipelines Using a Dynamic Fluid-Structure-Soil Simulation Fe Program." *International Journal of Offshore and Polar Engineering* 21(4): 308-315.

Tørnes, K., Zeitoun, H., Cumming, G. and Willcocks, J. (2009). "A Stability Design Rationale - a Review of Present Desgin Approaches". *Proceedings of the ASME 2009 28th International Conference on Ocean, Offshore and Arctic Engineering*, Honolulu, Hawaii, USA.

Verley, R. L. P., Lambrakos, K. F. and Reed, K. (1989). "Hydrodynamic-Forces on Seabed Pipelines." *Journal of Waterway Port Coastal and Ocean Engineering-Asce* 115(2): 190-204.

Verley, R. L. P. and Lund, K. M. (1995). "A Soil Resistance Model for Pipelines Placed on Clay Soils". *Proceedings of the International Offshore Mechanics and Arctic Engineering Symposium*.

Verley, R. L. P. and Reed, K. (1989). "Use of Laboratory Force Data in Pipeline Response Simulations". *Proceedings of the International Offshore Mechanics and Arctic Engineering Symposium*.

Verley, R. L. P. and Sotberg, T. (1992). "Soil Resistance Model for Pipelines Placed on Sandy Soils". *Proceedings of the International Offshore Mechanics and Arctic Engineering Symposium*.

Wagner, D. A., Murff, J. D., Brennodden, H. and Sveggen, O. (1989). "Pipe-Soil Interaction-Model." *Journal of Waterway Port Coastal and Ocean Engineering-Asce* 115(2): 205-220.

Wantland, G. M., O'Neill, M. W., Reese, L. C. and Kalajian, E. H. (1979). "Lateral Stability of Pipelines in Clay". *OTC*, Houston, Texas.

Youssef, B. S., Cassidy, M. J. and Tian, Y. (2010). "Balanced Three-Dimensional Modelling of the Fluid-Structure-Soil Interaction of an Untrenched Pipeline". *Proceeding of the 20th International Offshore (Ocean) and Polar Engineering Conference* Beijing, China.

Zeitoun, H., Tørnes, K., Cumming, G. and Branković, M. (2008). "Pipeline Stability - State of the Art". *Proceedings of the ASME 27th International Conference on Offshore Mechanics and Arctic Engineering*, Estoril, Portugal.

Zeitoun, H., Tørnes, K., Li, J., Wong, S., Brevet, R. and Willcocks, J. (2009). "Advanced Dynamic Stability Analysis". *Proceedings of the ASME 2009 28th International Conference on Ocean, Offshore and Arctic Engineering*, Honolulu, Hawaii, USA.

Zhang, J. (2001). "Geotechnical Stability of Offshore Pipelines in Calcareous Sand", University of Western Australia.

Zhang, J., Stewart, D. P. and Randolph, M. F. (2002). "Modelling of Shallowly Embedded Offshore Pipelines in Calcareous Sand." *Journal of Geotechnical and Geoenvironmental Engineering ASCE* 128(5): 363-371.

LANDSLIDE GEOMORPHOLOGY ALONG THE EXMOUTH PLATEAU CONTINENTAL MARGIN, NORTH WEST SHELF, AUSTRALIA

J.V. Hengesh[1], J.K. Dirstein[2] and A.J. Stanley[2]
[(1)] Centre for Offshore Foundation Systems at The University of Western Australia, M053, 35 Stirling Highway, Crawley, WA, Australia 6009; Email: james.hengesh@uwa.edu.au.
[(2)] TotalDepth,Pty 21 Churchill Ave, Subiaco, WA, Australia 6008; Email: jim@td.iinet.net.au

ABSTRACT

3D exploration seismic data were interpreted to investigate the locations and characteristics of submarine slope failures along the continental slope in the offshore Carnarvon Basin on Australia's North West Shelf. Seisnetics™, a patented genetic algorithm was used to process the 3D seismic data to extract virtually all peak and trough surfaces in an unbiased and automated manner. The extracted surfaces were combined in a 3D visual database to develop a seafloor digital terrain model that extends from the continental slope to the Exmouth Plateau. The 3D data were used to map the subsurface extent and geometry of landslide failure planes, as well as to estimate the thickness and volumes of slide deposits. This paper describes the geomorphic characteristics of six of the survey areas.

Geomorphic mapping shows the presence of slope failures ranging from small (<3 km across) to moderate (<10 km across) scale debris flows, rotational block failures, translational slides and topple failures, as well as large scale (>20 km across) mass transport complexes (MTC). The features are associated with debris flow chutes, turbidity flow channels, and debris fields. Analysis of failure planes show prominent grooves or striations related to the mobilization of slide material down both the continental slope and Exmouth Plateau and into the Kangaroo Syncline.

Submarine slope failures can occur at the continental shelf break in approximately 200 m to 300 m of water and run out to the Exmouth Plateau surface in approximately 1,100 m to 1,400 m water depths. The largest individual slides in the survey areas have widths of >30 km and minimum run-out lengths of 75 km, though associated turbidity flow deposits likely extend much further. The subsurface expression of the large MTCs illustrates a history of sediment accumulation along the mid-slope followed by repeated slope failure and debris run-out.

Sediment accumulation and slope failure processes are actively occurring along the continental slope and submarine landslides thus are a major driver of hazard to subsea infrastructure development. Smaller slides seem to occur more frequently than large slides and thus may pose a greater hazard to subsea infrastructure than large infrequent MTCs.

1 INTRODUCTION

As global energy demand continues to grow, numerous potential field developments are being identified in deep water along Australia's North West Shelf. A significant number of potential developments have been identified at depths of 500 to 1000 metres (m) or more, and several hundred kilometres from shore. Developments at these water depths necessarily mean that infrastructure elements are located below the continental slope, export systems might involve crossing the slope, and so system components potentially could be negatively affected by geohazards originating along the slope.

The primary driver of geohazard risk at these water depths will be slope failures and associated mass transport deposits. These types of failures can be amongst the largest earth movements in the world (Moore et al., 1989; Hampton et al., 1996; Masson *et al*., 2006) involving thousands of cubic kilometres of material, but it is not necessarily these large catastrophic failures that pose the greatest risk to marine infrastructure. Relatively frequent small failures can impose sufficient loads on infield and export systems to jeopardize system integrity.

The current publically available bathymetric data lack sufficient resolution to identify these features and so our research is being completed to map and characterize submarine slope failures using 3D exploration seismic data. This paper presents examples of several types of submarine slope failures and processes recognized along part of the continental slope adjacent to the Exmouth Plateau on Australia's North West Shelf.

1.1 GEOLOGICAL SETTING

The Exmouth Plateau encompasses part of the offshore Carnarvon Basin (Figure 1). This area is located on the northwestern margin of the Australian continent approximately 800 km to 1000 km south of the tectonically active boundary between the Australian and Eurasian tectonic plates.

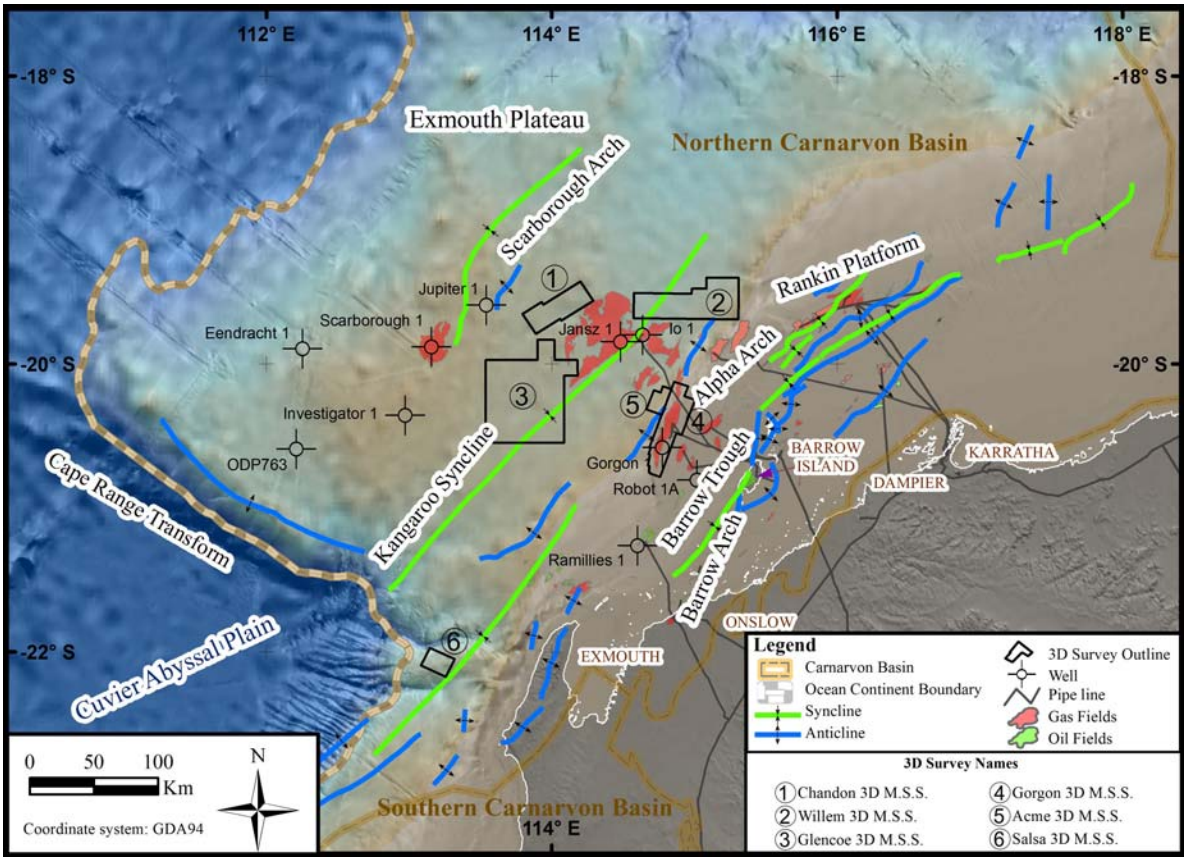

Figure 1: Regional tectonic and physiographic setting of the Exmouth Plateau. Grey polygons represent survey locations. Dark gray lines represent locations of sections shown on Figure 2. Coloured circles represent earthquake epicentre locations.

Sediments within the Carnarvon Basin (onshore and offshore) range in age from Silurian to Holocene and comprise 12 primary sedimentary sequences that reflect major depositional episodes (Hocking, 1990). Figure 2 shows two regional scale geological sections that illustrate the stratigraphic and structural relationships across Exmouth Plateau (modified from AGSO North West Shelf Study Group, 1994). The sedimentary sequences are each bound by erosional unconformities. There are three Palaeozoic sequences that formed during the Silurian, Devonian to early Carboniferous, and Late Carboniferous to Permian (Hocking, 1990). These deposits accumulated in a series of intra-continental rift basins that form the southern part of the late Palaeozoic-early Mesozoic Westralian Superbasin of Yeates *et al*. (1987).

Triassic to earliest Cretaceous sequences of the northern Carnarvon Basin (Figure 1) reflect development of the rift system related to fragmentation of Gondwanaland and separation of greater India from the western margin of the Australian craton. The sedimentary sequences formed in a variety of settings including a pre-rift trough during Triassic time, a rift valley in Jurassic time, and post-breakup troughs and trailing margin shelves during Cretaceous time (Hocking, 1990; Exon and Buffler, 1992; Exon *et al*., 1992; Baillie *et al*., 1994). The Late Cretaceous, Palaeocene to Early Eocene, Eocene, Oligocene to middle Miocene, and late Miocene to Holocene sequences are dominated by carbonate sediments that formed through progradation of the continental shelf (Hocking, 1990; Burchette and Wright, 1992) and carbonate-dominated hemipelagic sedimentation (von Rad and Haq, 1992; Boyd *et al*., 1992).

Many continental slopes define the transition from continental crust to oceanic crust. However, the Carnarvon Basin deposits that form the Exmouth Plateau represent a fragment of continental material that was stranded during the rifting process. It is bound by rift-related normal faults at the craton margin (AGSO North West Shelf Study Group, 1994) and is bound by abyssal planes on the north, west, and south. Therefore the continental slope on the Exmouth Plateau represents the transition from the continental shelf (proper) to a stranded continental fragment that stalled during the rifting process. Geological evidence of syn-rifting subaerial lava flows at the ocean-continent boundary (Figure 1), fluvial/subaerial depositional environments for pre-rift sedimentary sequences, as well as subsidence modelling (Kaiko and Tait, 2001) indicate that 1 km to 4 km of subsidence has occurred (from east to west) across the Exmouth continental margin between late Jurassic and Pleistocene time. This subsidence is a combination of post-rift tectonic

subsidence, thermal sagging, and sediment loading and is the driving mechanism that has led to the depressed elevation (i.e., deeper water depths) of the continental fragment that forms the Exmouth Plateau part of the Carnarvon Basin.

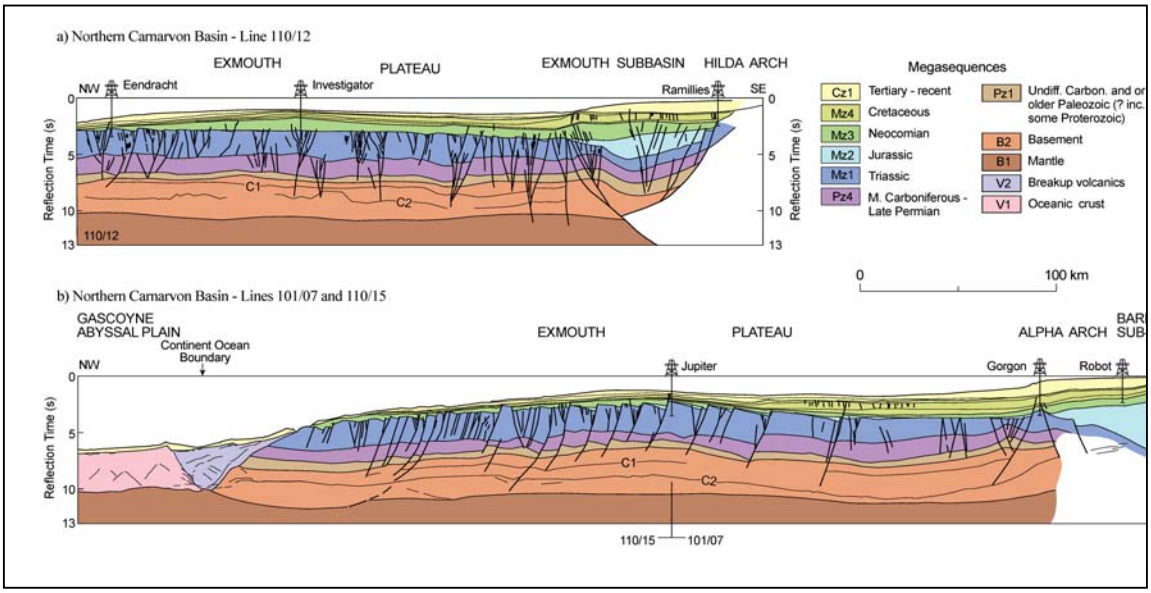

Figure 2: Regional geological sections showing major stratigraphic and structural relations across the Exmouth Plateau. Modified from AGSO North West Shelf Study Group (1994).

Former rift related extensional structures have undergone both transform and contractional reactivation leading to structural inversion of basin sequences both onshore and offshore. Reported relief across these structures varies from 300 m to 900 m (Hengesh *et al*., 2011a; Densley *et al*., 2000). This structural reactivation is widely attributed to the Neogene to Recent reorganization of the northern Australian plate boundary, but some structures may be as old as Cretaceous (Figure 3) (Boyd *et al*., 1992; Keep and Moss, 2000; Kaiko and Taite, 2001; Cathro and Karner, 2006; Keep *et al*., 2007). Some of these inversion structures underlie the continental slope and are targets for exploration activity. These inversion structures also are sources of gas and fluid venting as well as potential earthquake sources. Thus, slopes above inversion structures are susceptible to failure from several different triggering mechanisms (Hengesh *et al*., 2011b).

1.2 PHYSIOGRAPHY OF THE EXMOUTH CONTINENTAL SLOPE

The location and general physiography of the Exmouth Plateau is shown on Figures 1 and 4. The primary physiographic features in the Exmouth Plateau area include: (a) the continental shelf; (b) upper, middle, and lower continental slope; and (c) Kangaroo Syncline and Scarborough Arch. The continental shelf is generally defined as extending from the nearshore environment to the shelf break at approximately 200 m water depth. The continental slope is characterised by submarine canyon systems, smooth sedimentary fans and abrupt landslide scars. The elevation change across the slope is typically 400 m to 600 m. Average slopes along the canyon systems are in the order of 3 to 7 degrees (following interfluves), while the average slopes across the landside complexes are much higher with common 30 to 70 degree slopes.

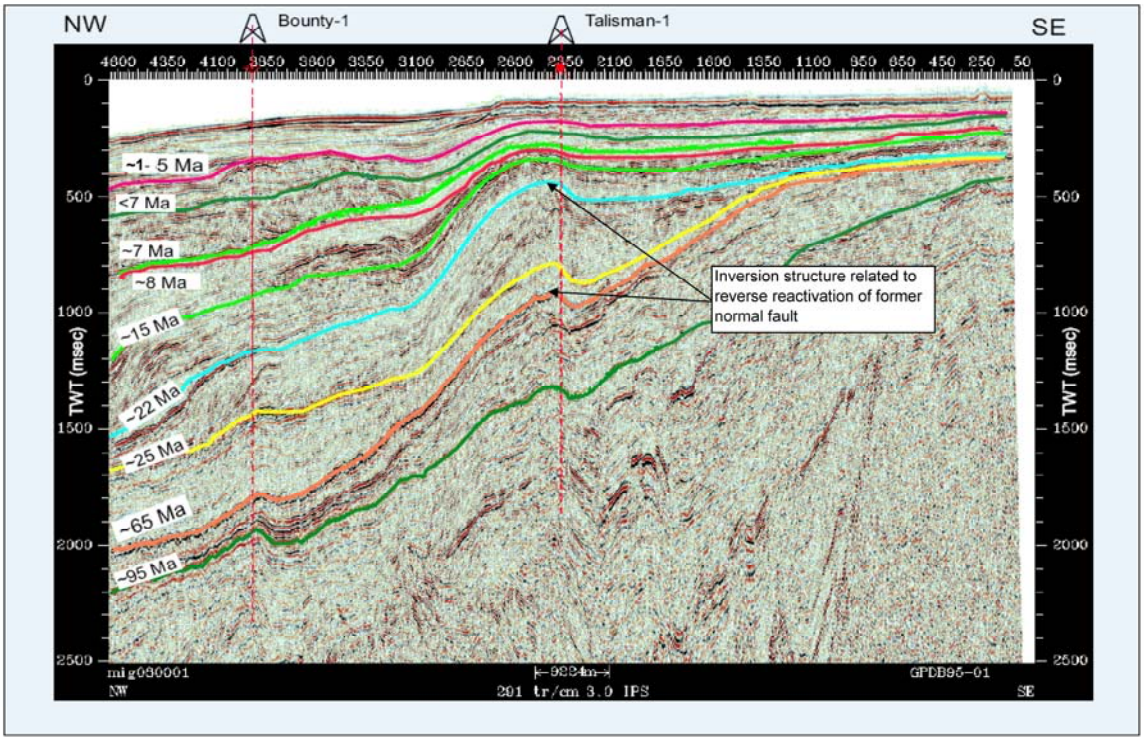

Figure 3: Example of late to post-Neogene inversion structure underlying the continental slope. Modified from Kaiko and Tait, 2001.

The continental slope extends from the shelf break to the Kangaroo Syncline at about 1,400 m water depth, where the lower slope adjoins the Exmouth Plateau. The plateau is a 350 km wide arch (in an east-west direction) that extends from the Kangaroo syncline at the base of the continental slope (~1,400 m depth), over the arch (~1100 m depth), to the continent-ocean boundary at approximately (~5000 m depth).

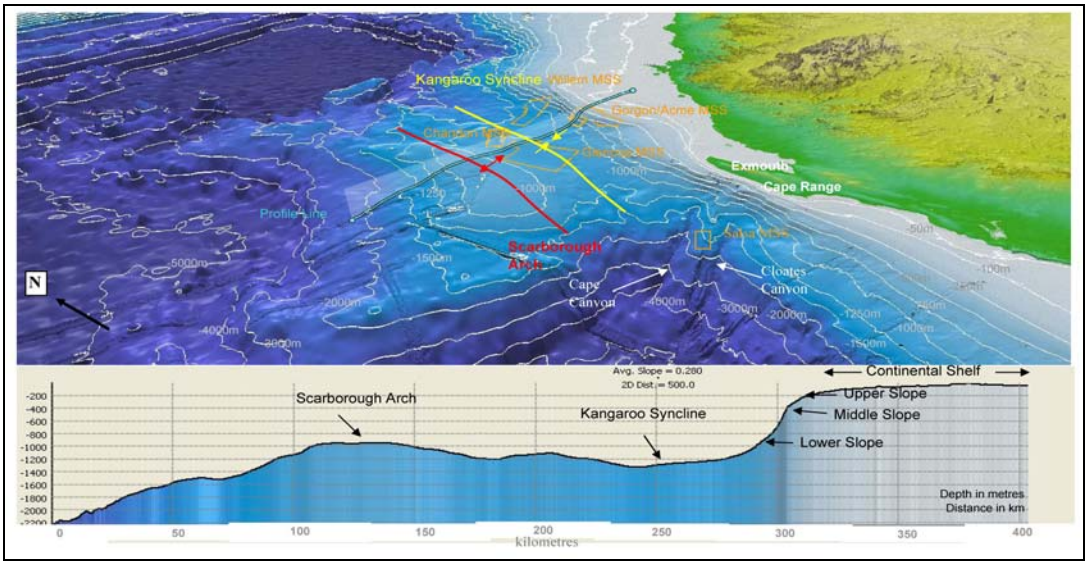

Figure 4: Oblique view to northeast across Exmouth Plateau showing major physiographic features and survey locations. Bathymetric data from Geoscience Australia. Vertical exaggeration 20 times.

Two important factors must be kept in mind when assessing the marine geomorphology and physiography in this region: (1) sedimentation rates in the pelagic environment are exceedingly low (von Rad and Haq, 1992) and thus even pronounced features in the landscape can have significant antiquity; and (2) hemipalagic sedimentation mantles former

seafloor features and thus the present seafloor geomorphology may in fact be mimicking a relict buried seabed. Relict seabed morphology can retain expression even under tens of metres of sediment.

2 LANDSLIDE PROCESSES ALONG EXMOUTH CONTINENTAL

The locations of submarine landslides along the North West Shelf are largely controlled by the relict seafloor topography that formed following Late Triassic to earliest Cretaceous continental rifting. The main relict topographic features where landslides occur include the continental slope and submarine canyons, the outer margins of the Exmouth Plateau, and along both the east and west facing limbs of Scarborough Arch (Figure 4).

Late Miocene to Recent collision of the Banda Arc and Australian continental plate and tectonic re-organization of Australia's northern plate boundary (Audley-Charles, 1986a, 1986b, 2004; Keep and Haig, 2010) has resulted in the reactivation of some faults along the former rifted margin of Western Australia (Whitney and Hengesh, 2013). The reverse reactivation of some of the former normal faults has resulted in the structural inversion of post-rift basin infills and has caused local arching and warping of the former relict sea-floor. Structures such as the Scarborough Arch and Kangaroo syncline (Figure 4) have increased seafloor slope gradients and reduced the stability of shallow, unconsolidated sediments.

Submarine landslides along the North West Shelf generally occur in Quaternary hemipelagic foraminiferal nanno-fossil ooze. These deposits have very high porosity, water content, void ratios and low strength profiles (Figure 5) (von Rad and Haq, 1992). Typical shear strength gradients in these shallow Quaternary age calcareous sediments are in the order of ~1 kiloPascal (kPa) per metre. These low shear strengths result in low residual stability of slopes and, given a triggering opportunity, a high slope hazard potential. The weak calcareous deposits overlie more competent Eocene and older sediments. Across parts of the Exmouth Plateau, the competent substrate includes polygonally faulted nanno-fossil chalk (von Rad and Haq, 1992). Figure 6 shows examples of the polygonally faulted substrate and a stacked series of large mass transport complexes (MTC) in the Willem survey area.

In other locations, such as the Bonaventure survey on the outer Exmouth Plateau (Dirstein *et al*., 2013), submarine landslides appear to be ancient features now draped by tens of metres to a few hundreds of metres of pelagic sediment. The large amount of sedimentary drape can indicate significant antiquity to these former landslide features. Because the sedimentation rates across the deep water parts of the Exmouth Plateau can be as low as 0.02 mm/yr (von Rad and Haq, 1992), the overlying sedimentary drape can be several million years old in these areas.

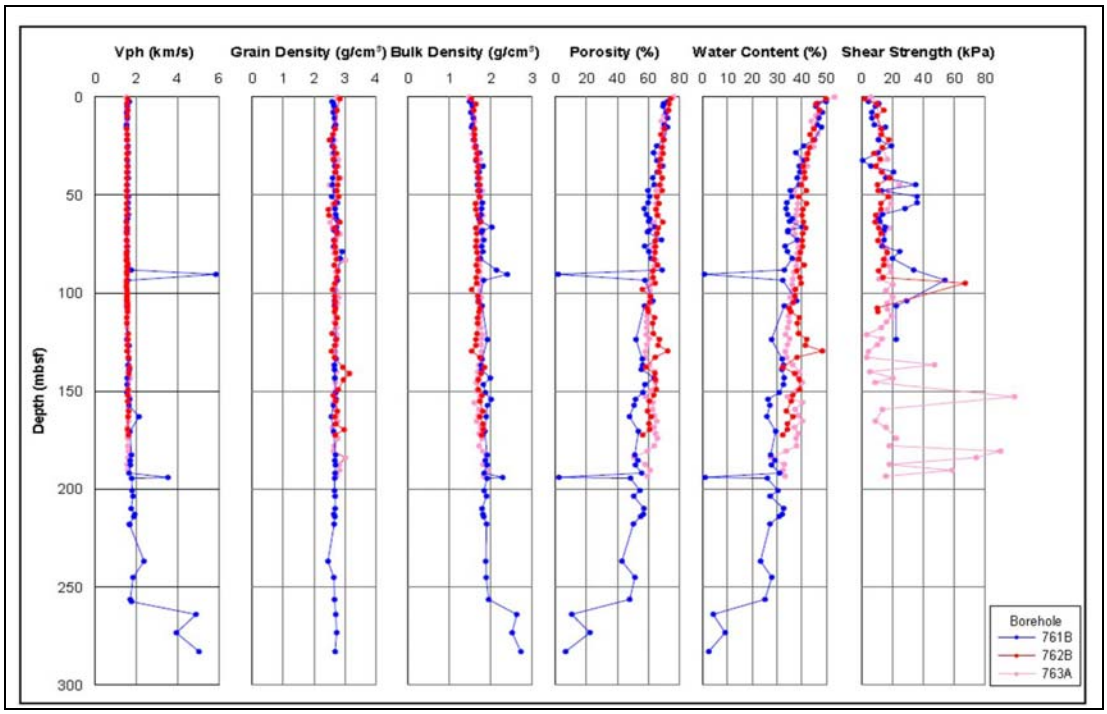

Figure 5: Sediment data from Ocean Drilling Project borings (ODP 761, 762, and 763) (von Rad and Haq, 1992).

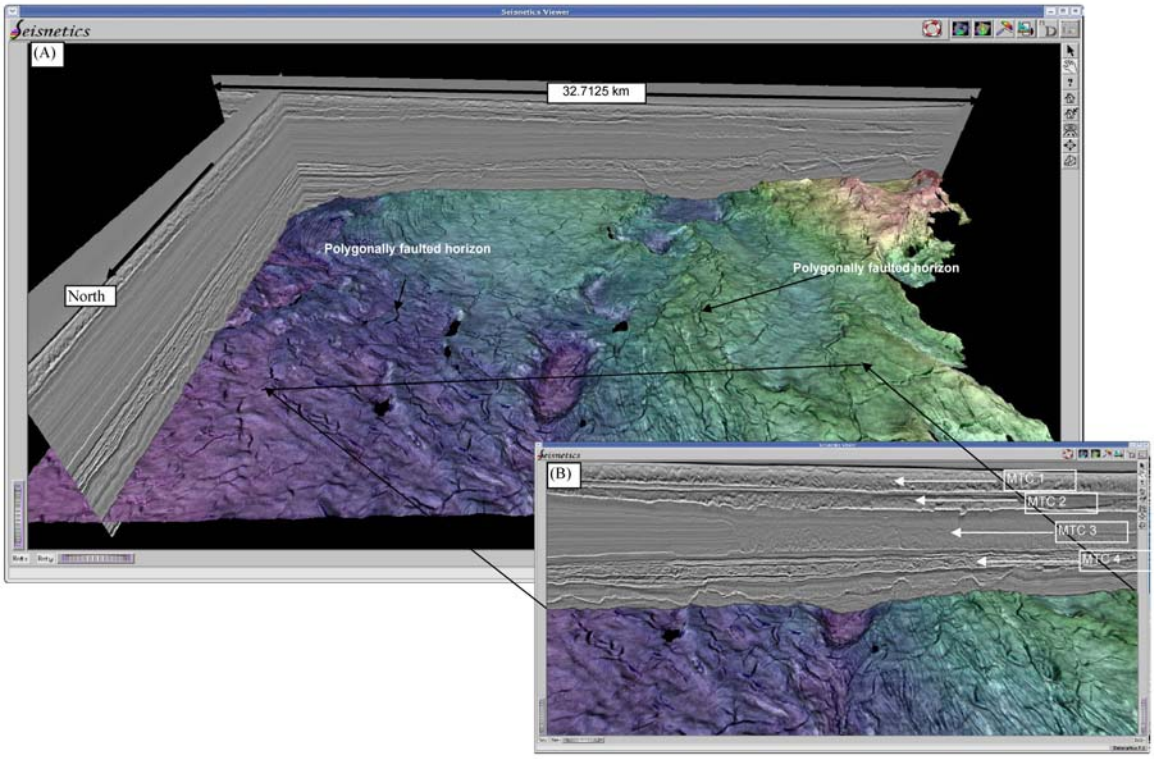

Figure 6: 3D perspective view to south across western end of Willem 3D seismic survey. The figure displays the combined Two-Way-Time and Amplitude attributes of GeoPopulation™ 130 from a subvolume of the Willem 3D survey in Seisnetics™. (A) The coloured horizon is a polygonally faulted chalk near the base of the nanno fossil ooze mobile section. (B) Arrows on inset image illustrate position of stacked submarine mass transport complexes (MTC) above the polygonally faulted chalk.

Sea-floor digital terrain models (DTM) were developed from open-file 3D exploration seismic data using Seisnetics™ (Dirstein and Fallon, 2011), a patented genetic algorithm that extracts virtually all trough and peak surfaces from 3D seismic data in an unbiased and automated manner. The extracted surfaces were combined in the 3D visual database and then the x,y,z coordinate data were imported to Fledermaus to develop the seafloor DTMs. The exploration 3D seismic data typically have bin spacing of 12.5 m to 25 m thus provide good resolution of seafloor features. The DTM's were used as a basis to map geomorphic features and assess processes occurring along the Exmouth Plateau continental slope. 2D profiles and 3D horizon maps also were used to assess the subsurface stratigraphy, seismic geomorphology, and characteristics of submarine landsides. Examples are shown for the Gorgon/Acme, Willem, Chandon, Glencoe and Salsa surveys.

2.1 GORGON/ACME SURVEY AREAS

The Gorgon survey covers an approximately 75-by-17 km area along the Exmouth continental slope (Figures 4 and 7). This has been combined with the smaller Acme survey, which provides partial coverage of the lower slope beneath the Gorgon survey area. The continental slope in the Gorgon area extends from approximately 200 m to 700 m water depth and includes four distinct morphologies including (from north to south): (a) the 35 km long 250 m high Slide 1 landslide headscarp; (b) the 20 km-long Slide 2 area of incipient slope failure lying above both submarine canyons and the Slide 1 headscarp; (c) a system of submarine canyons and debris flow chutes (referred to as Southern Canyons) and (d) a relatively smooth, sedimentary apron (fan) with little evidence of canyon formation or mass wasting. Concentrated fluid and gas expulsion features (pock marks) are common in the northern and central parts of the survey area and appear spatially associated with the Slide 1 and Slide 2 landslide failures; the expulsion features are less common in the Southern Canyons area, and are uncommon in the areas where there is a smooth sedimentary apron.

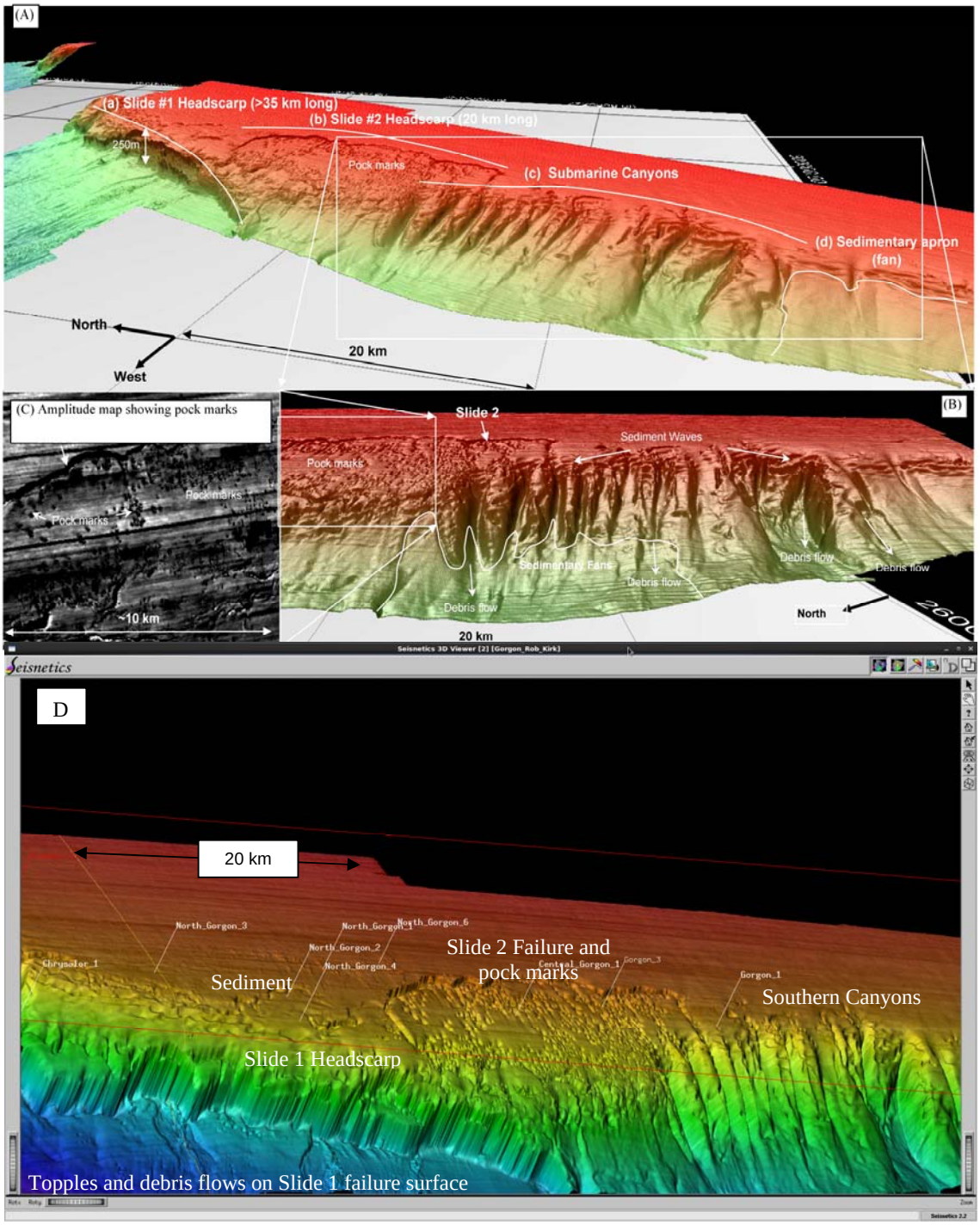

Figure 7: Perspective views of seafloor along Gorgon 3D survey area. (A) Shows four prominent morphological features along the Gorgon escarpment: (a) Slide #1 headscarp; (b) Slide #2 complex; (c) Submarine canyon system; and (d) Sedimentary apron or fan complex. Note also the extensive fields of pock marks in Slide #2 area. Inset image (B) shows the presence of sediment waves at top of submarine canyon complex and debris flow chutes. Inset (C) shows pock marks in Slide #2 complex. Some pock marks are up to 300 m across. Inset (D) shows perspective view of Gorgon Scarp including significant wells and Slide 1, Slide 2, and Southern Canyons (from Seisnetics 3D viewer).

The submarine canyon system in the southern part of the survey area has an average slope gradient of about 2 to 5 degrees: 4 to 8 degrees in the upper canyons; 2 to 4 degrees in the middle part of the canyons; and 1 to 3 degrees along the lower canyon and fan complexes. The individual canyons are approximately 5 to 8 km long and generally 0.8 to 1.6

km wide, though one canyon is 4.5 km wide (Figure 7(B)). Sedimentary fans are present at the base of the canyons and sediment waves have built up at the heads of the canyons. Relatively small (a few kilometres across) debris flows or translational failures are present at the base of the canyons and on the sedimentary fan, indicating instability of these slopes under static conditions. Sediment waves have formed near the top of the slope along the shelf break and provide sediment sources for down slope transport through the canyon systems and down the continental slope.

The landslide failure (labelled Slide 1 on Figure 7A) that occurred in the northern part of the Gorgon survey area extends from the upper slope in about 350 m of water to the lower continental slope in approximately 700 m of water. The slope gradient is 30 to 70 degrees and locally may be vertical (Figure 8). The slide is a minimum of 35 km wide and has a minimum run out length of 75 km, from the head scarp to the base of the lower slope in the Kangaroo syncline (Table 1). The basal failure surface coincides with a stratigraphic horizon that can be followed in the 3D seismic volume beneath the scarp and into the un-failed portions of the upper continental slope suggesting stratigraphic control on the location of the basal failure plain and slide geometry (Figures 8 and 9). The slide thickness was about 300 m. Note also the near vertical fault that projects from approximately 5.2 seconds two-way time (TWT) in the underlying inversion structure to the base of the landslide failure (Figure 9). This is a deep structure and if seismically active could be the source of the earthquake that triggered the Slide 1 and Slide 2 failures. A secondary kink band located several hundred metres west of the main fault extends to the near sub-bottom which implies recent structural deformation along the fault zone. The stratigraphy along the fault shows subtle drag folding. This folding increases the dip along east block of the fault (along the continental slope), creating a dip slope condition that reduces stability along the slope.

Extensive pockmarks and expulsion features are recognized on sea-floor terrane models (Figures 7D and 8). These features occur both within the slide mass, within drape over the former slide plane, and locally outside of landslide related features (Figure 8). Offset shallow stratigraphy and the thin layer of drape suggest that the slide is of late Quaternary age. Localised debris fields lie beneath the landslide headscarp and may be related to small scale debris avalanche or topple failures from the oversteepened scarp (Figure 8).

The submarine landslides observed within the Gorgon survey area are similar in scale to the large-scale MTC deposits observed in the subsurface of the Willem survey area (Figure 6). The slide geometry and MTC thicknesses suggest landslide volumes >50 km^3, but most likely between 50 km^3 and 100 km^3 Topple failures, debris avalanches, and debris flows sourced from the headscarp represent secondary retrogressive slope failures along the primary slide feature (Figure 8). These secondary failures can be several kilometres across with run-outs of 5 to 15 km. Erosion of the seabed also is occurring at the base of submarine canyons; these failures tend to be thin translational failures.

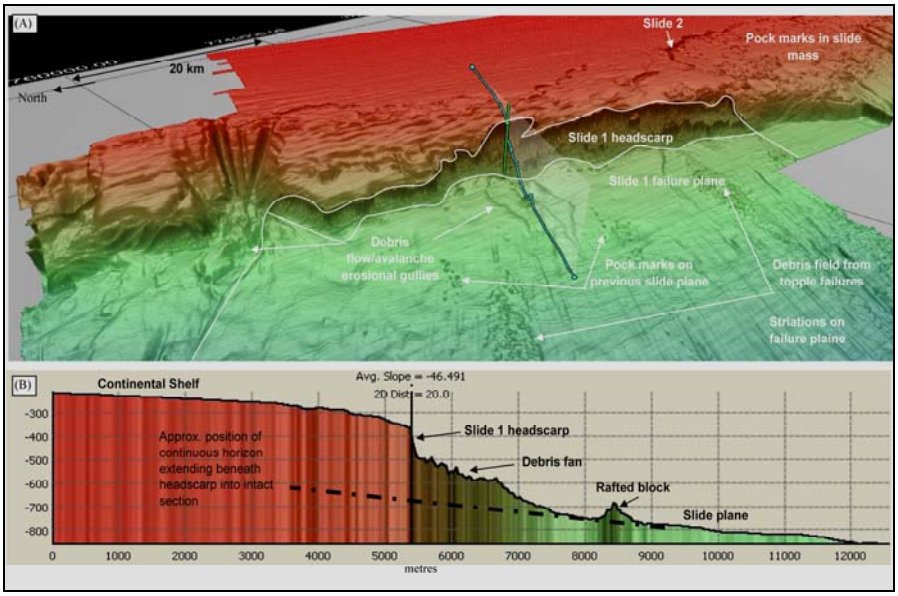

Figure 8: (a) Perspective view to east across Gorgon Slide #1 scarp. Note also the pockmarks, debris fields from topple failures and erosional channels near debris flow chutes. (b) Bathymetric profile across the scarp in the Gorgon survey area.

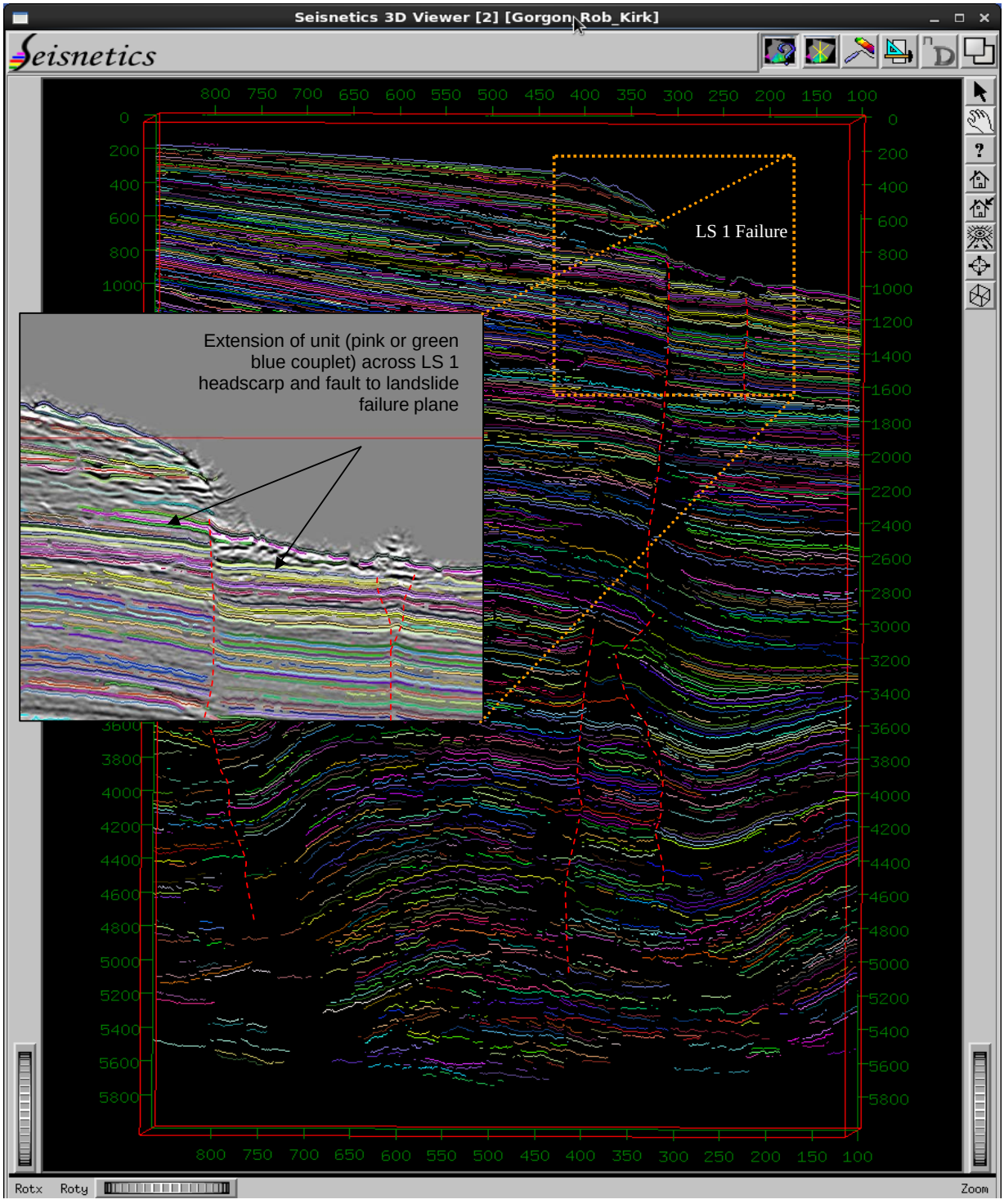

Figure 9: Cross line profiles of Gorgon 3D seismic survey showing Geopopulations™ associated with every mappable horizon. The pink horizon or the green blue couplet shown by arrows on inset diagram illustrate position of possible stratigraphic units that controlled the basal failure plain of the Gorgon Slide #1 failure. Note also the control of the headscarp position by the underlying fault.

2.2 WILLEM SURVEY

The Willem survey covers an area approximately 75 km long by 35 km wide along the Exmouth continental slope (Figure 4) 50 km northeast of the Gorgon survey. In this area the continental slope extends from approximately 250 to 1000 m depth (Figure 10). The survey area only captures a part of the upper continental slope, but includes a large part of the lower slope (Figure 10). The upper part of the continental slope has an average slope gradient of 7 degrees, while the lower slope has an average gradient of 1 degree.

The seabed rendering illustrates the presence of large debris fields below the escarpment extending approximately 55 km from the slope to the eastern edge of Kangaroo syncline (Figure 10). The debris field includes large (20 m to 60 m above seabed) landslide blocks located up to 13 km from the continental slope, and smaller debris blocks that extend to the Kangaroo syncline. These debris field deposits have been draped by hemipelagic sedimentation and sediment transported down slope, and have been eroded and incised by other younger debris flow deposits. Some of these younger debris flow deposits are observed extending over 35 km across the underlying debris fields on the lower slope (Figures 10 and 11). These underlying, older debris field deposits are associated with the nested large-scale MTC deposits observed at depth in the seismic volume (Figure 6).

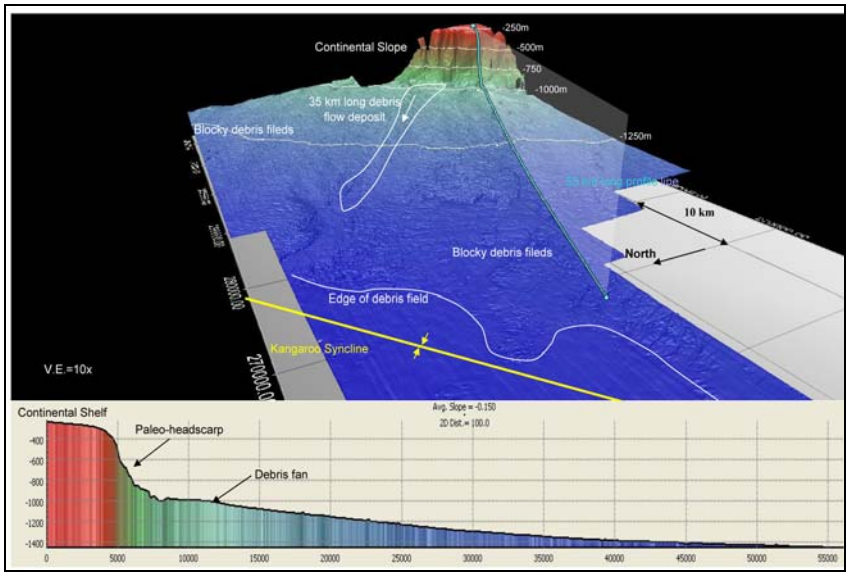

Figure 10: Seabed rendering of Willem survey area showing Kangaroo Syncline, continental slope in distance, MTC debris field along lower slope and other debris flow deposits overlying MTC debris field.

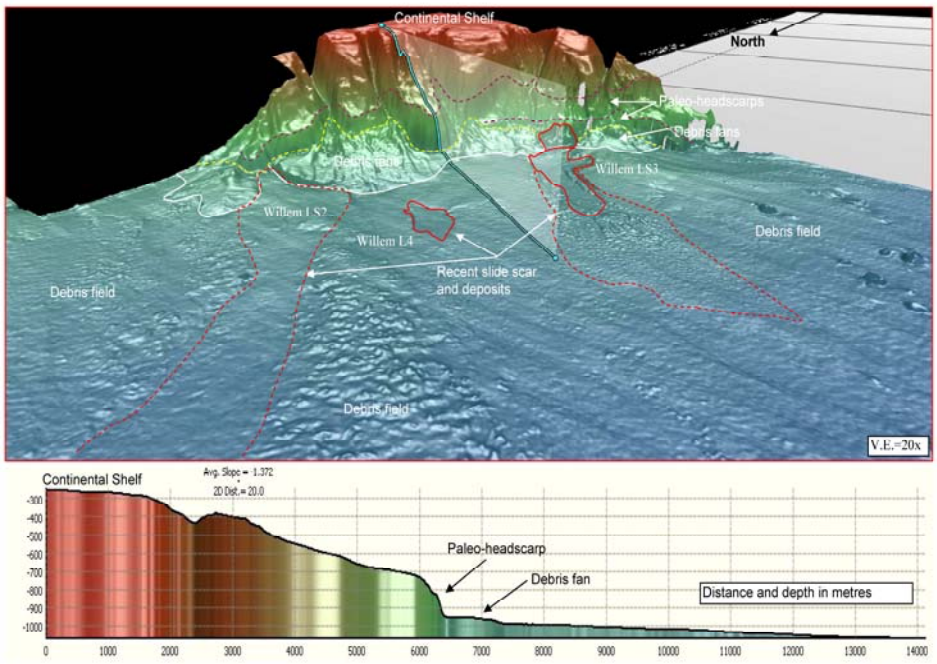

Figure 11: Palaeo landslide headscarp at base of Willem slope. Note also sedimentary fan development, and debris flow failure of fan complexes. Profile line is 14 km long and average slope gradient is 1.3 degrees.

In the Willem survey area the continental slope is oversteepened at its base. A partially buried scarp with slopes between 20^o and 66° is present at the base of the continental slope (Figure 11). This is inferred to be a palaeo-landslide headscarp. The headscarp is now partially buried by debris fans (Figure 11) shed from the slope. The debris fans dominantly form at the base of submarine canyons and coalesce into a complex of individual fans along the base of the palaeo-landslide headscarp. These fans have failed in two ways: (a) global failures of the entire fan complex leading to Mass Transport Complexes (Figure 6) and slide volumes of tens of cubic kilometres, and (b) local failures of individual fans at the base of canyons that have produced either rotational/debris flow events or translational slides that run down the lower continental slope. Several examples are shown on Figure 11. The southernmost example (Willem LS3) is about 1.7 km to 3 km wide and produced a scar approximately 7 km long. This failure is approximately 20 to 30m deep and occurred on a failure plane with a slope of 0.37^o to 0.95° (Table 1). The debris field from this event extends approximately 5 km beyond the slide scar. A retrogressive failure has expanded the landslide upslope into the debris fan complex (which has steeper seabed slopes of 5^o to 15°). The headscarp of the retrogressive failure is 60 m to 80 m high. The slope on the headscarp is up to 72°.

The large scale MTC deposits observed at depth (Figure 6) are on the order of 80 m to 100 m thick. The basal failure planes beneath these deposits show linear striations that illustrate direction of transport of the landslide mass. The striations shown on the horizon surface in Figure 12 comprise three populations: those coming from the continental shelf to the east; those coming from the Scarborough Arch to the west; and those moving down slope through the Kangaroo Syncline. The curvilinear striations indicate some slides initially moved straight down slope, but then turned northward into the Kangaroo syncline and likely continued down the axis of the syncline trough toward the Argo abyssal plain. A summary of slide parametres from the survey areas is included in Table 1.

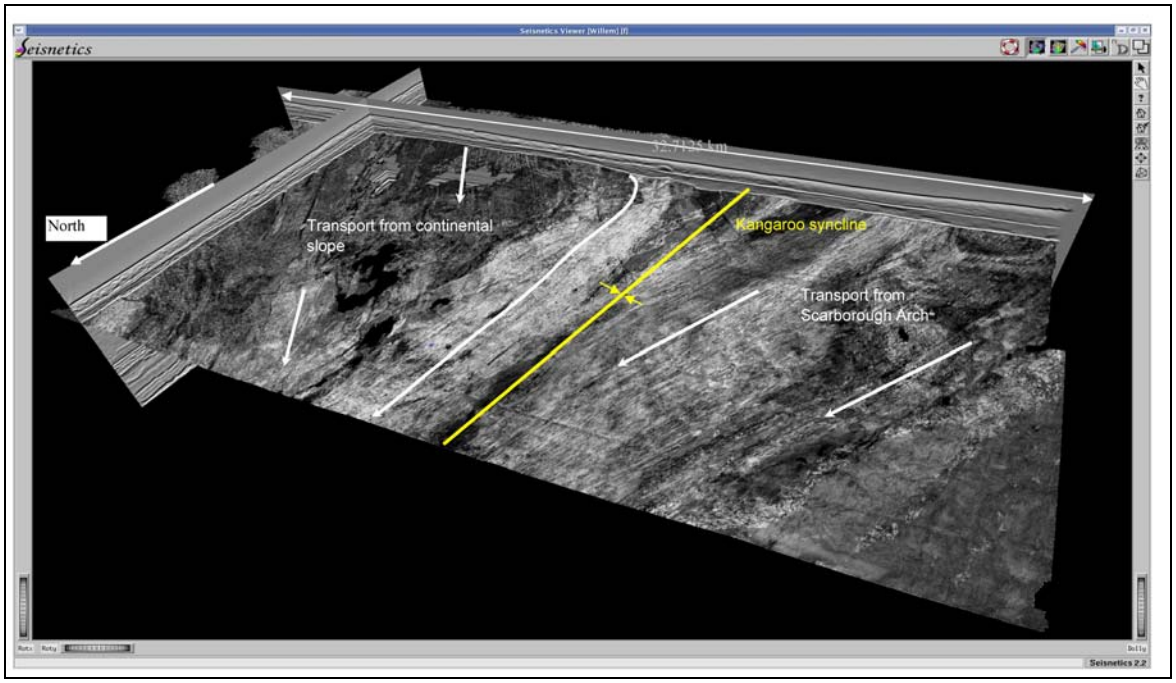

Figure 12: Striations on basal failure plane of MTC deposit, Willem survey.

Table 1: Summary of landslide parameters

Slide	Fairway Length (LS scar) (m)	Runout Length (Debris Field) (m)	Width (min) (m)	Width (max) (m)	Thick-ness (m)	Height Drop Failure zone (m)	Total Drop of Failure and Runout (m)	~Area (km^2)	~Vol. (km^3)	Ave Dip Failure Plane angle (degrees)/ distance (m)	Ave Stable Slope angle (degrees)/ distance (m)	Headscarp Ave Slope angle (degrees)/ distance (m)	Failure Mechanism	Velocity of down slope failure (qualitative)
Gorgon LS 1	8000	75000	35000	65000	300	500	800	540.0	162.00	2.0/7000	3.5/5000	21/270	Rotational/ debris flow	Rapid
Willem LS 1	16000	>40000	16000	22000	40	200	550	432.0	17.28	0.71/17000	0.9/1600	45/25	Translational	Moderate
Willem LS 2	7500	>40000	950	1400	55	110	550	12.38	0.68	0.8/7000	1.5/500	10/200	Rotational/ debris flow	Rapid
Willem LS 3	6000	5000	1700	3000	25	60	150	19.20	0.48	0.95/1110; 0.37/3500	0.67/5200	10.7/200	Translational	Rapid
Willem LS 4	2600	2600	1200	1200	8	35	65	4.68	0.04	0.5/2000	0.72/1800	2.3/166	Translational	Rapid
Chandon LS 1	11000	?	15000	17000	50	120	??	258.5	12.93	0.28/780	1.38/2780; 0.31/7460	10.8/450	Rotational	Slow
Glencoe LS 1	60000	?	30000	70000	25	80	80	3900	97.50	0.03/30000	0.16/10000	2.2/400	Translational	Slow
Salsa LS 1	15000	?	12000	16000	60	600	?	300	18.00	0.83/4940; 2.3/6000	1.3 to 2.4	5.5/520	Translational	Slow

2.3 CHANDON SURVEY AREA

The Chandon survey covers an area of approximately 17-by-25 km on the eastern limb of Scarborough Arch (Figure 4). The Chandon slide occurs on an east-facing slope between the Scarborough Arch and Kangaroo Syncline and extends from a depth of approximately -1180 m to at least -1300 m (Figure 13), and likely extends to a depth 1550 m in Scarborough trough. The Chandon slide is transporting sediment from Scarborough Arch eastward into the Kangaroo syncline. The slide has a width of 15-20 km and a visible length of 11 km, but a likely total length of >30 km. The average slope gradient within the slide mass is less than 0.28 degree, however, steeper slopes of 1.4° and possibly up to several degrees are present down slope (out of the survey area (Figure 4). The slide has a rotational failure mechanism and the mass is composed of rotational slide blocks (Figure 13) that are mobilized above the extremely low angle failure plane. At the point of initial detachment from the headscarp, the rotational blocks are up to 40 m high and 1.5 km across and 6 km long. The low angle of the failure plane and internal coherence are evidence that this is a "slow" failure. A distinctive feature of the slide morphology is the lateral mote that follows the base of the head scarp (Figure 14). Large gas/fluid expulsion features are present above the headscarp on the south side of the landslide complex. These gas/fluid vents are 650 m to 2000 m across and form a field of pockmarks that is at least 8 km across. The association the gas expulsion features with the landslide suggests gas/fluid expulsion may have been the triggering mechanism for this event. The process of gas/fluid expulsion may localize future slope failures in this area.

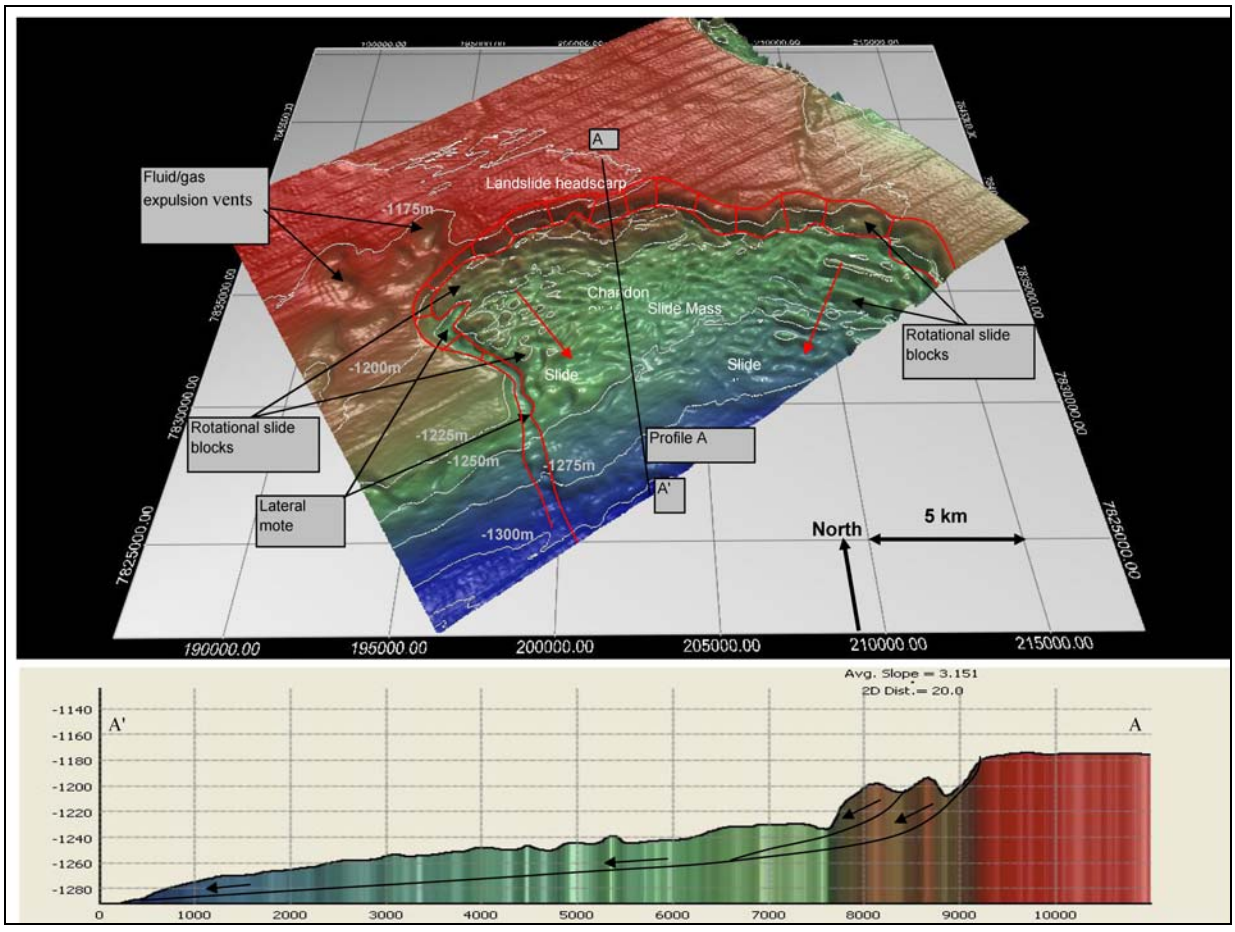

Figure 13: Seafloor rendering of the Chandon slide, northeastern Scarborough Arch. Regional relations suggest the slide should connect to a larger slide down slope and extend approximately 35 km to the trough axis. The slide mass shown is 17 km wide and 10 km long (to the limit of survey).

2.4 GLENCOE SURVEY AREA

The Glencoe survey encompasses an area of approximately 60-by-65 km in the central trough of the Kangaroo syncline and part of the eastern limb of Scarborough Arch, about 20 km southwest of the Chandon survey area (Figure 4). The axis of the Kangaroo syncline in the survey area is characterized by very gentle slopes. The seabed along the syncline axis slopes from south to north between 0.08° and 1.5°. The western part of the survey area is characterized by a greater

than 65 km long topographically sharp 10 m to 20 m high curvilinear scarp with a down to the east sense of displacement (Figure 14). The slope leading from the axis of the Kangaroo syncline up to the scarp is characterized by a rhythmic ripple type structure (Figure 14 and 15). The ripples have amplitudes of up to 2 m, but the amplitude is highest near the scarp and diminishes down slope toward the axis of the Kangaroo syncline. The ripples (Figures 15A and B) are formed by drape that overlies or mantles blocks of displaced sediment (Fig 15C) that lies above a low angle failure plane. The blocks of displaced sediment appear to be rafted along the low angle detachment and the edges of the failure are defined by distinct lateral margins seen in the seismic horizon (Figure 15A). The white ovals on Figure 15C also show areas of gas migration associated with the displaced blocks. The average gradient of the slope, over the 20 km distance leading up to the scarp, is 0.032°; this also approximates the dip of the failure plane (Table 1). The coherent displaced blocks that characterize the Glencoe slide are likely a form of mega-flow failure. The presence of gas suggests this might be a triggering mechanism; however, pock marks are not common on the surface. Therefore, another mechanism, such as earthquake loading, may have triggered this failure. The low angle of the failure plane and internal coherence are evidence that this is a “slow” failure.

Slope gradients across the southeastern corner of the survey area, on the extreme lowermost part of the continental rise are generally less than 0.2 degrees. However, debris or earth flow lobes are observed in this part of the survey area in water depths of 1120 m to 1220 m (Figures 14 and 16). These form the leading edge of a landslide complex and lower continental slope deposits that originated 75 km to the east along the slope (Figure 4). The sediment lobes shown on Figure 16 are each about 10 km to 12 km wide and the easternmost lobe shows crevasse fields, internal shears, and prominent lateral shear margins (Figure 17). Secondary flows are present on the edges of the lobes. The lobes are interpreted to be the front of a landslide complex that has moved down the lower continental slope and into the Kangaroo Syncline. The lobes are likely moving slowly, perhaps analogous to a glacier.

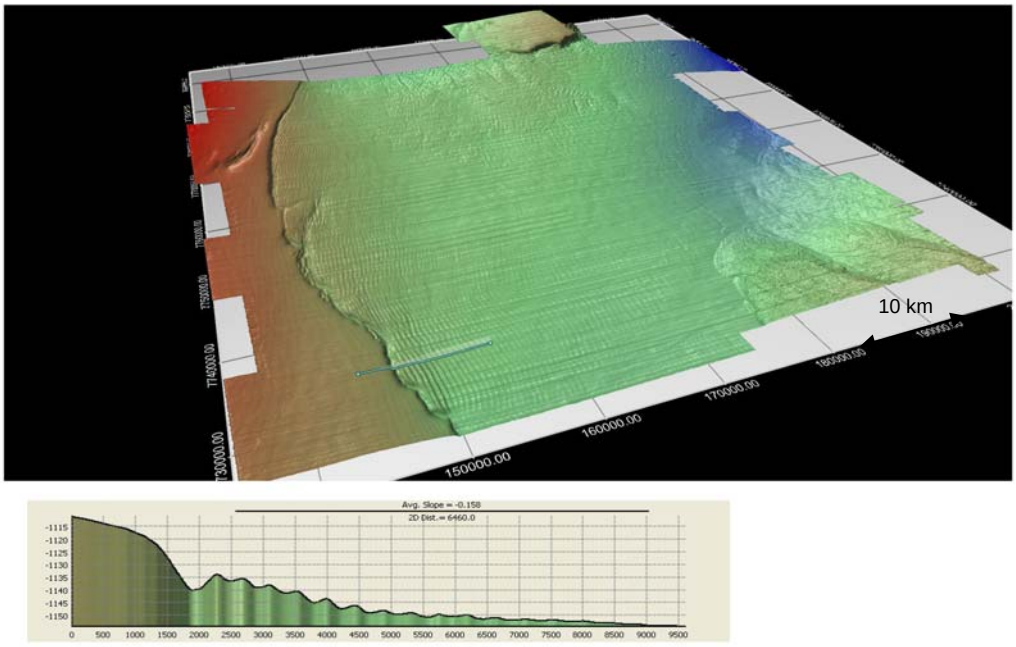

Figure 14: Seafloor rendering of the Glencoe survey area, eastern flank of Scarborough Arch. Arcuate scarp is the headscarp of a >65 km long landslide complex. Seaflor ripples are drape over landslide blocks at depth.

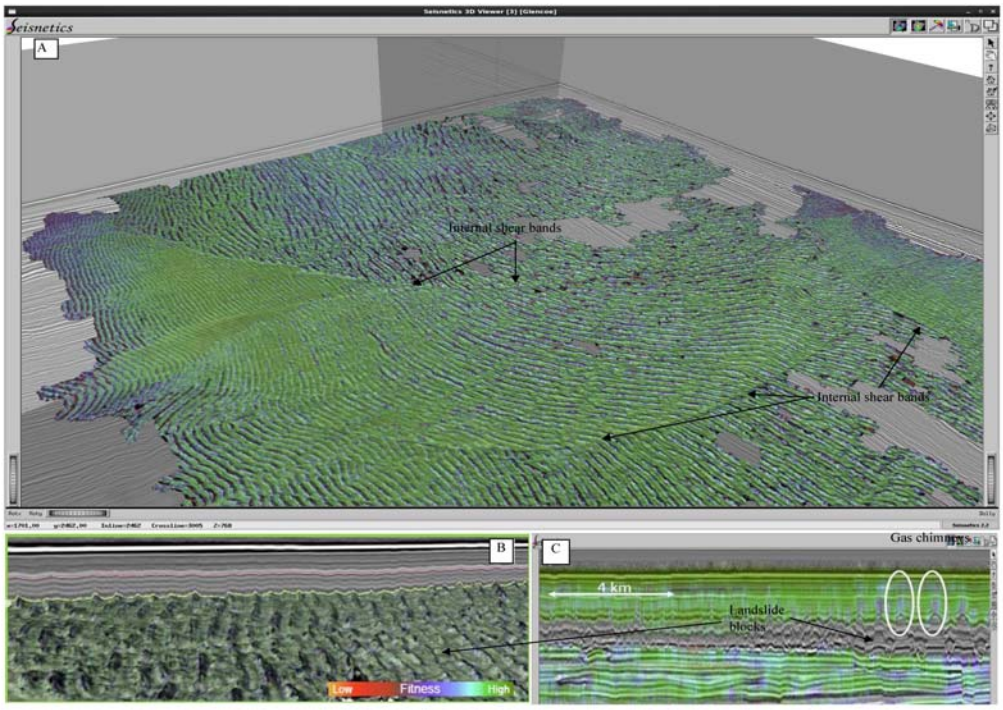

Figure 15: Seismic horizon from Glencoe Survey showing internal deformation of slide complex. (A) shows displaced landslide blocks and internal shear bands. (B) shows close up of landslide blocks; and (C) shows further close up of blocks and associated gas chimneys. Images are "fitness" plots where green colours suggest coherent wave properties, while blue and purple colours suggest some alteration of the soil properties. The alteration may be related to gas or fluid expulsion.

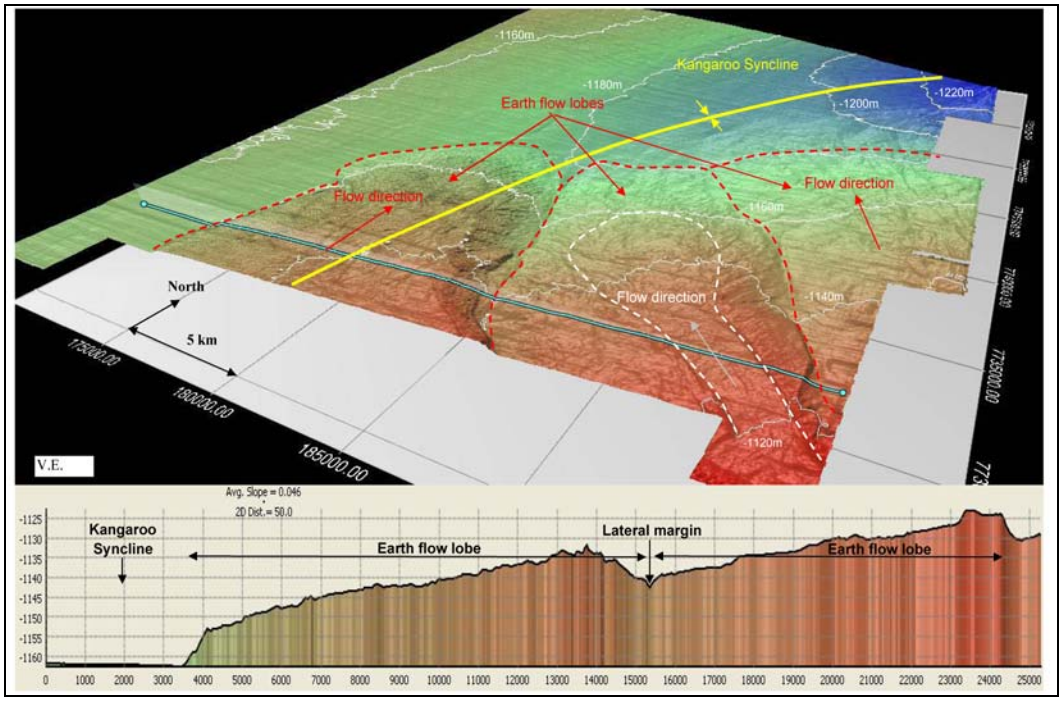

Figure 16: (a) Ten kilometre wide debris flow lobes within the Glencoe survey area in the centre of Kangaroo Syncline, 75 km from the continental slope. (b) Bathymetric profile across debris lobe in the Kangaroo Syncline.

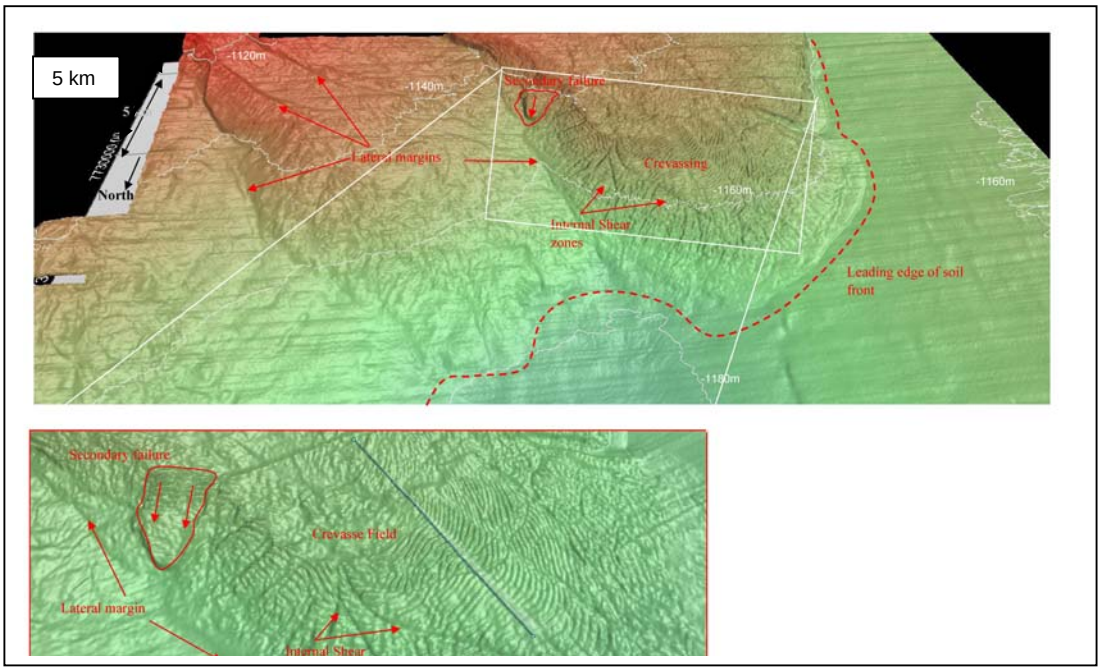

Figure 17: Close up views of debris flow lobes shown in Figure 16. Close up view illustrates the presence of crevasse fields, internal shears, and lateral shear margins.

2.5 SALSA SURVEY AREA

The location and general physiography of the Salsa Survey area is shown on Figures 1 and 4. The area is located on a ridge spur between two major canyons on the middle part of the continental slope; these are the Cape Range and Cloates submarine canyons. The continental slope typically extends from the shelf break to the abyssal plain, but in the Cuvier region of Western Australia the continental slope includes three distinct steps: (a) between 200 m and 1000 m depths the slope dips seaward 2 to 3 (locally 5) degrees; (b) at approximately 1000 m the slope encounters an 80 km-wide plateau surface that dips ~1 degree toward the west and continues to a depth of approximately 2000 m; and (c) between 2000 m and 4000 m the slope dip increases again to 3 to 4 degrees and the slope descends to the Cuvier abyssal plain. The plateau between 1000 m and 2000 m depth represents the southern offshore continuation of the Northern Carnarvon Basin and is analogous to the Exmouth Plateau.

The Salsa Survey lies in approximately 1,250 m to 1,875 m water depth (Figure 18). The axis of the ridge spur plunges approximately 0.4° to the west, and the dips on the north and south facing slopes of the ridge spur vary from 1 to 2.5°. The survey partially captures two large landslide complexes, which occur on the north and south slopes of the ridge spur (Figure 19). The landslide on the north slope (Salsa LS 1) is a minimum of 15 km long and 12 km wide (Table 1). The headscarp of the landslide is approximately 60 m high and the overall elevation drop, from the top of the slide to the bottom is about 600 m. The average slope gradient of the slide mass varies from 0.83° on the upper flat part of the slide complex to 2.3° on the lower steepened part of the complex (Table 1). The gradient of the nearby unfailed slope varies from 1.3° to 2.4°. However, the base of the slope near the canyon is up to 15°. The slide mass is complex and composed of numerous nested slope failures. The main features include failures at the slope break near the base of the slide, a main slide mass, and a series of retrogressive slope failures near the upper part of the slide (Figure 19).

The top of the Salsa LS1 slide complex is characterized by a longitudinal mote (Figure 19), much like the Chandon slide and Glencoe slides. This is a channel like feature that connects a series of pock marks, or expulsion vents. The pock marks are 500 to 1000m across and can be up to 50m deep. The pock marks, or vents, coincide quite closely with the position of the landslide headscarp and may indicate an association between fluid expulsion and landslide triggering.

The Salsa Slide is a large complex failure with multiple retrogressive failures along the top and sides of the slide. It is less coherent than either the Chandon or Glencoe slides and therefore is inferred to have been a somewhat more rapid failure. However, a section of drape (landslide deposits from the upper slope) over the slide deposits suggests that at least in the upper part the slide is not currently active, however, the lower part of the slide complex on the steep slope near the canyon may still be active.

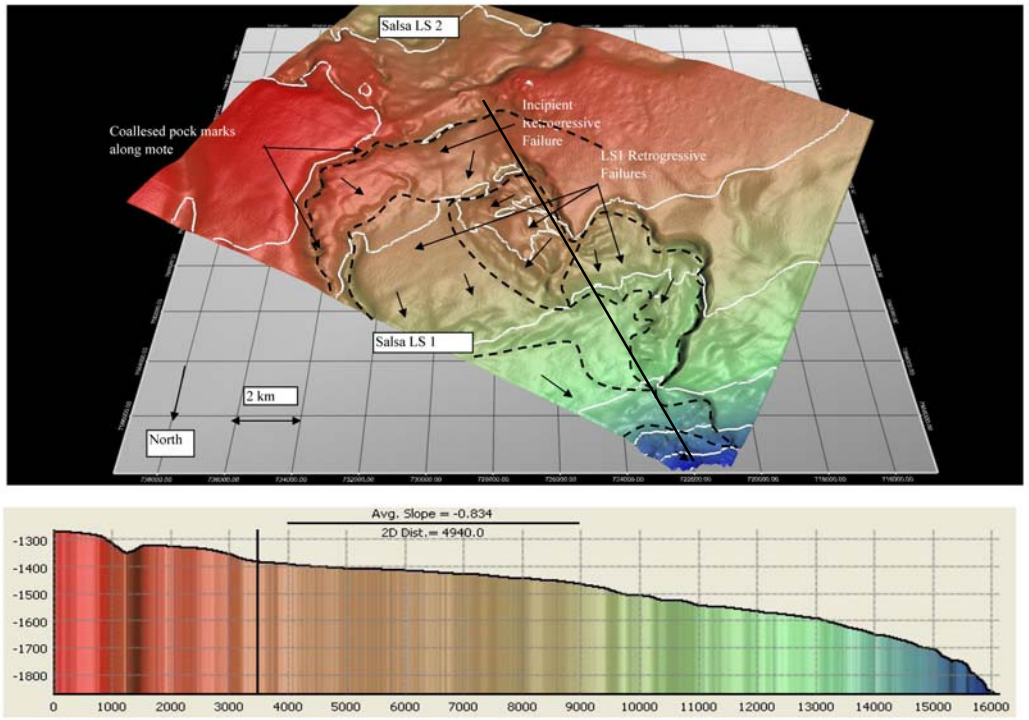

Figure 18: Overview of landslide complex from the Salsa survey area and associated bathymetric profile.

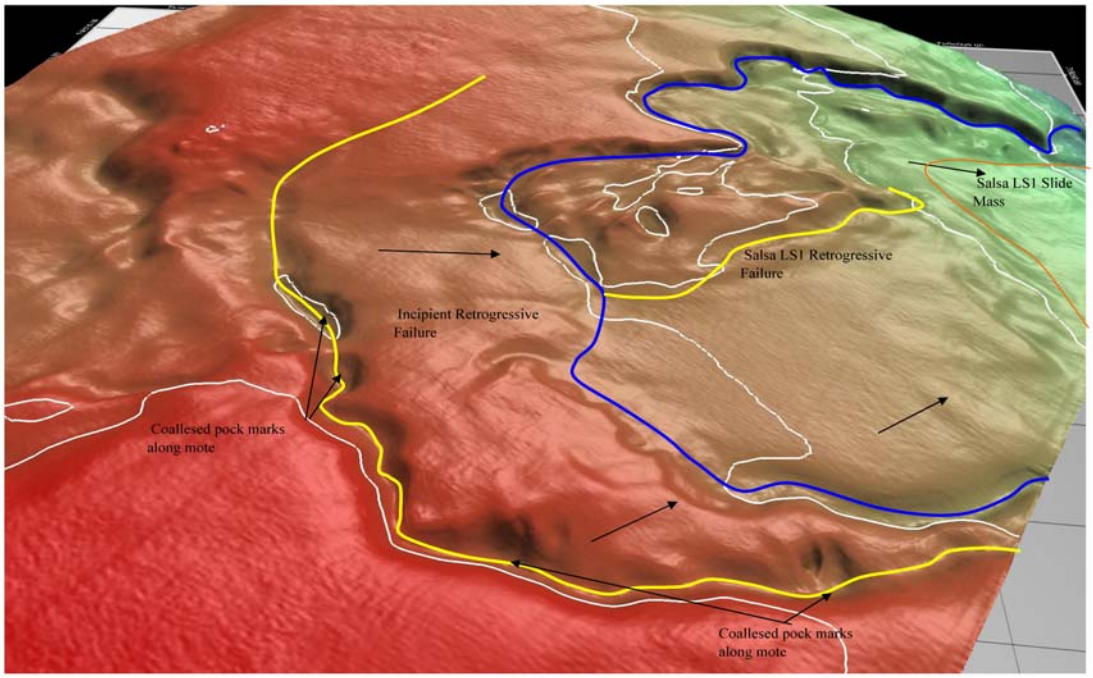

Figure 19: Close up of Salsa landslide complex showing association with gas/fluid expulsion features and retrogressive failures. Grid lines are 2 km.

3 DISCUSSION

Seafloor digital terrain models (DTMs) were produced from six 3D seismic volumes located along the Exmouth Plateau continental slope, along the eastern limb of Scarborough Arch, and along the Cape and Cloates Canyons (Figures 1 and 4). The DTMs were produced to assess seafloor geomorphology and types of processes occurring across this approximately 240 km long segment of the continental margin. Deep water projects such as Gorgon, Pluto, Scarborough, and Jansz-Io are all progressing along this part of the North West Shelf and therefore improving our understanding of seabed processes will help to reduce the risk to these and future projects in the area.

The Gorgon/Acme and Willem surveys are located along the continental slope and the Willem survey extends across the lower slope to the Kangaroo Syncline (Figure 4). The large scale morphology of this part of the continental slope is characterized both by undisturbed sedimentary fans, submarine canyon systems and submarine landslide complexes (Figure 7).

A range of geomorphic features on the seabed indicate that surficial geomorphic processes play an important role in the evolution of the continental slope and landslides are probably the dominant mechanism by which sediment is transported down the slope. The types of landslides observed along these parts of the continental slope include: small translational failures and slumps (<3 km across); moderate scale debris flows, debris avalanches, and topple failures (<10 km across); and large scale mass transport complexes (>20 km across). The small failures and slumps have the greatest likelihood of occurrence on steeper slopes with unstable sediment accumulations, such as the sedimentary fans at the base of canyons, near sediment waves at the tops of the canyons, or along sedimentary aprons such as the one that blankets the slope in the southern part of the Gorgon and Willem survey areas (Figures 7 and 10). The moderate scale failures appear most likely to occur along the sedimentary fan complex that has accumulated at the base of submarine canyons, or at the base of palaeo-headscarps from past mass failure events (i.e. the Gorgon and Willem scarps). The debris fields from topple failures beneath the Gorgon scarp (Figure 8), and the recent slide scars and deposits shown on Figure 10 provide examples of these types of moderate scale failures. We infer that these types of failures are primarily driven by gravitational instability related to over-steepened scarps, or areas with rapid sediment accumulation (fans). Evidence of pock-marks in the canyons and on the sedimentary fans indicate that fluid over-pressures also might play a role in triggering the moderate scale failures.

Large scale mass transport events such as those that formed the Gorgon Slide 1 failure (Figures 7 and 8), or the buried series of MTCs shown on Figure 6 from the Willem survey area, involve deep seated translational failures that may be up to 200 m or 300 m thick, 20->30 km wide, and 50 km to 75 km long. The volumes for these events therefore can be in the order of a hundred cubic kilometres, or more. We speculate that deep seated failures of these magnitudes likely require a triggering mechanism such as an earthquake and/or gas expulsion event. The association of reactivated faults (Figures 3 and 9), inversion structures, gas reservoirs and seafloor expulsion features (pock marks: Figure 7D) suggests there may be a tectonic control on seafloor stability (Hengesh *et al*., 2011b). Large-scale mass transport events may occur near areas where fault reactivation has inverted former basin structures along the rifted margin. The structural inversions can locally increase slope gradient (driving force), provide a source for gas/fluid release (venting) that reduces soil effective stress, and can generate localized earthquake strong ground shaking that increases lateral loads and reduces effective stresses through pore pressure changes. Due to the unusually weak calcareous soils on the North West Shelf any of these factors may be sufficient to trigger a large-scale mass wasting event.

The Chandon, Glencoe and Salsa slope failures have a different character to the debris flows and mass transport complexes along the continental slope. The Chandon slide appears to be both a rotational failure near the headscarp and a translational failure within the slide mass. The translational part of the slide mobilizes the rotated soil blocks within the slide mass and transports them down slope (Figure 13). The failure is interpreted to be a slow moving translation of large soil blocks on a very low angle failure plane. The slide appears to be the upper retrogressive failure of a larger landslide complex that exists down slope. The very low angle slopes in these areas likely prevent the failures from gaining significant speed or energy. The failures appear to be slow and thus the soil mass can stay relatively intact compared to failures on steeper slopes.

Submarine landslides from both the continental slope and Scarborough arch are creating meta-stable deposits that are moving down slope and into the Kangaroo Syncline, or down Cape Range and Cloates Canyons. Striations on failure planes from buried MTCs indicate movement into the syncline from both directions and the continued northward down slope movement within the syncline axis (Figure 10). Figures 16 and 17 show examples of soil lobes on the seafloor that have mobilized from the continental slope more than 75 km away. Although the driving process for these soil lobes is probably slow moving soil creep, the soil lobes will pose unusual geotechnical conditions and could impose strains on subsea infrastructure systems, especially in the areas where crevasses have formed or along the lateral margins. Although the Kangaroo Syncline appears flat on many bathymetric maps, a careful understanding of the seafloor conditions and route options is important to minimize risks.

Together, all of these landslide types form elements of a slope process model. Within a slope process model the types and frequency of landslide occurrence tend to follow a "power law" (ten Brink *et al*., 2006), meaning that like many natural processes there is a relationship between the magnitude of an event and its frequency of occurrence. Specifically, there are many more small slope failures than large ones. Though the large failures are the most impressive, even smaller failures can jeopardize pressure integrity of a field development or export system. Therefore, it is very important that the data acquisition programmes carried out in support of site investigations and engineering design be fit-for-purpose. Although regional 3D exploration seismic data are suitable for general screening purposes, these data are not suitable for detailed mapping and characterization of the sea-bed to support detailed design and engineering. The 3D exploration data are useful for identifying the types of failures from infrequent moderate to large events, such as the landslide complexes along the Gorgon scarp and Scarborough arch (Figure 4), but these data are not suitable for identifying small failures (e.g. tens of metres) that still could impose unacceptable loads on sea-bed developments. It is recommended that additional high resolution swath bathymetry datasets be collected using Autonomous Underwater Vehicles (AUV) for future slope process risk assessments in this area and other deep water, far shore areas of the North West Shelf.

4 CONCLUSIONS

Our analysis of Open File exploration seismic data has identified several types of slope failures along submarine slopes on Exmouth Plateau. The landslides range in size from less than a kilometre to greater than 30 kilometres across and show a range of failure mechanisms from small debris flows and topple failures to large scale Mass Transport Complexes (MTC). Some of the observed characteristics of these slides are summarized below:

- Slide lengths vary from 2.6 km to 60 km in length;
- Slide widths vary from <1 km to 70 km in width;
- Slide thicknesses vary from 8 m to 300 m;
- Slide volumes range from 40 m^3 to over 100 km^3 and
- All slides occur on slopes less than 2 degrees, and most slides occur on slopes less than 1 degree.

The characteristics of the landslide deposits suggest different velocities of failure events. For example the relatively intact soil blocks observed in the Chandon and Glencoe slides are used to infer that these events were relatively slow failures, while the large dispersed debris fields observed at the Gorgon LS 1 and Willem LS 2, 3, and 4 sites are used to infer that these were relatively rapid failures. The velocity of landslide failure is an important consideration for performance analysis of subsea infrastructure that may lie in the path of these events.

Although a quantitative analysis of slope failures and triggering mechanisms has not yet been carried out, the geomorphic observations provide indications of the types of mechanisms that might be controlling slope processes along the Exmouth slope. Small to moderate failures such as debris flows in canyons and on fans, and translational failures on the lower slope may be occurring under sediment loading and gravitational instabilities; in other words these are likely to be static slope failures. However, the large MTC's such as observed at Gorgon and in the Willem subsurface appear to be related to observed factors including increased stratigraphic dips above inversion structures, fluid and gas expulsion, and near surface faulting. We recognize a frequent association of fluid expulsion features and slope failures (e.g. Gorgon Slide #2) and so this may be a common triggering mechanism. Seismic loading also is a likely triggering mechanism and the association of slides with potential seismic sources will be a topic of ongoing research.

5 REFERENCES

Audley-Charles, M. G. (1986a). Rates of Neogene and Quaternary tectonic movements in the Southern Banda Arc based on micropalaeontology, Journal of the Geological Society, London, Vol. 143, 1986, pp. 161-175.

Audley-Charles, M. G. (1986b). Timor-Tanimbar Trough: the foreland basin of the evolving Banda Orogen. In: Foreland Basins (Edited by Allen, P. A. and Homewood, P.). Spec. Pub. Int. Assoc. Sedimentology, 8, pp. 92-102.

Audley-Charles, M.G. (2004). Ocean trench blocked and obliterated by Banda forearc collision with Australian proximal continental slope. Tectonophysics Vol. 389, pp. 65-79.

Australian Geological Survey Organisation (AGSO) North West Shelf Study Group (1994). Deep reflections on the North West Shelf: changing perspectives of basin formation, in Purcell, P. G. and Purcell, R. R. (eds.), The Sedimentary Basins of Western Australia, Proceedings of the Petroleum Exploration Society of Australia, Perth, pp. 63-74.

Baillie, P.W, Powell, C.M., Li, Z.X., and. Ryan, A.M (1994). The tectonic framework of Western Australia's Neoproterozoic to Recent sedimentary basins, in Purcell, P. G., and Purcell, R. R. (eds.), The Sedimentary Basins of Western Australia, Proceedings of the Petroleum Exploration Society of Australia, Perth, pp. 45-62.

Boyd, R. Williamson, P., and Haq, B. (1992). Seismic stratigraphy and passive margin evolution of the southern Exmouth plateau, in von Rad, Haq, B.U., et al., (eds.), Proceedings of the Ocean Drilling Program, Scientific Results, Vol. 122.

Burchette, T. P., and Wright, V. P. (1992). Carbonate ramp depositional systems. Sedimentary Geology, Vol. 79, No. 1, pp. 3-57.

Cathro, D.L. and Karner, G.D. (2006). Cretaceous-Tertiary inversion history of the Dampier sub-basin, northwest Australia: Insights from quantitative basin modelling, Marine and Petroleum Geology, Vol. 23, pp. 503-526.

Densley, M. R., Hillis, R. R., & Redfearn, J. E. P. (2000). Quantification of uplift in the Carnarvon Basin based on interval velocities. Australian Journal of Earth Sciences, 47(1), pp. 111-122.

Dirstein, J.K. and Fallon G.N. (2011). Automated Interpretation of 3D Seismic Data Using Genetic Algorithms, ASEG Preview Vol. 201, no. 151, pp. 30-37.

Dirstein, J.K., Hengesh, J.V. and Stanley, A.J. (2013). Identification of Fluid Flow Features in the Seafloor and Subsurface and their Implications for Prospect and Geohazard Assessment: Examples from the Australian Northwest Shelf, Western Australian Basin Symposium (WABS), Perth, WA, 18-21 August 2013.

Exon, N.F. and Buffler, R.T. (1992). Mesozoic Seismic Stratigraphy and Tectonic Evolution of the Western Exmouth Plateau, in von Rad, U. and Haq, B. U. (eds), Proceedings of the Ocean Drilling Program, Scientific Results, Vol. 122.

Exon, N. F., Haq, B.U. and von Rad, U. (1992). Exmouth Plateau Revisited: Scientific Drilling and Geological Framework, in von Rad, U., Haq, B. U. (eds), Proceedings of the Ocean Drilling Program, Scientific Results, Vol. 122.

Geoscience Australia (2009). The Australian Bathymetry and Topography Grid, June 2009; COPYRIGHT, Commonwealth of Australia, (Geoscience Australia) 2009.

Hampton, M.A., Homa, J.L. and Locat, J. (1996). Submarine Landslides, Reviews of Geophysics, v34, no.1, pp. 33-59.

Hengesh, J.V., Wyrwoll, K.H. and Whitney, B.B. (2011a). Neotectonic deformation of northwestern Australia and implications for oil and gas development. Proc. 2nd International Symposium on Frontiers in Offshore Geotechnics (ISFOG), Perth, Western Australia, Ed. Gourvenec & White, Taylor & Francis.

Hengesh, J. V., Whitney, B.B., and Rovere, A. (2011b). A Tectonic Influence on Seafloor Stability along Australia's North West Shelf, in Proceedings of the Twenty-first (2011) International Offshore and Polar Engineering Conference, Maui, Hawaii, USA, June 19-24, 2011, pp. 596-566, Copyright © 2011 by the International Society of Offshore and Polar Engineers (ISOPE), ISBN 978-1-880653-96-8 (Set); ISSN 1098-6189 (Set).

Hocking, R.M. (1990). Field Guide for the Carnarvon Basin, Geological Survey of Western Australia, Record 1990/11.

Kaiko, A.R., and Tait, A.M. (2001). Post-rift tectonic subsidence and palaeo-water depths in the northern Carnarvon Basin, Western Australia, APPEA Journal, pp. 368-379.

Keep, M. and Moss, S.J. (2000). Basement reactivation and control of Neogene structures in the Outer Browse Basin, Northwest Shelf, Exploration Geophysics, Vol. 31, pp. 424-432.

Keep, M., Harrowfield, M., and Crowe, W. (2007). The Neogene tectonic history of the North West Shelf, Australia, Exploration Geophysics, Vol. 38, pp. 151-174.

Keep, M. & Haig D.W. (2010). Deformation and exhumation in Timor: distinct stages of a young orogeny. Tectonophysics Vol. 483, pp. 93–111.

Masson, D.G., Harbitz, C.B., Wynn, R.B., Pedersen, G. and Lovholt, F. (2006). Submarine landslides: processes, triggers and hazard prediction. Phil. Trans. R. Soc., A, vol. 364, pp. 2009-2039.

Moore, J.G., Clague, D.A., Holcomb, R.T., Lipman, P.W., Normark, W.R. and Torresan, M.E. (1989). Prodigeous submarine landslides on the Hawaiian Ridge, Journal of Geophysical Research, Vol. 94, No. B12, pp. 17,465-17,484.

ten Brink, U.S., Geist, E.L. and Andrews, B.D. (2006). Size distribution of submarine landslides and its implication to tsunami hazard in Puerto Rico, Geophys. Res. Lett., 33, L11307, doi:10.1029/2006GL026125.

von Rad, U. and Haq, B.U. (1992). Proceedings of the Ocean Program, Scientific Results, Leg 122, College Station, Texas, USA, Ocean Drilling Program, doi:10.2973/odp.proc.sr.122.

Whitney, B.B. and J. Hengesh (2013). Geological constraints on Mmax values from Western Australia: Implications for seismic hazard assessments. Australian Geomechanics Society Journal. Western Australian Geotechnics. Vol. 48, no 2. p. 15-26.

Yeates, A. N., Bradshaw, M. T., Dickins, J. M., Brakel, A. T., Exon, N. F., Lanford, R. P., Mulholland, S. M., Totterdell, J. M., and M. Yeung (1987). The Westralian Superbasin, an Australian link with Tethys: in McKenzie, K.G. (ed.), Shallow Tethys 2: 2nd International Symposium on Shallow Tethys, Wagga Wagga, pp. 199–213.